

EARLY RESULTS TOWARDS THE CANADIAN GEOID IN THE THREE-SPACE SCENARIO

HUAINING YANG

April 2005



**TECHNICAL REPORT
NO. 229**

EARLY RESULTS TOWARDS THE CANADIAN GEOID IN THE THREE-SPACE SCENARIO

Huaining Yang

Department of Geodesy and Geomatics Engineering
University of New Brunswick
P.O. Box 4400
Fredericton, N.B.
Canada
E3B 5A3

April 2005

© Huaining Yang 2005

PREFACE

This technical report is an unedited reproduction of a report submitted in partial fulfillment of the requirements for the degree of Master of Science in Engineering in the Department of Geodesy and Geomatics Engineering, April 2005. The research was supervised by Drs. Petr Vanicek and Marcelo Santos, and it was financially supported by the Natural Sciences and Engineering Research Council of Canada.

As with any copyrighted material, permission to reprint or quote extensively from this report must be received from the author. The citation to this work should appear as follows:

Yang, H. (2005). *Early Results Towards the Canadian Geoid in the Three-Space Scenerio*. M.Sc.E. thesis, Department of Geodesy and Geomatics Engineering Technical Report No. 229, University of New Brunswick, Fredericton, New Brunswick, Canada, 152 pp.

Abstract

The three space Stokes-Helmert scheme of the precise gravimetric geoid determination has been theoretically developed and numerically realized in UNB.

A transformation of observed values of terrestrial gravity in Real space, from No topography space into Helmert space on geoid surface, is accomplished by a series of gravity reductions and corrections. Helmert co-geoid can be decomposed into two parts: the low-frequency part, called reference co-geoid is determined from satellite data directly; the high-frequency part, called residual co-geoid is determined by the solution of geodetic boundary value problem using derived terrestrial gravity. The co-geoid is transformed to the geoid by correcting from the primary indirect effects.

The final Canadian geoid has been compared with GPS/Leveling data. Difference due to the long wavelength part of the differences is obvious and other systematic errors, such as the bias and vertical deflection between the geometric geoid model and gravimetric geoid model, definitely exist.

Acknowledgements

I would like to convey my heartfelt appreciation to Prof. Petr Vaníček for his theoretical contribution to the precise geoid determination, constructive guidance, cautious revision of this manuscript, and insistent push. I would like to deeply express my gratitude to Prof. Marcelo Santos for his academic guidance, financial support, and kindly patience.

I am indebted to Dr. Jianliang Huang, Mr. Marc Véronneau for providing me with all necessary elevation data and the associated information.

My thanks go to Dr. Jianhu Zhao, Dr. Robert Tenzer, Mr. Robert Paul, Dr. Auto Ellmann, Mrs. Azadeh Koohzare and Mr. Mustafa Berber for their help and friendship.

Contents

Abstract	ii
Acknowledgements	iii
Table of contents	iv
List of Tables	viii
List of Figures	ix
List of Abbreviations	xii
List of Symbols	xiv
1 Introduction	1
1.1 Geoid definition	1
1.2 Geoid determination	2
1.3 Thesis objective and structure	3
2 Theoretical Background	5
2.1 Geodetic boundary value problem	5
2.2 Construction of harmonic space	8
2.3 Stokes-Helmert's scheme	9
2.3.1 General introduction to methodology	9
2.3.2 Evaluation of gravity anomaly on the Earth's surface	11
2.3.3 Definition of gravity disturbance and its relation to gravity anomaly	14

2.3.4 Evaluation of NT gravity anomaly on the Earth's surface	16
2.3.5 Downward continuation of gravity anomaly in NT-space	19
2.3.6 Transformation of gravity anomaly from NT-space into H-space	20
2.3.7 Evaluation of the Helmert co-geoid	23
2.3.8 Primary indirect effect	26
2.3.9 Summary of the Stokes-Helmert's scheme	30
3 The Precise Geoid Determination Software Package	33
3.1 Introduction of the Software Package	33
3.2 Specification of input files	38
3.2.1 Heights	38
3.2.2 Gravity data	41
3.2.3 Topographical density data (laterally varying)	41
3.2.4 Other standard input data	42
3.3 Problems encountered during data processing	43
3.3.1 Production of mean orthometric heights files	43
3.3.2 Generation of the input files for PGDP component programs DAE_NTspace, DAE_Hspace, SIAE_NTspace, SIAE_Hspace and PIAE	45
3.3.3 Preparation of "Inner_zone.dat" for the programs, SITE_NTspace, SITE_Hspace, and PITE	47
3.3.4 Preparation and management of the Detailed DTM files	48
3.3.5 Programs of Reference field and Reference spheroid	50
3.3.6 Evaluation of required region for each file	51
3.3.7 Additional comments	51

3.4 Special technical skills required for calculation	53
3.4.1 Requirement for familiarity with one computer language	53
3.4.2 Capability of writing scripts in Linux	53
3.4.3 Mastering GMT to make graphical plots	54
3.5 Descriptive statistics of program operation	54
4 Numerical Results and Their Interpretation	57
4.1 Direct topographical effect and direct condensed topographical effect	58
4.1.1 STC and SCTC	59
4.1.2 DTE-density and DCTE-density	63
4.1.3 DTE and DCTE	69
4.2 Atmospheric effects	72
4.3 Secondary indirect effect of topographical evaluated in NT-space and H-space respectively, and PITE	78
4.4 Ellipsoidal correction and geoid-quasigeoid correction	79
4.5 Downward continuation	86
4.6 Helmert Reference Gravity Anomaly and Helmert Reference Spheroid	87
4.7 Residual Helmert gravity anomaly and residual spheroid	87
4.8 Geoid model and the comparison of results with GPS/Leveling data	94
4.9 Comparison between Canadian geoid models produced in UNB	95
4.10 Comparison Canadian geoid models between UNB's and GSD's	99
5 Conclusions and recommendation	103
References	107

Appendix A	115
Appendix B	121
Appendix C	150
Vita	

List of Tables

3.1 Function of each program in the UNB Precise Geoid Determination Package ...	37
3.2 DEM_5m files covering Canada	46
3.3 Statistics of computational time span for the production of digital geoid	56
4.1 Terrain and condensed terrain effects on gravity – near-zone (mGal)	61
4.2 Terrain and condensed terrain effects on gravity – far-zone (mGal)	64
4.3 Anomalous density effects (mGal)	66
4.4 DTE and DCTE on gravity (mGal)	70
4.5 All effects of atmospheric masses on gravity (mGal)	74
4.6 Secondary indirect topographical effect on gravity (mGal)	80
4.7 Ellipsoidal correction and Geoid-quasigeoid correction (mGal)	83
4.8 Gravity anomaly in NT-space and downward contribution (mGal)	88
4.9 Reference gravity anomaly (mGal) and reference spheroid (m)	90
4.10 Residual gravity anomaly (mGal) and residual co-geoid (m).....	92
4.11 Geoid and compared differences with GPS/Leveling (m)	96

List of Figures

1.1 Relationship between the geoid, orthometric height and geodetic height	2
2.1 Stokes-Helmert's scheme	11
2.2 Parameters used in the definition of gravity anomalies	12
2.3 Flowchart of the Stokes-Helmert's scheme	32
3.1 Flowchart of the UNB <i>Precise Geoid Determination Package</i> (PGDP)	36
3.2 Mean DTM with 5' by 5' resolution (m)	40
3.3 Coverage relation between Near_zone.dat and Computation_points.dat	46
3.4 Coverage relation between Inner_zone.dat and Computation_points.dat	47
3.5 Example of the scheme of detailed DTM files	49
4.1 Scheme of integration domain	60
4.2 Terrain effect on gravity – near zone (mGal)	61
4.3 Condensed terrain effect on gravity – near zone (mGal)	62
4.4 Terrain effect on gravity – far zone (mGal)	64
4.5 Condensed terrain effect on gravity – far zone (mGal)	65
4.6 Anomalous topographical density effect on gravity (mGal)	66
4.7 Condensed anomalous topographical density effect on gravity (mGal)	67
4.8 Direct topographical effect on gravity (mGal)	70
4.9 Direct condensed topographical effect on gravity (mGal)	71
4.10 Integration scheme for the atmospheric effects	72

4.11 Direct atmospheric effect on gravity (mGal)	74
4.12 Direct condensed atmospheric effect on gravity (mGal)	75
4.13 Secondary indirect atmospheric effect on gravity (mGal)	76
4.14 Secondary indirect condensed atmospheric effect on gravity (mGal)	77
4.15 Secondary indirect topographical effect on gravity (mGal)	80
4.16 Secondary indirect condensed topographical effect on gravity (mGal)	81
4.17 Primary indirect topographical effect on geoid (m)	82
4.18 Ellipsoidal correction to the gravity disturbance (mGal)	83
4.19 Ellipsoidal correction for the spherical approximation (mGal)	84
4.20 Geoid-quasigeoid correction on gravity (mGal)	85
4.21 NT gravity anomaly on the Earth's surface (mGal)	88
4.22 NT gravity anomaly on the geoid (mGal)	89
4.23 Helmert reference gravity anomaly (mGal)	90
4.24 Helmert reference spheroid (m)	91
4.25 Residual gravity anomaly in H-space (mGal)	92
4.26 Residual co-geoid (m)	93
4.27 Canadian geoid model (m)	96
4.28 Locations of GPS/Leveling points	97
4.29 Comparing results with GPS/Leveling data (m)	97
4.30 Geoid model based on two-space Stokes-Helmert scheme (m)	98
4.31 Difference between two Canadian geoid models (m)	98
4.32 CGG2000 of GSD (m)	101
4.33 Difference between Geoid_UNB2004 and CGG2000 (m)	101

4.34 Comparison between CGG2000 and GPS/Levelings (m)	102
---	-----

List of Abbreviations

CDED	Canadian Digital Elevation Data
CGG2000	Canadian Gravimetric 2000
DAE-NT	direct atmospheric effect referred to the Earth's surface
DCAE-H	direct condensed atmospheric effect referred to the geoid
DCTE	direct condensed topographical effect
DCTE-density	condensed anomalous topographical density effect
DCTE-H	direct condensed topographical effect in Helmert space
DEM_5m	Digital Elevation Data with the resolution 5' by 5'
DEM_30s	Digital Elevation Data with the resolution 30" by 30"
DTE	direct topographical effect
DTM	Digital Terrain Model
DTDM	Digital Topographical Density Model
DTE-density	anomalous topographical density effect
EGM96	Earth Geopotential Model 96
GA-E-NT	gravity anomaly on the Earth's surface in No topography space
GA-G-NT	gravity anomaly on the geoid in No topography space
GBVP	geodetic boundary value problem
GGM02	GRACE Gravity Model 02

GMT	Generic Mapping Tool
GPS	Global Positioning System
GRS80	Geodetic Reference System 1980
GSD	Geodetic Survey Division of Natural Resources Canada
H-space	Helmet space
NT-space	No Topography space
PGDP	precise geoid determination package
PIAE	primary indirect atmospheric effect referred to the geoid
PITE	primary indirect topographical effect referred to the geoid
Reference-GA	Helmert reference gravity anomaly
R-space	Real space
SCTC	spherical condensed terrain correction effect
SCTC-far-zone	spherical condensed terrain correction effect over the far zone
SCTC-near-zone	spherical condensed terrain correction effect over near zone
SIAE-NT	secondary indirect atmospheric effect in No Topography space
SIAE-H	secondary indirect condensed atmospheric effect in Helmert space
SICAE-H	secondary indirect condensed atmospheric effect in Helmert space
SICTE-H	secondary indirect condensed topographical effect in Helmert space
SITE-H	secondary indirect condensed topographical effect in Helmert space
SITE-NT	secondary indirect topographical effect in No Topography space
STC	spherical terrain correction effect
STC-far-zone	far zone contribution to the spherical terrain correction effect
STC-near-zone	near zone contribution to the spherical terrain correction effect

List of Symbols

a	... major semi-axis of the reference ellipsoid
b	... minor semi-axis of the reference ellipsoid
f	... polar flattening of the reference ellipsoid
h	... geodetic height
g	... magnitude of gravity
m	... Clairaut's constant
r	... geocentric radius in spherical coordinates
r_g	... geocentric radius of the geoid in spherical coordinates
r_t	... geocentric radius of the topography in spherical coordinates
r_o	... geocentric radius of the ellipsoid in spherical coordinates
r_{lim}	... geocentric radius of the upper limit of atmosphere
G	... universal gravitational constant
H	... orthometric height
H^N	... normal height between telluroid and ellipsoid surfaces
K	... spherical Poisson integral kernel
N	... geoidal height
N^H	... co-geoid height

$N_{\text{ref}}^{\text{H}}$... reference co-geoidal height
R	... radius of the reference sphere
S	... spherical Stokes's integration kernel
T	... disturbing gravity potential
$T_{\text{ref}}^{\text{H}}$... low-frequency gravity disturbing potential
V	... gravitational potential generated by the Earth
V^a	... gravitational potential of atmospheric masses
V^{ct}	... gravitational potential of the masses condensed on the geoid
V^s	... gravitational potential generated by the masses below the geoid
V^t	... gravitational potential generated by the topographical masses
W	... actual gravity potential
W_0	... gravity potential on the geoid
U	... normal gravity potential
δg	... gravity disturbance
δV^t	... residual gravitational potential of the topographical masses
δV^a	... residual gravitational potential of the atmospheric masses
Δg	... gravity anomaly
Δg^{FA}	... free air gravity anomaly
Δg^{H}	... gravity anomaly in Helmert space
Δg^{NT}	... gravity anomaly in No Topography space
Δg^{SB}	... simple Bouguer gravity anomaly

$\Delta g_{\text{ref}}^{\text{H}}$... Helmert's reference gravity anomaly
$\delta\rho$... anomalous topographical density
γ	... normal gravity
$\varepsilon_{\delta g}$... ellipsoidal correction to the gravity disturbance
ε_n	... ellipsoidal correction for the spherical approximation
ζ	... height anomaly
λ	... geocentric longitude
ξ	... meridional component of the deflection of the vertical
ρ^a	... radially distributed atmospheric density
ρ_o	... mean density of topographical masses
ϕ	... geocentric latitude
γ_0	... magnitude of normal gravity on the reference ellipsoid
Ω	... computation point
Ω	... pair of angular spherical coordinates
Ω_o	... total pairs of angular spherical coordinates
Ω'	... integration point
Ω_{ψ_o}	... near-zone integration sub-domain

Chapter 1

Introduction

1.1 Geoid definition

The geoid is defined as an equipotential surface of the Earth corresponding to the mean sea level approximately, which is the most natural representation of the Earth's shape. In the strict mathematical sense, this surface intersects the direction of gravity at right angles everywhere. Generally, it is too complicated to serve as the computational surface on which to solve geometrical problems such as point positioning.

The reference ellipsoid is customarily considered as a geocentric ellipsoid which best fits the geoid globally with the same volume as the geoid and the same mass as the Earth. Its minor axis is always parallel to the Earth's principal polar axis of inertia. This geocentric reference ellipsoid that generates normal gravity is used to approximate the geoid.

The geometrical separation between the geoid and the reference ellipsoid is called the geoidal height (or geoidal undulation) and is denoted by N . The orthometric height H is the height above the geoid and the geodetic height h is the height above the reference ellipsoid. These three parameters are related by the following equation (Vaniček and Krakiwsky, 1986):

$$h = N + H. \tag{1.1}$$

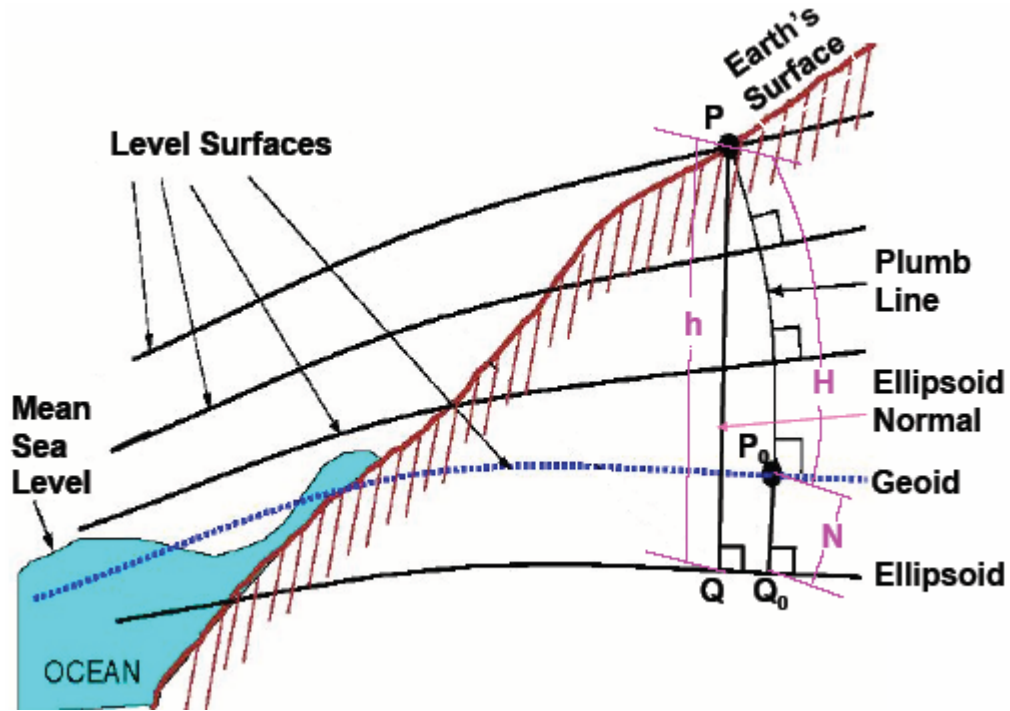


Figure 1.1: Relationship between the geoid, orthometric height and geodetic height.

Adapted from Smith, NGS (2000)

In Figure 1.1, the level surface represents the equipotential surface; N denotes geoidal height which is the distance along the ellipsoid normal (Q_0 to P_0); H is orthometric height, the distance along plumb line (P_0 to P); and h is the ellipsoid height or geodetic height, the distance along the ellipsoid normal (Q to P).

1.2 Geoid determination

Since the geoid serves as a geodetic datum for vertical positioning and it is also valuable in geophysics, physical oceanography and elsewhere, many efforts in geodesy

are focused on its accurate determination. Usually, the geoid can be calculated by using either geometric or gravimetric approaches.

With the successful development of Global Positioning System (GPS) and its capability of measuring geodetic height fairly accurately, geoidal height can be calculated by a simple subtraction of geodetic height from orthometric height evaluated using spirit levelling. Due to the limited number of GPS/Levelling points, this geometric solution cannot provide a high-resolution geoid model over a large region. In this situation the cost-efficient gravimetric method is adopted.

One of the widely used gravimetric approaches to determining the geoid is the Stokes-Helmert's technique, which was theoretically developed and properly refined at the University of New Brunswick (UNB). The associated software package was designed to numerically realize the local digital geoid based on the available gravity and elevation data. The detailed explanation of the Stokes-Helmert's theory, the introduction to the associated software package, the numerical results' presentation and the corresponding analysis will be shown in a later chapter.

1.3 Thesis objective and structure

The main objective of this research is to test the software package and come up with suggestions for improvements in the realm of user friendliness by understanding and mastering the theoretical background of the Stokes-Helmert's approach, and being familiar with the precise geoid determination package, which contains programs and related accessories.

The Stokes-Helmert approach, a mathematical model for the determination of precise gravimetric geoid, is described in Chapter (2). Firstly, the geodetic boundary value problem is introduced. To solve the problem, a harmonic space is created by applying the Helmert second condensation technique. Then each procedure in the Stokes-Helmert method is explained and the formulae are presented, which make up the theoretical methodology behind the corresponding programs.

During the computation, one must learn the flowchart of the precise geoid determination package, each program's function, the required input data files, the method of generating the input data files, the solution of frequently encountered problems in running programs, and the necessary special technique skills, which are all fully investigated in Chapter (3). My contribution here has been the correction of two main programs, NT_anomaly and Helmert_anomaly, and the preparation of several auxiliary programs for data format transformation and data manipulation.

Chapter (4) is composed of the explanation for realization of the computational methods in programs, and the analysis of the numerical results of each procedure, shown by graphical plots and statistical tables respectively. The chapter concludes with the comparison between the present Canadian geoid model and the previous one produced at UNB.

The conclusions are summarized in Chapter (5). Additionally, recommendations for further research in the area of the precise geoid determination are presented.

Chapter 2

Theoretical background

2.1 Geodetic boundary value problem

Let us begin with an explanation of the concept of the geopotential number (Baeschlin, 1960) which relates the basic orthometric height (Vaníček and Krakiwsky, 1986),

$$C = W_0 - W = \int_{P_0}^P g dl , \quad (2.1)$$

where g is the mean value of gravity along the plumb line between the point P_0 on the geoid and the point P ; dl represents the leveling increment; and W and W_0 denote the gravity potential of the point and of the geoid, respectively.

According to Eqn. (2.1), the geopotential number is the product of gravity multiplied by the height increment between the equipotential surface, where the point is located and the geoid surface along the plumb line. Geoidal height can be solved analogously after the determination of the potential difference between the geoid and the ellipsoidal surface. The big issue is to pursue this potential difference.

As defined, the geoid is an equipotential surface and is denoted by W equal to W_0 , both a constant, which is approximated by an Earth-referenced ellipsoid. Throughout this thesis, the Geodetic Reference System 1980 (GRS80) is used as the geocentric

reference ellipsoid generating a smooth potential field U , the normal potential. The normal potential on the reference ellipsoid is chosen to be equal to the real potential on the geoid $U_0 = W_0$ (Heiskanen and Moritz, 1967).

Now we are concerned with (i) the difference between the actual gravity potential and the normal potential, which is called the disturbing potential T , and (ii) especially with T on the geoid $T(r_g, \Omega)$,

$$\forall \Omega \in \Omega_0 : \quad T(r_g, \Omega) = W(r_g, \Omega) - U(r_g, \Omega), \quad (2.2)$$

where Ω is the solid spherical angle denoted by the pair (ϕ, λ) , the geocentric co-latitude and longitude; Ω_0 stands for the total geocentric solid angle; r is the geocentric radius of the point; and r_g is the geocentric radius of a point on the geoid. The argument (r, Ω) represents the position in three dimensions. All of the following formulae are valid over the whole Earth, i.e., Ω belongs to Ω_0 .

If the function T is harmonic outside the geoid, it satisfies Laplace's differential equation in space everywhere above the geoid,

$$\forall r \geq r_g : \quad \nabla^2 T(r, \Omega) = 0 \quad (2.3)$$

with the following condition suited over the geoid surface as a boundary:

$$\left. \frac{\partial T(r, \Omega)}{\partial r} \right|_{r=r_g} + \frac{2}{R} T(r_g, \Omega) = -\Delta g(r_g, \Omega), \quad (2.4)$$

which is the spherical approximation of the "Fundamental Gravimetric Equation" (Heiskanen and Moritz, 1967) and

$$\Delta g(r_g, \Omega) = g(r_g, \Omega) - \gamma_0(\phi), \quad (2.5)$$

where $\Delta g(r_g, \Omega)$ is the gravity anomaly on the geoid; R is the mean radius of the Earth; $g(r_g, \Omega)$ is the gravity on the geoid; and γ_0 is the normal gravity on the reference ellipsoid.

The asymptotic condition of function T at infinity is expressed by

$$\lim_{r \rightarrow \infty} T(r, \Omega) = 0. \quad (2.6)$$

Eqns. (2.3), (2.4) and (2.6) form a fixed, linear boundary-value problem called the geodetic boundary value problem (GBVP) in physical geodesy, which is suitable for determining the disturbing potential T on the geoid (Heiskanen and Moritz, 1967).

The solution of T for the above discussed boundary values, is given by Stokes formula (Stokes, 1849)

$$T(r_g, \Omega) = \frac{R}{4\pi} \iint_{\Omega_0} \Delta g(r_g, \Omega') \cdot S(\psi(\Omega, \Omega')) d\Omega', \quad (2.7)$$

where Δg is the gravity anomaly referred to the geoid, $\psi(\Omega, \Omega')$ is the spherical distance between the computation point Ω and integration point Ω' , and S denotes a spherical Stokes function relating the computation point Ω and integration point Ω' .

Next the geoidal height N is derived by applying Bruns formula (Bruns, 1878)

$$N = \frac{T(r_g, \Omega)}{\gamma_0}. \quad (2.8)$$

To determine the geoid, the boundary value, gravity anomaly must be evaluated on the geoid by applying the downward continuation from the topographical surface onto the geoid.

2.2 Construction of harmonic space

Due to the existence of topography and atmosphere, the most significant problem in solving the GBVP arises from the application of Stokes's formula which requires a harmonic space on and above the geoid.

One of the most common condensation techniques, Helmert's second condensation method (Heiskanen and Moritz, 1967: Sec. 3-7), was adopted in the Stokes-Helmert scheme to satisfy these requirements. In this procedure, the topographical masses (masses between the geoid and the topographical surface) are condensed along the plumb line onto the geoid surface as an infinitesimally thin layer with a surface density given as the product of the average column density of topographical masses with the height of the topographical surface.

The gravitational potential V generated by the Earth may be split into two parts:

$$V = V^g + V^t, \quad (2.9)$$

where V^g is the potential generated by the masses below the geoid and V^t is the potential generated by the topographical masses. Based on Helmert's condensation method, the decomposition of the topographical masses reads

$$V^t = V^{ct} + \delta V^t, \quad (2.10)$$

where V^{ct} is the potential of the masses condensed on the geoid and δV^t is the residual topographical potential.

An abstract space obtained after such a condensation is called Helmert space (H-space); consequently, a parameter with a superscript h indicates that it is defined in H-Space. Real space (R-space) is used to refer to the original space. According to the

techniques of Helmert's second condensation, the gravity field in H-space (called Helmert's gravity field) has the following characteristics:

- The isostatic equilibrium of the crust and the features of the gravity field are retained essentially intact, because the total mass of the Earth is preserved;
- Helmert's disturbing potential at the Earth's surface becomes smoother than the actual one; and
- Stokes' formula is applicable on the geoid in H-space without violating the required assumption of harmonicity.

2.3 Stokes-Helmert's scheme

The second Helmert condensation technique is applied in conjunction with Stokes' approach as the most straightforward method of solving the GBVP. The combination of these two main ideas is referred to as the "Stokes-Helmert scheme".

2.3.1 General introduction to methodology

The Stokes-Helmert scheme, which was initially constructed by Vaníček and Martinec (1994), uses the Helmert condensation idea for precise geoid determination and the theoretical properties of Stokes's solution in Helmert space. Over the last decade, it was revised and significantly improved at UNB in the so called Two-space scenario (involving the R-space and the H-space). More recently, it was followed by a development of the theory to accommodate the three-space scenario (Vaníček and Tenzer, 2003), additionally including the "No Topography" space (also referred to as

Bouguer space or NT-space) obtained by removing all of the topographical and atmospheric masses. The main idea behind it is that the disturbing potential is sought from a gravity anomaly in H-space, which leads to geoid determination based on Bruns formula. The objective of the scheme is to provide a theory accurate enough for calculating the geoidal height to one centimetre accuracy. The biggest obstacle to achieving this level of accuracy is in the mitigation of input data errors and improvement in area coverage.

The main principle of this scheme (shown in Figure 2.1), as originally conceived by Vaníček and Martinec (1994), can be characterized as follows:

- The construction and transformation of the gravity anomaly $\Delta g(r_t, \Omega)$ from R-space into NT-space by removing all of the topographical and atmospheric masses to obtain a harmonic space and gravity anomaly with comparatively smoother pattern;
- The downward continuation of the gravity anomaly from the earth's surface to the geoid in NT-space;
- Transformation of the gravity anomaly $\Delta g^{NT}(r_g, \Omega)$ referred to co-geoid from NT-space into H-space by the addition of the layer of condensed topographical and atmospheric masses onto the co-geoid surface, which is used in Stokes's integral to evaluate the disturbing potential $T^H(r_g, \Omega)$;
- Reformulation of the GBVP by decomposition of Helmert's gravity field into the low and high frequency field;

- Solution of Stokes formula for the high-frequency Helmert's gravity field by use of the modified spheroidal Stokes kernel and evaluation of the Helmert reference spheroid from a satellite geopotential model; and
- Transformation of the geoid from H-space back into R-space by adding the primary indirect topographical effect (PITE).

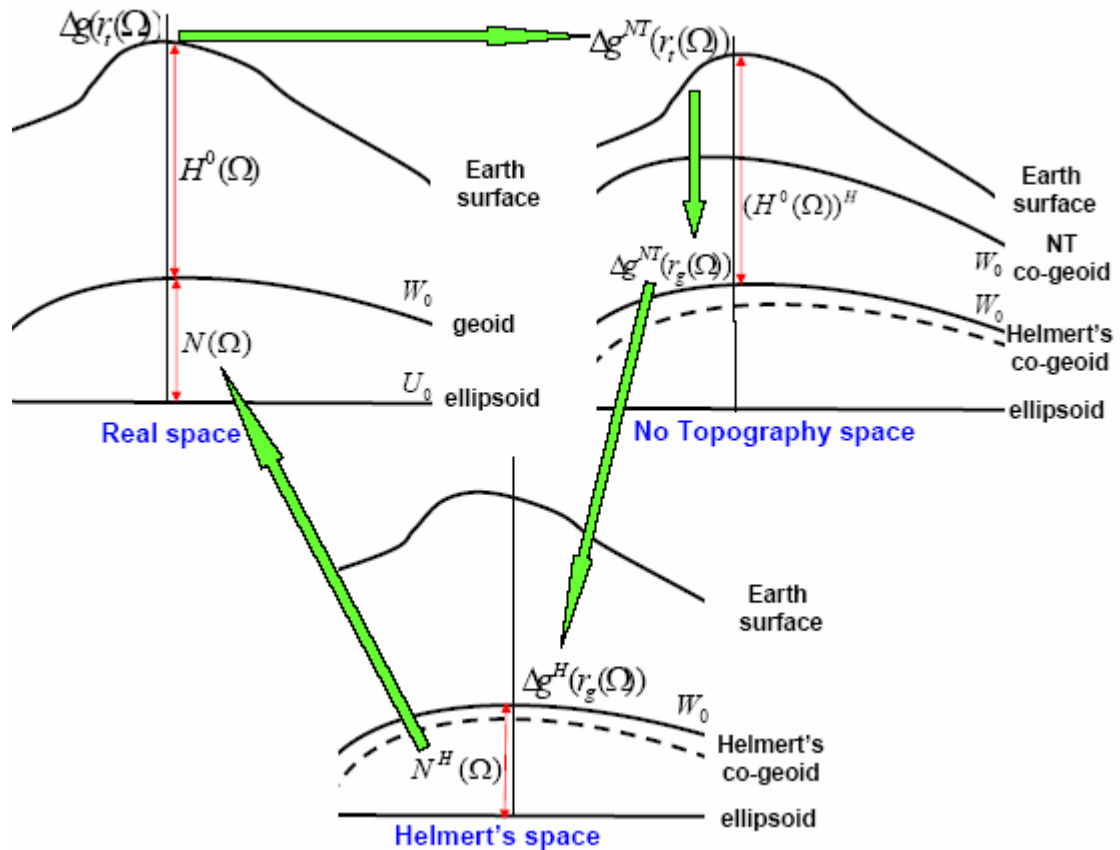


Figure 2.1: Stokes-Helmert's scheme

2.3.2 Evaluation of gravity anomaly on the Earth's surface

The gravity anomaly on the Earth's surface $\Delta g(r_i, \Omega)$ (Figure 2.2) (Vaniček *et al.*, 1999) is defined by

$$\Delta g(r_t, \Omega) = g(r_t, \Omega) - \gamma(r_o(\Omega) + H^N(\Omega)), \quad (2.11)$$

where r_t and r_o are the geocentric radius of a point on the Earth's surface and on the ellipsoid surface respectively; H^N is the normal height between telluroid (Molodenskij *et al.*, 1960) and ellipsoid surfaces; ζ is the quasigeoidal height, usually called the height anomaly; g is the observed gravity on the Earth's surface; and γ is the normal gravity referred to the telluroid.

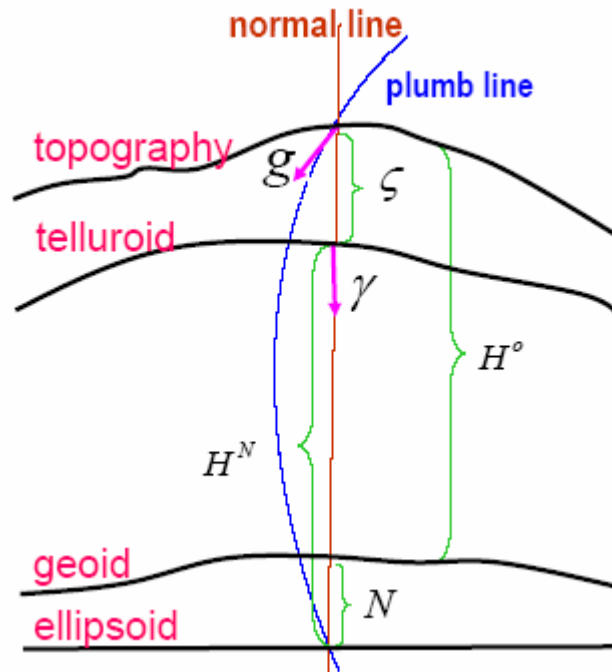


Figure 2.2: Parameters used in the definition of gravity anomalies

The difference between normal gravity $\gamma(r_t, \Omega)$, referred to the earth's surface, and the normal gravity $\gamma(r_o(\Omega) + H^N(\Omega))$ referred to the telluroid $r(\Omega) \cong r_o(\Omega) + H^N(\Omega)$ can be expressed as follows (Vaniček *et al.*, 1999):

$$\gamma(r_t, \Omega) - \gamma[r_o(\Omega) + H^N(\Omega)] \cong \gamma(r_t, \Omega) - \gamma_o(\Omega) - \left. \frac{\partial \gamma(r, \Omega)}{\partial n} \right|_{r=r_o} H^N(\Omega). \quad (2.12)$$

To evaluate the gravity anomaly $\Delta g(r_t, \Omega)$, the normal heights $H^N(\Omega)$ should be used. In practice, orthometric heights $H^o(\Omega)$ of gravity observations at the Earth's surface are used instead. The geoid-quasigeoid correction (Molodenskij *et al.*, 1960) should be applied which is approximately described as a linear function of the simple Bouguer gravity anomaly $\Delta g^{SB}(r, \Omega)$,

$$H^N(\Omega) - H^o(\Omega) \cong H^o(\Omega) \frac{\Delta g^{SB}(r_t, \Omega)}{\gamma_o(\Omega)}. \quad (2.13)$$

The simple Bouguer gravity anomaly $\Delta g^{SB}(r_t, \Omega)$ reads

$$\Delta g^{SB}(r_t, \Omega) = g(r_t, \Omega) - \gamma[r_o(\Omega) + H^o(\Omega)] - 2\pi G \rho_o H^o(\Omega), \quad (2.14)$$

where G is Newton's gravitational constant. The third term on the right-hand-side of Eqn. (2.14) stands for the gravitational attraction generated by the infinite Bouguer plate (of mean topographical density ρ_o and thickness equal to the orthometric height $H^o(\Omega)$ of the computation point).

Considering the formula for the free-air gravity anomaly $\Delta g^{FA}(r_t, \Omega)$ (Heiskanen and Moritz, 1967),

$$\begin{aligned} \Delta g^{FA}(r_t, \Omega) &= g(r_t, \Omega) - \gamma[r_o(\Omega) + H^o(\Omega)] \\ &= g(r_t, \Omega) - \gamma_o(\Omega) - \left. \frac{\partial \gamma(r, \Omega)}{\partial n} \right|_{r=r_o} H^o(\Omega) \end{aligned} \quad (2.15)$$

and combining Eqns. (2.11) and (2.15) together, the gravity anomaly $\Delta g(r_t, \Omega)$ becomes

$$\Delta g(r_t, \Omega) = \Delta g^{FA}(r_t, \Omega) - \frac{\Delta g^{SB}(r_t, \Omega)}{\gamma_o(\Omega)} \frac{\partial \gamma(r, \Omega)}{\partial n} \Big|_{r=r_o} H^o(\Omega). \quad (2.16)$$

The second term on the right-hand-side of Eqn. (2.16) is called the geoid-quasigeoid correction denoted by $\chi(r_t, \Omega)$, which can be simplified using the spherical approximation (Heiskanen and Moritz, 1967)

$$\chi(r_t, \Omega) \cong \frac{2}{R} H^o(\Omega) \Delta g^{SB}(r_t, \Omega). \quad (2.17)$$

The gravity anomaly $\Delta g(r_t, \Omega)$ subsequently takes the following form,

$$\Delta g(r_t, \Omega) = \Delta g^{FA}(r_t, \Omega) + \frac{2}{R} H^o(\Omega) \Delta g^{SB}(r_t, \Omega). \quad (2.18)$$

In respect to actual observed gravity data, the gravity anomaly $\Delta g(r_t, \Omega)$ may be regarded as an available ‘measurable’ quantity.

2.3.3 Definition of gravity disturbance and its relation to gravity anomaly

The gravity disturbance $\delta g(r, \Omega)$ is defined by the difference of the gravity $g(r, \Omega)$ and the corresponding normal gravity $\gamma(r, \Omega)$ (Vaniček *et al.*, 1999)

$$\delta g(r, \Omega) = g(r, \Omega) - \gamma(r, \Omega). \quad (2.19)$$

The relation between the gravity disturbance $\delta g(r, \Omega)$ and the disturbing potential $T(r, \Omega)$ in Eqn. (2.2) reads as follows (Vaniček *et al.*, 1999)

$$\delta g(r, \Omega) = -\frac{\partial T(r, \Omega)}{\partial r} + \varepsilon_{\delta g}(r, \Omega), \quad (2.20)$$

where $\varepsilon_{\delta g}(r, \Omega)$ is the ellipsoidal correction to the gravity disturbance defined by (Bomford, 1971)

$$\varepsilon_{\delta g}(r, \Omega) \cong g(r, \Omega) f \sin 2\varphi \xi(r, \Omega), \quad (2.21)$$

where a , b and $f = (a - b)/a$ denote the semi-axes and the first numerical flattening of the geocentric reference ellipsoid; φ is the geodetic latitude; and $\xi(r, \Omega)$ is the meridional component of the deflection of the vertical (Vaníček and Krakiwsky, 1986).

The gravity disturbance $\delta g(r_t, \Omega)$ is related to the gravity anomaly $\Delta g(r_t, \Omega)$ on the Earth's surface by the following formula (Vaníček *et al.*, 1999),

$$\Delta g(r_t, \Omega) = \delta g(r_t, \Omega) + \gamma(r_t, \Omega) - \gamma(r_o + H^N(\Omega)). \quad (2.22)$$

The difference between gravity anomaly and gravity disturbance accounts for the change in normal gravity referred to the earth's surface and referred to the telluroid, and is denoted by $\Gamma(r_t, \Omega)$. Using Bruns formula, $\Gamma(r_t, \Omega)$ may be rewritten to a sufficient accuracy (Vaníček and Martinec, 1994) as

$$\begin{aligned} \Gamma(r_t, \Omega) &= \gamma(r_t, \Omega) - \gamma(r_o + H^N(\Omega)) \\ &\cong \left. \frac{\partial \gamma(r, \Omega)}{\partial n} \right|_{r=r_t} \zeta(\Omega) = \left. \frac{\partial \gamma(r, \Omega)}{\partial n} \right|_{r=r_t} \frac{T(r_t, \Omega)}{\gamma(r_o + H^N(\Omega))}, \end{aligned} \quad (2.23)$$

where $\zeta(\Omega)$ is the height anomaly, and the derivative of normal gravity is taken with respect to the normal n to the reference ellipsoid. Applying the spherical approximation, Eqn. (2.21) becomes (Vaníček and Martinec, 1994)

$$\Gamma(r_t, \Omega) = -\frac{2}{R} T(r_t, \Omega) - \varepsilon_n(r_t, \Omega), \quad (2.24)$$

where $\varepsilon_n(r_t, \Omega)$ is the ellipsoidal correction for the spherical approximation,

$$\varepsilon_n(r_t, \Omega) \cong 2 \left[m + f \left(\cos 2\varphi - \frac{1}{3} \right) \right] \frac{T(r_t, \Omega)}{R}, \quad (2.25)$$

where $m = \omega^2 a^2 b / GM$ denotes Clairaut's constant (Heiskanen and Moritz, 1967), and $R = \sqrt[3]{a^2 b}$ is the mean radius of the Earth.

Based on Eqns. (2.20), (2.22) and (2.24), the following formula is produced (Vaniček *et al.*, 1999)

$$\Delta g(r_t, \Omega) = - \left. \frac{\partial T(r, \Omega)}{\partial r} \right|_{r=r_t} + \varepsilon_{\delta g}(r_t, \Omega) - \frac{2}{R} T(r_t, \Omega) - \varepsilon_n(r_t, \Omega), \quad (2.26)$$

which is the so-called fundamental gravimetric equation of physical geodesy. It is equally valid for the real, No Topography, and Helmert spaces.

2.3.4 Evaluation of NT gravity anomaly on the Earth's surface

The NT-space is produced after removal of the external (i.e., topographical and atmospheric) masses situated above the geoid and, consequently, causing considerable changes in the original gravity potential and the corresponding gravity field.

Considering in No Topography gravity potential space, the geoid-generated disturbing gravity potential $T^{\text{NT}}(r_t, \Omega)$ becomes harmonic above the geoid surface (Vaniček *et al.*, 2003),

$$T^{\text{NT}}(r_t, \Omega) = T(r_t, \Omega) - V^t(r_t, \Omega) - V^a(r_t, \Omega), \quad (2.27)$$

where $T(r_t, \Omega)$ denotes the disturbing gravity potential; $V^a(r, \Omega)$ represents gravitational potential generated by the atmospheric masses.

Combining the fundamental formula of physical geodesy (Eqn. (2.26)), the geoid-generated disturbing gravity potential $T^{\text{NT}}(r_t, \Omega)$ in Eqn. (2.27), and the definition of gravity anomaly Eqn. (2.16), the geoid-generated gravity anomaly $\Delta g^{\text{NT}}(r_t, \Omega)$ can be derived (Vaniček *et al.*, 2003)

$$\begin{aligned} \Delta g^{\text{NT}}(r_t(\Omega)) = & \Delta g^{\text{FA}}(r_t(\Omega)) + \frac{2}{R} H^o(\Omega) \Delta g^{\text{SB}}(r_t, \Omega) + \varepsilon_{\text{og}}(r_t(\Omega)) - \\ & - \varepsilon_n(r_t(\Omega)) + \left. \frac{\partial V^t(r, \Omega)}{\partial r} \right|_{r=r_t(\Omega)} + \left. \frac{\partial V^a(r, \Omega)}{\partial r} \right|_{r=r_t(\Omega)} + \\ & + \frac{2}{r_t(\Omega)} V^t(r_t(\Omega)) + \frac{2}{r_t(\Omega)} V^a(r_t(\Omega)), \end{aligned} \quad (2.28)$$

where the fifth term on the right-hand-side of Eqn. (2.28) represents the direct topographical effect on the gravitational attraction. The sixth term represents the direct atmospheric effect on gravitational attraction. The seventh and eighth terms stand for the secondary indirect topographical effect, and the secondary indirect atmospheric effect, respectively, on gravitational attraction. The negative radial derivative of the gravitational potential $V^t(r, \Omega)$ defines the gravitational attraction of the topographical masses (Martinec, 1993); the gravitational attraction of the atmospheric masses is given by the negative radial derivative of the gravitational potential $V^a(r, \Omega)$ of the atmospheric masses.

For the evaluation of the effect of atmospheric and topographical masses on the gravitational attraction, a numerical Newtonian integration using a spherical model over the whole earth was adopted. The effect of lateral variation of topographical density is also taken into consideration.

The gravitational potential $V'(r_i(\Omega))$ of the topographical masses is given by (Martinec and Vaníček, 1994b; Martinec, 1998)

$$\begin{aligned}
V'(r_i(\Omega)) &= 4\pi G\rho_o \frac{R^2}{r_i(\Omega)} H^o(\Omega) \left[1 + \frac{H^o(\Omega)}{R} + \frac{1}{3} \left(\frac{H^o(\Omega)}{R} \right)^2 \right] \\
&+ G\rho_o \iint_{\Omega' \in \Omega_o} \int_{R+H^o(\Omega)}^{R+H^o(\Omega')} l^{-1}[r_i(\Omega), \psi(\Omega, \Omega'), r'] r'^2 dr' d\Omega' \\
&+ G \iint_{\Omega' \in \Omega_o} \delta\rho(\Omega') \int_R^{R+H^o(\Omega')} l^{-1}[r_i(\Omega), \psi(\Omega, \Omega'), r'] r'^2 dr' d\Omega'.
\end{aligned} \tag{2.29}$$

The first term on the right-hand-side of Eqn. (2.31) is the gravitational potential of the spherical Bouguer shell (of mean topographical density ρ_o and thickness equal to the orthometric height $H^o(\Omega)$ of the computation point (r, Ω)) (Wichiencharoen, 1982). The second term represents the gravitational potential of the spherical roughness term, while the third term represents the effect of the anomalous topographical density $\delta\rho(\Omega)$ distribution on the gravitational potential.

The direct topographical effect on the gravitational attraction (Martinec and Vaníček, 1994a; Martinec, 1998) reads

$$\begin{aligned}
\frac{\partial V'(r, \Omega)}{\partial r} \Big|_{r=r_i(\Omega)} &= -4\pi G\rho_o \frac{R^2}{r_i^2(\Omega)} H^o(\Omega) \left[1 + \frac{H^o(\Omega)}{R} + \frac{1}{3} \left(\frac{H^o(\Omega)}{R} \right)^2 \right] + \\
&+ G\rho_o \iint_{\Omega' \in \Omega_o} \int_{R+H^o(\Omega)}^{R+H^o(\Omega')} \frac{\partial l^{-1}[r, \psi(\Omega, \Omega'), r']}{\partial r} \Big|_{r=r_i(\Omega)} r'^2 dr' d\Omega' + \\
&+ G \iint_{\Omega' \in \Omega_o} \delta\rho(\Omega') \int_R^{R+H^o(\Omega')} \frac{\partial l^{-1}[r, \psi(\Omega, \Omega'), r']}{\partial r} \Big|_{r=r_i(\Omega)} r'^2 dr' d\Omega'.
\end{aligned} \tag{2.30}$$

The first term on the right-hand-side of Eqn. (2.32) is the negative value of the gravitational attraction of the spherical Bouguer shell (Wichiencharoen, 1982). The second term stands for the negative value of the gravitational attraction of the spherical roughness term, i.e. (the spherical terrain correction) and the third term represents the negative value of the effect of the anomalous topographical density $\delta\rho(\Omega)$ distribution on the gravitational attraction.

The gravitational potential $V^a(r, \Omega)$ of the atmospheric masses is expressed by (Novak, 2000)

$$V^a(r_t, \Omega) = G \iint_{\Omega' \in \Omega_0} \int_{R+H^o(\Omega)}^{R+H_{lim}} \rho^a(r') l^{-1}[r_t(\Omega), \psi(\Omega, \Omega'), r'] r'^2 dr' d\Omega' + \quad (2.31)$$

$$+ G \iint_{\Omega' \in \Omega_0} \int_{R+H_{lim}}^{r_{lim}} \rho^a(r') l^{-1}[r_t(\Omega), \psi(\Omega, \Omega'), r'] r'^2 dr' d\Omega',$$

where $\rho^a(r)$ is the spherically distributed atmospheric density; r_{lim} is the upper limit of the atmosphere; and $l[r, \psi(\Omega, \Omega'), r']$ denotes the spatial distance between points (r, Ω) and (r', Ω') , where the latter point runs along the topography $R + H_{lim}$.

The direct atmospheric effect on gravitational attraction is given by the radial derivative of the gravitational potential of the atmospheric spherical roughness term (Novák, 2000)

$$\left. \frac{\partial V^a(r, \Omega)}{\partial r} \right|_{r=r_t(\Omega)} = G \iint_{\Omega' \in \Omega_0} \int_{R+H^o(\Omega)}^{R+H_{lim}} \rho^a(r') \left. \frac{\partial l^{-1}[r, \psi(\Omega, \Omega'), r']}{\partial r} \right|_{r=r_t(\Omega)} r'^2 dr' d\Omega'. \quad (2.32)$$

2.3.5 Downward continuation of gravity anomaly in NT-space

The gravity anomaly in the NT-space has a smooth character. To obtain boundary values on the geoid, the gravity anomalies are continued from the Earth's surface downward onto the geoid in the NT-space. This process is known as the downward continuation problem, and is described by the Poisson integral equation.

The Poisson integral is given by the following formula (Kellogg, 1929)

$$\Delta g^{\text{NT}}(r_i, \Omega) = \frac{R}{4\pi r_i(\Omega)} \iint_{\Omega' \in \Omega_0} K[r_i, \psi(\Omega, \Omega'), R] \Delta g^{\text{NT}}(R, \Omega') d\Omega', \quad (2.33)$$

where $K[r_i(\Omega), \psi(\Omega, \Omega'), R]$ is the spherical Poisson integral kernel (Sun and Vaníček, 1998); and $\Delta g^{\text{NT}}(R, \Omega')$ is the vector of the gravity anomalies referred to the co-geoid surface (approximated by the reference sphere).

Due to the harmonicity in NT-space, Poisson's solution to the Dirichlet problem of upward continuation can be employed. The integral can be seen as an operator that transforms the gravity anomalies on the geoid into the gravity anomaly at any point outside the geoid. When the gravity anomalies on the geoid are known, the gravity anomaly at any point outside the earth can, theoretically, be derived by the integral. In fact, however, the known gravity anomalies are at the Earth's surface and the unknown gravity anomalies are at the geoid. The problem we are confronted with is, in fact, an inverse problem.

2.3.6 Transformation of gravity anomaly on the geoid surface from NT-space into H-space

To minimize the change in gravity field caused by the removal of the external masses, the gravity anomalies $\Delta g^{\text{NT}}(\mathbf{R}, \Omega)$ referred to the geoid surface in spherical approximation are transformed from the No Topography space into the Helmert space.

Helmert's gravity anomaly $\Delta g^{\text{H}}(\mathbf{R}, \Omega)$ referred to the geoid surface is evaluated by adding the effect on the gravitational attraction of the condensed topographical and condensed atmospheric masses to the NT gravity anomaly $\Delta g^{\text{NT}}(\mathbf{R}, \Omega)$ (Vaníček *et al.*, 2003),

$$\Delta g^{\text{H}}(\mathbf{R}, \Omega) = \Delta g^{\text{NT}}(\mathbf{R}, \Omega) - \left. \frac{\partial V^{\text{ct}}(r, \Omega)}{\partial r} \right|_{r \rightarrow \mathbf{R}} - \frac{2}{\mathbf{R}} V^{\text{ct}}(\mathbf{R}, \Omega) - \left. \frac{\partial V^{\text{ca}}(r, \Omega)}{\partial r} \right|_{r \rightarrow \mathbf{R}} - \frac{2}{\mathbf{R}} V^{\text{ca}}(\mathbf{R}, \Omega). \quad (2.34)$$

The second term on the right-hand-side of Eqn. (2.34) represents the direct effect of the condensed topographical masses on the gravitational attraction. The third term represents the secondary indirect effect of the condensed topographical masses on the gravitational attraction. The fourth and fifth terms stand for the direct effect of the condensed atmospheric masses, and the secondary indirect effect of the condensed atmospheric masses, respectively, on the gravitational attraction.

The gravitational potential $V^{\text{ct}}(\mathbf{R}, \Omega)$ of the condensed topographical masses in Eqn. (2.34) is given by (Martinec, 1998),

$$\begin{aligned} V^{\text{ct}}(\mathbf{R}, \Omega) = & 4\pi G \rho_0 \mathbf{R} H^0(\Omega) \left[1 + \frac{H^0(\Omega)}{\mathbf{R}} + \frac{1}{3} \left(\frac{H^0(\Omega)}{\mathbf{R}} \right)^2 \right] \\ & + G \rho_0 \iint_{\Omega' \in \Omega_0} \frac{r^3(\Omega') - r^3(\Omega)}{3} l^{-1}[\mathbf{R}, \psi(\Omega, \Omega'), \mathbf{R}] d\Omega' \\ & + G \iint_{\Omega' \in \Omega_0} \delta\rho(\Omega') \frac{r^3(\Omega') - \mathbf{R}^3}{3} l^{-1}[\mathbf{R}, \psi(\Omega, \Omega'), \mathbf{R}] d\Omega', \end{aligned} \quad (2.35)$$

where the first term on the right-hand-side is the gravitational potential of the condensed spherical Bouguer shell; the second term stands for the gravitational potential of the spherical roughness term of the condensed topographical masses; and the third term represents the effect of the anomalous condensed topographical density distribution on the gravitational potential.

The direct effect of the condensed topographical masses on the gravitational attraction reads as (Vaníček *et al.*, 2003),

$$\begin{aligned}
& -\left. \frac{\partial V^{ca}(r, \Omega)}{\partial r} \right|_{r \rightarrow R^+} = 4\pi G \rho_o H^o(\Omega) \left[1 + \frac{H^o(\Omega)}{R} + \frac{1}{3} \left(\frac{H^o(\Omega)}{R} \right)^2 \right] \\
& - G \rho_o \iint_{\Omega' \in \Omega_o} \frac{r^3(\Omega') - r^3(\Omega)}{3} \frac{\partial l^{-1}[r, \psi(\Omega, \Omega'), R]}{\partial r} \Big|_{r \rightarrow R} d\Omega' \\
& - G \iint_{\Omega' \in \Omega_o} \delta\rho(\Omega') \frac{r^3(\Omega') - R^3}{3} \frac{\partial l^{-1}[r, \psi(\Omega, \Omega'), R]}{\partial r} \Big|_{r \rightarrow R} d\Omega',
\end{aligned} \tag{2.36}$$

where the first term on the right-hand-side is the gravitational attraction of the condensed spherical Bouguer shell; the second term stands for the gravitational attraction of the spherical roughness term of the condensed topographical masses; and the third term represents the effect of the anomalous condensed topographical density distribution on the gravitational attraction.

The gravitational potential $V^{ca}(R, \Omega)$ of the condensed atmospheric masses takes the following form (Novák, (2000)):

$$\begin{aligned}
V^{ca}(R, \Omega) = G \iint_{\Omega' \in \Omega_o} \int_{r'=R+H^o(\Omega')}^{R+H_{lim}} \rho^a(r') r'^2 dr' l^{-1}[R, \psi(\Omega, \Omega'), R] d\Omega' \\
+ G \iint_{\Omega' \in \Omega_o} \int_{r'=R+H_{lim}}^{r_{lim}} \rho^a(r') r'^2 dr' l^{-1}[R, \psi(\Omega, \Omega'), R] d\Omega'.
\end{aligned} \tag{2.37}$$

The direct effect of the condensed atmospheric masses on gravitational attraction can further be expressed as (Vaníček *et al.*, 2003),

$$\begin{aligned} -\left. \frac{\partial V^{ca}(r, \Omega)}{\partial r} \right|_{r \rightarrow R^+} &= -G \iint_{\Omega' \in \Omega_0} \int_{r'=R+H^o(\Omega')}^{R+H_{lim}} \rho^a(r') r'^2 dr' \left. \frac{\partial l^{-1}[r, \psi(\Omega, \Omega'), R]}{\partial r} \right|_{r \rightarrow R^+} d\Omega' \\ &- G \iint_{\Omega' \in \Omega_0} \int_{r'=R+H_{lim}}^{r_{lim}} \rho^a(r') r'^2 dr' \left. \frac{\partial l^{-1}[r, \psi(\Omega, \Omega'), R]}{\partial r} \right|_{r \rightarrow R^+} d\Omega'. \end{aligned} \quad (2.38)$$

The gravity anomaly on the geoid in H-space is then used as the boundary value in the spherical Stokes formulation.

2.3.7 Evaluation of the Helmert co-geoid

Helmert co-geoid $N^H(\Omega)$ can be evaluated by applying the Stokes integral formula (Eqn. (2.7)) (Stokes, 1849) and Bruns formula (Eqn. (2.8)) (Bruns, 1878) as follow (Heiskanen and Moritz, 1967)

$$N^H(\Omega) = \frac{R}{4\pi\gamma_o(\phi)} \iint_{\Omega' \in \Omega_0} \Delta g^H(R, \Omega') S(\psi(\Omega, \Omega')) d\Omega', \quad (2.39)$$

where $\Delta g^H(R, \Omega)$ is Helmert's gravity anomaly referred to the reference sphere of radius R . The homogenous and isotropic spherical Stokes function $S(\psi(\Omega, \Omega'))$, is given by (Heiskanen and Moritz, 1967) as

$$S(\psi(\Omega, \Omega')) = \sum_{n=2}^{\infty} \frac{2n+1}{n-1} P_n(\cos \psi(\Omega, \Omega')). \quad (2.4)$$

To implement the surface integration according to the Stokes integral in Eqn. (2.39), the gravity anomalies $\Delta g^H(R, \Omega)$ have to be known over the entire Earth. In practice, data on gravity anomalies over the entire Earth are not available. For this reason, the

summation over n in the Stokes function given by Eqn. (2.40) can be separated into low-degree and high-degree parts (Vaniček and Kleusberg, 1987),

$$S(\psi(\Omega, \Omega')) = \sum_{n=2}^{\ell} \frac{2n+1}{n-1} P_n(\cos \psi(\Omega, \Omega')) + \sum_{n=\ell+1}^{\infty} \frac{2n+1}{n-1} P_n(\cos \psi(\Omega, \Omega')). \quad (2.41)$$

Considering Eqn. (2.41), Eqn. (2.39) becomes (Martinec, 1993)

$$\begin{aligned} N^H(\Omega) &= N_{\text{ref}}^H(\Omega) + N_{n>\bar{n}}^H(\Omega) \\ &= \frac{R}{4\pi\gamma_o(\phi)} \iint_{\Omega' \in \Omega_o} \Delta g^H(R, \Omega') \sum_{n=2}^{\ell} \frac{2n+1}{n-1} P_n(\cos \psi(\Omega, \Omega')) d\Omega' \\ &\quad + \frac{R}{4\pi\gamma_o(\phi)} \iint_{\Omega' \in \Omega_o} \Delta g^H(R, \Omega') \sum_{n=\ell+1}^{\infty} \frac{2n+1}{n-1} P_n(\cos \psi(\Omega, \Omega')) d\Omega'. \end{aligned} \quad (2.42)$$

$N_{\text{ref}}^H(\Omega)$ and $N_{n>\ell}^H(\Omega)$ represent the reference co-geoid (spheroid) and the high-frequency (residual) co-geoid respectively (Novák *et al.*, 2001). This approach is based on determination of the reference spheroid from the satellite derived potential coefficients (Vaniček and Kleusberg, 1987). Surface integration by the Stokes integral formula is employed to compute the high-frequency part of the co-geoid solely from terrestrial gravity data.

2.3.7.1 Reference field and spheroid in Helmert's space

The reference spheroid is computed from a satellite-derived spherical harmonic global model. Due to the attenuation of the strength of the Earth's gravity, only the low-frequency component of the Earth's gravity field can reliably be detected in this way. Generally, a value of 20 is employed as the threshold value of degree ℓ . It is believed that the frequencies up to this degree can correctly be derived from satellite dynamics,

and do not have to be further improved by terrestrial gravity data in a combined global geopotential model.

The low-frequency gravity disturbing potential $T_{ref}^H(r_g, \Omega)$ can be estimated from the low-frequency spherical satellite-determined harmonic coefficients of a global geopotential model as follows (Vaniček and Featherstone, 1998)

$$T_{ref}^H(r_g, \Omega) = \frac{GM}{r_g} \sum_{n=2}^{\ell} \left(\frac{R}{r_g} \right)^n (\delta \bar{C}_{nm} \cos m\lambda + \bar{S}_{nm} \sin m\lambda) \bar{P}_{nm}(\cos \phi) \quad (2.43)$$

where $\delta \bar{C}_{nm}$ and \bar{S}_{nm} are the fully normalized potential coefficients of degree n and m order, which have been reduced by the even zonal harmonics of the reference ellipsoid, and $\bar{P}_{nm}(\cos \phi)$ are the fully normalized associated Legendre functions.

In similarity, Helmert's reference gravity anomaly $\Delta g_{ref}^H(r_g, \Omega)$ can be expressed as follows (Vaniček and Featherstone, 1998)

$$\Delta g_{ref}^H(r_g, \Omega) = \frac{GM}{r_g^2} \left(\frac{R}{r_g} \right)^n (n-1) \sum_m^n (\delta \bar{C}_{nm} \cos m\lambda + \bar{S}_{nm} \sin m\lambda) \times \bar{P}_{nm}(\cos \phi) . \quad (2.44)$$

The reference spheroid is given by the reference co-geoidal heights $N_{ref}^H(\Omega)$. Applying Bruns formula, the reference co-geoidal height $N_{ref}^H(\Omega)$ reads

$$N_{ref}^H(\Omega) = \frac{T_{ref}^H(r_g, \Omega)}{\gamma_o(\phi)} . \quad (2.45)$$

2.3.7.2 GBVP in Helmert's space

The GBVP is used for the determination of the high-frequency co-geoid that is residual to the reference spheroid which has been described in detail in section 2.1. At this point,

two terms should be further explained: (i) boundary values and (ii) the modified spheroidal Stokes integral.

The boundary value, given as the residual gravity anomaly at the geoid, is defined (Vaníček and Kleusberg, 1987) as

$$\Delta g_{n>l}^H(r_g, \Omega) = \Delta g(r_g, \Omega) - \Delta g_{ref}^H(r_g, \Omega). \quad (2.46)$$

In practical terms, the integration domain Ω_0 can be divided into a spherical cap called the near-zone integration sub-domain Ω_{ψ_0} (defined on the interval $\psi \in \langle 0, \psi_0 \rangle$) (Vaníček and Kleusberg, 1987) and the far-zone integration sub-domain $\Omega_0 - \Omega_{\psi_0}$ (on the interval $\psi \in \langle \psi_0, \pi \rangle$). Based on Eqn. (2.39), the near zone contribution to the residual co-geoid is calculated. The contribution of the gravity data outside the cap is referred to as the truncation error, and is minimized by the modified kernel. It is estimated from a global gravity field model (of a higher degree and order than the reference satellite-derived field).

Thus the Helmert residual co-geoid is evaluated by the Stokes integral in the Helmert gravity space using the residual gravity anomalies. The Helmert co-geoid is then obtained as a sum of the Helmert reference spheroid and residual co-geoidal heights.

2.3.8 Primary indirect effect

Now the effect of the difference between the gravitational potential of actual topographical masses and the gravitational potential of the condensed masses referred to the Helmert geoid should be taken into account; this quantity is usually called the

Primary Indirect Effect on potential. To transform the geoid from H-space into real space, the primary indirect topographical and atmospheric effects on the geoidal heights are evaluated.

Helmert's disturbing gravity potential referred to the geoid surface is defined as (Vaniček *et al.*, 2003)

$$T^H(\mathbf{R}, \Omega) = T(\mathbf{R}, \Omega) - \delta V^t(\mathbf{R}, \Omega) - \delta V^a(\mathbf{R}, \Omega), \quad (2.49)$$

where $\delta V^t(\mathbf{R}, \Omega)$ is the residual gravitational potential of the topographical masses; and $\delta V^a(\mathbf{R}, \Omega)$ is the residual gravitational potential of the atmospheric masses.

The residual gravitational potential of the topographical masses $\delta V^t(\mathbf{R}, \Omega)$ may be rewritten according to Eqn. (2.10) as

$$\delta V^t(\mathbf{R}, \Omega) = V^t(\mathbf{R}, \Omega) - V^{ct}(\mathbf{R}, \Omega). \quad (2.50)$$

Similar to the treatment of the residual gravitational potential of the topographical masses, the residual gravitational potential of the atmospheric masses $\delta V^a(\mathbf{R}, \Omega)$ is given by the difference of the gravitational potential $V^a(\mathbf{R}, \Omega)$ of the atmospheric masses and the gravitational potential $V^{ca}(\mathbf{R}, \Omega)$ of the condensed atmospheric masses (Vaniček *et al.*, 1999):

$$\delta V^a(\mathbf{R}, \Omega) = V^a(\mathbf{R}, \Omega) - V^{ca}(\mathbf{R}, \Omega). \quad (2.51)$$

The primary indirect effect on geoidal heights which shows the relation between the geoidal height $N(\Omega)$ and the co-geoidal height $N^H(\Omega)$ is defined (Martinec, 1993) as

$$\begin{aligned} \delta N(\Omega) &= N(\Omega) - N^H(\Omega) = \frac{T(\mathbf{R}, \Omega)}{\gamma_o(\phi)} - \frac{T^H(\mathbf{R}, \Omega)}{\gamma_o(\phi)} \\ &= \frac{\delta V^t(\mathbf{R}, \Omega)}{\gamma_o(\phi)} + \frac{\delta V^a(\mathbf{R}, \Omega)}{\gamma_o(\phi)}. \end{aligned} \quad (2.52)$$

The first term on the right-hand-side of Eqn. (2.52) is the primary indirect topographical effect on the geoidal heights; the second term represents the primary indirect atmospheric effect on geoidal heights.

2.3.8.1 Primary indirect topographical effect

The gravitational potential $V^t(\mathbf{R}, \Omega)$ of the topographical masses referred to the geoid surface is given by (Martinec, 1993) as

$$\begin{aligned}
V^t(\mathbf{R}, \Omega) &= 4\pi G \rho_o H^o(\Omega) \left[R + \frac{1}{2} H^o(\Omega) \right] \\
&+ G \rho_o \iint_{\Omega' \in \Omega_o} \int_{r'=R+H^o(\Omega)}^{R+H^o(\Omega')} l^{-1}[\mathbf{R}, \psi(\Omega, \Omega'), r'] r'^2 dr' d\Omega' \\
&+ G \iint_{\Omega' \in \Omega_o} \delta\rho(\Omega') \int_{r'=R}^{R+H^o(\Omega')} l^{-1}[\mathbf{R}, \psi(\Omega, \Omega'), r'] r'^2 dr' d\Omega'.
\end{aligned} \tag{2.53}$$

The gravitational potential $V^{ct}(\mathbf{R}, \Omega)$ of the condensed topographical masses referred to the geoid surface reads (Martinec, 1993)

$$\begin{aligned}
V^{ct}(\mathbf{R}, \Omega) &= 4\pi G \rho_o \frac{r_t^3(\Omega) - R^3}{3R} + \\
&+ G \rho_o \iint_{\Omega' \in \Omega_o} \frac{r_t^3(\Omega') - r_t^3(\Omega)}{3} l^{-1}[\mathbf{R}, \psi(\Omega, \Omega'), R] d\Omega' \\
&+ G \iint_{\Omega' \in \Omega_o} \delta\rho(\Omega') \frac{r_t^3(\Omega') - R^3}{3} l^{-1}[\mathbf{R}, \psi(\Omega, \Omega'), R] d\Omega'.
\end{aligned} \tag{2.54}$$

Eqns. (2.53), (2.54) and (2.50) are combined to yield the primary indirect topographical effect on the geoidal heights, which reads (Martinec, 1993)

$$\begin{aligned}
\frac{\delta V'(\mathbf{R}, \Omega)}{\gamma_o(\phi)} &= -4\pi G \rho_o \frac{[H^o(\Omega)]^2}{\gamma_o(\phi)} \left[\frac{1}{2} + \frac{H^o(\Omega)}{3R} \right] \\
&+ \frac{G}{\gamma_o(\phi)} \rho_o \iint_{\Omega' \in \Omega_o} \int_{r'=R+H^o(\Omega)}^{R+H^o(\Omega')} l^{-1}[\mathbf{R}, \psi(\Omega, \Omega'), r'] r'^2 dr' d\Omega' \\
&- \frac{G}{\gamma_o(\phi)} \rho_o \iint_{\Omega' \in \Omega_o} \frac{r_t^3(\Omega') - r_t^3(\Omega)}{3} l^{-1}[\mathbf{R}, \psi(\Omega, \Omega'), \mathbf{R}] d\Omega' \\
&+ \frac{G}{\gamma_o(\phi)} \iint_{\Omega' \in \Omega_o} \delta\rho(\Omega') \int_{r'=R}^{R+H^o(\Omega')} l^{-1}[\mathbf{R}, \psi(\Omega, \Omega'), r'] r'^2 dr' d\Omega' \\
&- \frac{G}{\gamma_o(\phi)} \iint_{\Omega' \in \Omega_o} \delta\rho(\Omega') \frac{r_t^3(\Omega') - R^3}{3} l^{-1}[\mathbf{R}, \psi(\Omega, \Omega'), \mathbf{R}] d\Omega'.
\end{aligned} \tag{2.55}$$

2.3.8.2 Primary indirect atmospheric effect

The gravitational potential $V^a(\mathbf{R}, \Omega)$ of the atmospheric masses referred to the geoid surface takes the following form (Novák, 2000),

$$\begin{aligned}
V^a(\mathbf{R}, \Omega) &= G \iint_{\Omega' \in \Omega_o} \int_{r'=R+H^o(\Omega')}^{R+H_{\text{lim}}} \rho^a(r') l^{-1}[\mathbf{R}, \psi(\Omega, \Omega'), r'] r'^2 dr' d\Omega' \\
&+ G \iint_{\Omega' \in \Omega_o} \int_{r'=R+H_{\text{lim}}}^{r_{\text{lim}}} \rho^a(r') l^{-1}[\mathbf{R}, \psi(\Omega, \Omega'), r'] r'^2 dr' d\Omega'.
\end{aligned} \tag{2.56}$$

The gravitational potential $V^{ca}(\mathbf{R}, \Omega)$ of the condensed atmospheric masses referred to the geoid surface reads (Novák, 2000))

$$\begin{aligned}
V^{ca}(\mathbf{R}, \Omega) &= G \iint_{\Omega' \in \Omega_o} \int_{r'=R+H^o(\Omega')}^{R+H_{\text{lim}}} \rho^a(r') r'^2 dr' l^{-1}[\mathbf{R}, \psi(\Omega, \Omega'), \mathbf{R}] d\Omega' \\
&+ G \iint_{\Omega' \in \Omega_o} \int_{r'=R+H_{\text{lim}}}^{r_{\text{lim}}} \rho^a(r') r'^2 dr' l^{-1}[\mathbf{R}, \psi(\Omega, \Omega'), \mathbf{R}] d\Omega'.
\end{aligned} \tag{2.57}$$

Considering Eqns. (2.54), (2.55) and (2.49) together, the primary indirect atmospheric effect on the geoidal heights is given as

$$\begin{aligned}
\frac{\delta V^a(\mathbf{R}, \Omega)}{\gamma_o(\phi)} &= \frac{G}{\gamma_o(\phi)} \iint_{\Omega' \in \Omega_o} \int_{r'=R+H^o(\Omega')}^{R+H_{lim}} \rho^a(r') \left(l^{-1}[\mathbf{R}, \psi(\Omega, \Omega'), r'] - l^{-1}[\mathbf{R}, \psi(\Omega, \Omega'), \mathbf{R}] \right) r'^2 dr' d\Omega' \\
&+ \frac{G}{\gamma_o(\phi)} \iint_{\Omega' \in \Omega_o} \int_{r'=R+H_{lim}}^{r_{lim}} \rho^a(r') \left(l^{-1}[\mathbf{R}, \psi(\Omega, \Omega'), r'] - l^{-1}[\mathbf{R}, \psi(\Omega, \Omega'), \mathbf{R}] \right) r'^2 dr' d\Omega'.
\end{aligned}
\tag{2.58}$$

2.3.9 Summary of the Stokes-Helmert's scheme

According to the above descriptions, the Stokes-Helmert's scheme can be summarized (see Figure 2.3) as follows:

- By the ellipsoidal corrections and the geoid-quasigeoid correction, the free air gravity anomaly is transformed into the gravity anomaly on the Earth's surface in R-space;
- The gravity anomaly on the Earth's surface in NT-space can be evaluated by adding the direct topographical and atmospheric effects on gravity (DTE and DAE), and the second indirect topographical and atmospheric effect on gravity (SITE-NT and SIAE-NT);
- The NT gravity anomaly is downward continued from the Earth's surface onto the geoid;
- Considering the direct condensed topographical and atmospheric effects on gravity (DCTE and DAE-H), the second indirect condensed topographical and atmospheric effect on gravity (SITE-H and SIAE-H), both taken on the geoid, the gravity anomaly referred to the geoid is transformed from NT-space into H-space;

- The reference gravity anomaly and the reference spheroid are evaluated. Then the residual gravity anomaly and the residual co-geoid are calculated by Stokes integral;
- The reference spheroid and the residual co-geoid are combined with PITE to arrive at the final geoid.

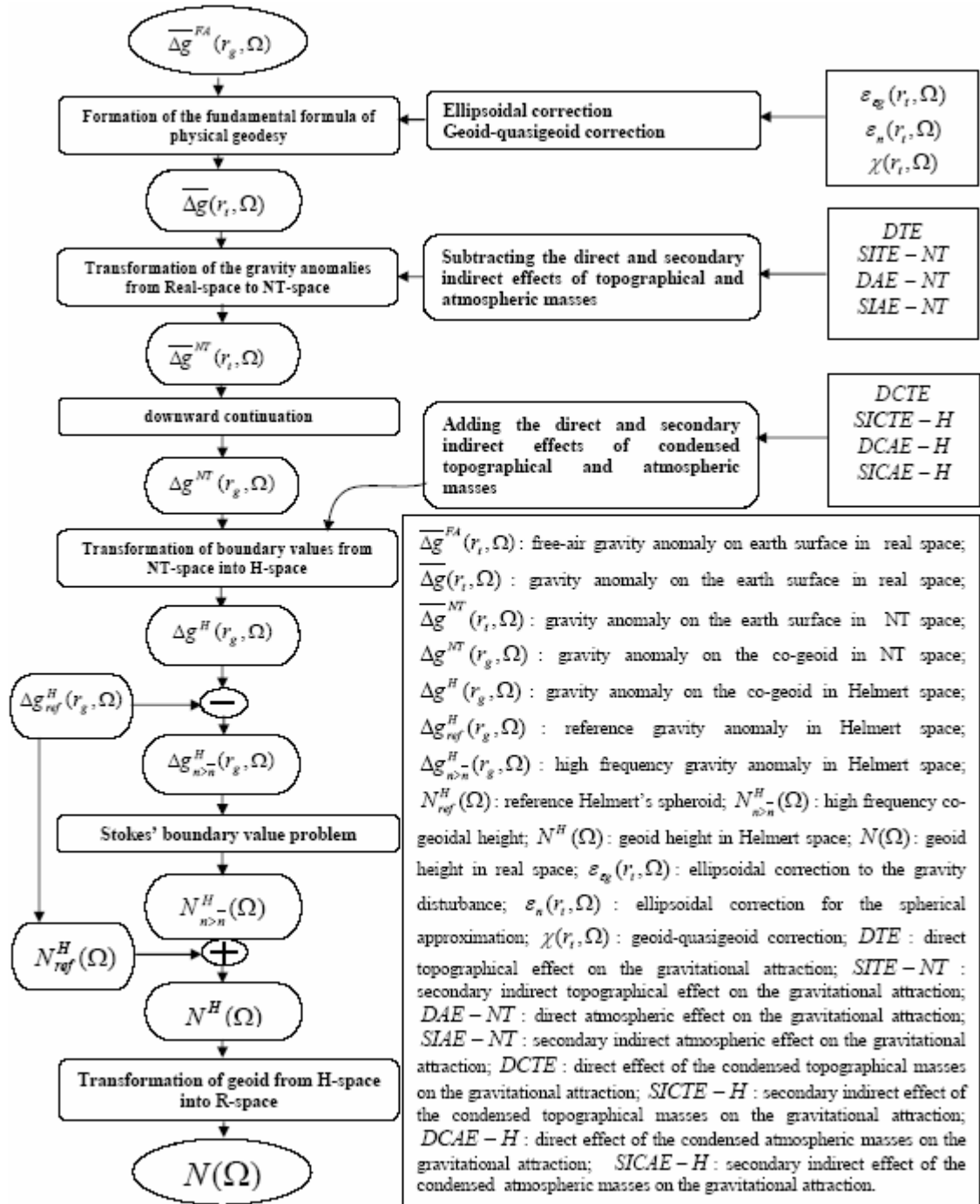


Figure 2.3: Flowchart of the Stokes-Helmert's scheme

Chapter3

The Precise Geoid Determination

Software Package

3.1 Introduction to the software package

The development of the Stokes-Helmert theory of determination of the gravimetric geoid in a three-space scenario and its refinement to achieve theoretical one-centimeter accuracy enabled the conception of a corresponding suite of programs called the *UNB Precise Geoid Determination Package* (PGDP); developed over the past decade at UNB, PGDP's main function is the numerical realization of a precise geoid model. Its development targets the objective of calculating geoidal height with one centimeter accuracy, providing that the accuracies and spacing of the required input data and their area coverage meet acceptable standards. Associated documentation considered as the reference manual, is comprised of three parts: (i) Manual I: the theoretical description of the Stokes-Helmert method of geoid determination; (ii) Manual II: the reference user's guide shows the function of each particular program for computation of the geoid; and (iii) Manual III: documentation of auxiliary programs enabling data manipulation and format transformation.

To calculate geoidal heights over Canada, the required data include: available terrestrial gravity data; digital elevation model; and other auxiliary data, such as digital topographical density model, global elevation model, and global potential model. Additionally, GPS/Leveling data are used as a standard to evaluate the accuracy of the final geoid model.

A flowchart of PGDP operations (see Figure 3.1) shows each computational step, related programs and required input files. Operations required to evaluate each gravity anomaly and the final geoid are shown in the sequence of boxes in the left-hand side of Figure 3.1. Associated programs are shown in the middle and on the right-hand side, along with the required input files. Table 3.1 introduces each program's function.

From the flowchart and the table, the computational procedure can be readily summarized as follows:

- For the transformation from the mean free air gravity anomaly $\overline{\Delta g}^{FA}(r_i, \Omega)$ into the mean gravity anomaly in NT-space $\overline{\Delta g}^{NT}(r_i, \Omega)$, the ellipsoidal corrections and the geoid-quasigeoid correction, the near zone and far zone terrain roughness effects on gravity (STC-near-zone and STC-far-zone), the anomalous topographical density effect on gravity (DTE-density), SITE-NT, SIAE-NT, and DAE-NT are taken into account. These are calculated by programs `Ellipsoidal_cor`, `Geoid_quasigeoid_cor`, `STC_near_zone` and `STC_far_zone`, `DTE_density`, `SITE_NTspace` and `SIAE_NTspace`, and `DAE_NTspace` respectively.

- After running program Downward_continuation program, the gravity anomaly referred to geoid in NT-space $\Delta g^{NT}(r_g, \Omega)$ is obtained from the mean gravity anomaly in NT-space $\overline{\Delta g}^{NT}(r_g, \Omega)$.
- Then the gravity anomaly referred to geoid in NT-space $\Delta g^{NT}(r_g, \Omega)$ is transformed into the gravity anomaly referred to the geoid in H-space $\Delta g^H(r_g, \Omega)$, by considering the near zone and far zone terrain roughness effects on gravity (SCTC-near-zone and SCTC-far-zone), the anomalous topographical density effect on gravity (DCTE-density), SICTE-H, SICAE-H, and DCAE-H. These are calculated by programs SCTC_near_zone and SCTC_far_zone, DCTE_density, SITE_Hspace and SIAE_Hspace, and DAE_Hspace respectively.
- The residual gravity anomaly $\Delta g_{n>\ell}^H(r_g, \Omega)$ is obtained from the Helmert gravity anomaly $\Delta g^H(r_g, \Omega)$ through subtracting the Helmert's reference gravity anomaly $\Delta g_{ref}^H(r_g, \Omega)$, calculated by program Reference_field.
- By employing Stokes_integral, the residual spheroid $N_{n>\ell}^H(r_g, \Omega)$ is arrived at. The addition of the reference spheroid, $N_{ref}^H(r_g, \Omega)$ calculated by program Reference_spheroid, results in Helmert co-geoid.
- Finally, considering the primary indirect topographical effect on geoid calculated using programs PITE and PIAE, the digital geoid is realized.

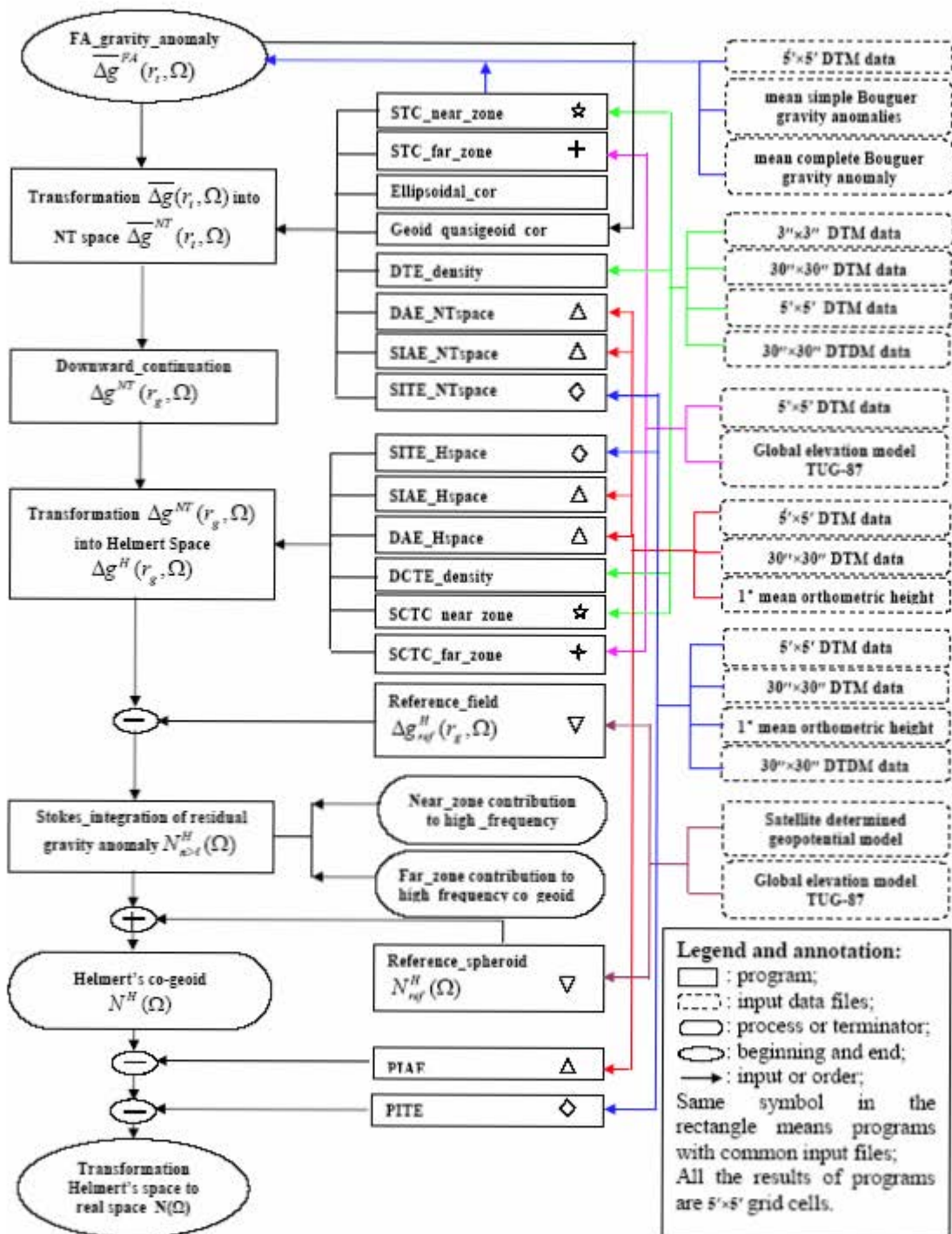


Figure 3.1: Flowchart of the UNB *Precise Geoid Determination Package* (PGDP)

PROGRAM	FUNCTION
FA_gravity_anomaly	computation of mean values of free-air gravity anomalies
STC_near_zone	computation of point values of the near-zone contribution to the gravitational attraction of the spherical terrain roughness term referred to the Earth's surface
STC_far_zone	computation of point values of the far-zone contribution to the gravitational attraction of the spherical terrain roughness term referred to the Earth's surface
Ellipsoidal_cor	computation of mean values of the ellipsoidal corrections to the boundary value problem
Geoid_quasigeoid_cor	computation of mean values of the geoid-quasigeoid correction to the boundary value problem
DTE_density	computation of mean or point values of the direct effect of the anomalous topographical density distribution referred to the Earth's surface
DAE_NTspace	computation of point values of the direct effect of atmospheric masses on the gravitational attraction referred to the Earth's surface
SIAE_NTspace	computation of point values of the secondary indirect effect of atmospheric masses on the gravitational attraction referred to the Earth's surface
SITE_NTspace	computation of point values of the secondary indirect effect of topographical masses on the gravitational attraction referred to the Earth's surface
NT_anomaly	computation of mean values of the "No Topography" gravity anomalies referred to the Earth's surface
Downward_continuation	downward continuation of the mean "No Topography" gravity anomalies from the Earth's surface onto the co-geoid
SITE_Hspace	computation of point values of the secondary indirect effect of condensed topographical masses referred to the geoid surface
SIAE_Hspace	computation of point values of the secondary indirect effect of condensed atmospheric masses on the gravitational attraction referred to the geoid surface
DAE_Hspace	computation of point values of the direct effect of condensed atmospheric masses on the gravitational attraction referred to the geoid surface
DCTE_density	computation of point values of the direct effect of the anomalous condensed topographical density distribution referred to the geoid surface
SCTC_near_zone	computation of point values of the near-zone contribution to the spherical condensed terrain roughness term referred to the geoid surface
SCTC_far_zone	computation of point values of the far-zone contribution to the spherical condensed terrain roughness term referred to the geoid surface
Helmert_anomaly	computation of point values of Helmert gravity anomalies referred to the co-geoid
Reference_field	computation of Helmert's reference gravity anomalies referred to the co-geoid
Stokes_integral	computation of Helmert residual co-geoid
Reference_spheroid	computation of Helmert reference spheroid
PIAE	computation of point values of the primary indirect atmospheric effect on the geoidal heights
PITE	computation of point values of the primary indirect topographical effect on the geoidal heights

Table 3.1: Function of each program in the UNB Precise Geoid Determination Package

3.2 Specification of input files

In the absence of a statements to the contrary, all original input files have been provided by Geodetic Survey Division (GSD) of Natural Resources Canada. At present, heights including local digital terrain model and global elevation model, gravity data, topographical density data and other are used as standard input data.

3.2.1 Heights

Two Digital Terrain Models (DTMs) are used for numerical computation: one is the detailed DTM; the other is the mean DTM with a relatively smooth character, obtained from the detailed DTM. The global elevation model TUG87 (Wieser, 1987) is also employed, which contains the spherical harmonic representation of the global topography to the degree and order of 180. The coefficients for the second power of global topography up to degree and order 90 are also available for evaluation of the effects due to the far-zone topographical masses.

3.2.1.1 Detailed Digital Terrain Model (DTM)

The Canadian Digital Elevation Data (CDED) used as the detailed DTM are often saved as binary files using “byn” as extension of the file name. Each file contains two sections: (i) an 80-byte header; and (ii) the actual data. The data are sorted in rows starting from north to south, and each row is sorted from west to east. All data are stored as short or long integers. The size of the file is 80 bytes plus the number of rows,

multiplied by the number of columns times the size of data in bytes. Elevations are stored as a short integer with a multiplication factor of 1. CDED files are of different resolutions determined photogrammetrically according to the latitude. One file of the detailed DTM below latitude 68° north contains the elevation within an area of 1° by 1° with a resolution of 3" by 3". Between latitude 68° and 80° north it covers an area of 1° by 2° with a resolution of 3" by 6" while, for areas above latitude 80° north, the coverage area is 1° by 4° with a resolution of 3" by 12". In addition, detailed American-sourced DTM data are also used. They are referred to as STRM, and come in binary format with a different header from CDED.

In this solution of the Stokes-Helmert scheme, the detailed DTM covers the Canadian landmass. It is required the evaluation of the effects on gravity of the following factors associated with topography: STC-near-zone, SCTC-near-zone, DTE-density and DCTE-density. The corresponding programs in the PGDP require detailed DTM's formatted, regardless of latitude, in a 3" by 3" geographical grid.

3.2.1.2 Mean Digital Terrain Models

Mean DTM files are also stored as integers in binary files sorted by rows from north to south, and each row sorted from west to east. In practical terms, the North American Digital Elevation Model data with a recommended resolution of 30" by 30", and derived from GTOPO30 (conventionally denoted herein as DEM_NA_30s.byn) is established as the original data set of mean orthometric heights. It can be used to generate mean orthometric height file with resolution 30" by 30" (DEM_30s) and with resolution 5' by 5' (DEM_5m). Figure 3.2 shows the 5' mean orthometric heights covering Canada.

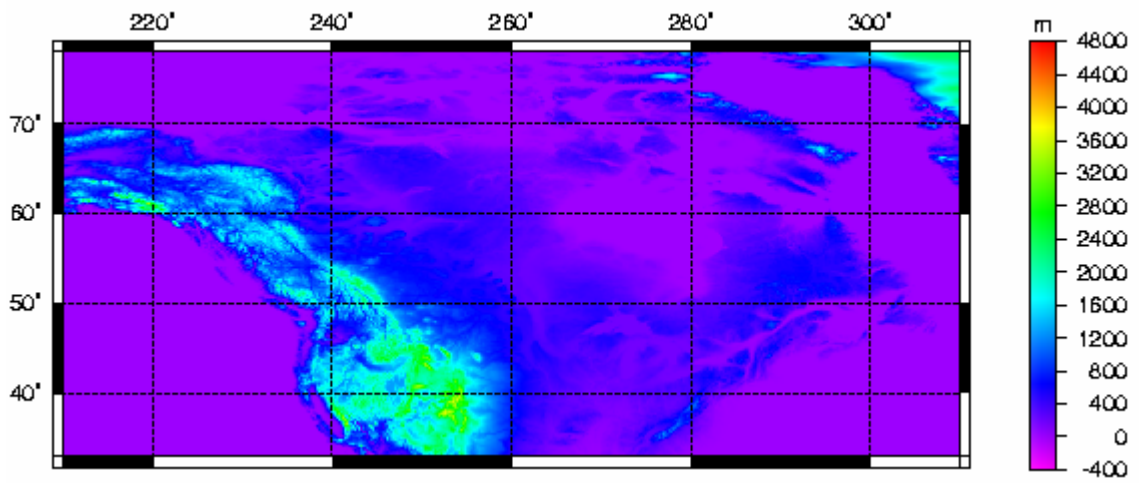


Figure 3.2: Mean DTM with 5' by 5' resolution (m)

3.2.2 Gravity data

In the absence of a homogeneous and properly densified network of point gravity anomalies (with known orthometric heights), terrestrial gravity data are available in mean form on 5' by 5' grid for both Simple and of Complete Bouguer gravity anomalies derived from point values, stored in an ASCII data file in a following format:

Latitude (deg), longitude (deg), gravity anomaly (mGal),
representing a series of data sets. In the meantime, however, averaging the “observed” point anomalies in a geographic cell suppresses the observational errors in data collection and smoothes the gravity field. The degree of smoothness depends on the areal extent of the cell. Practically, in geoid determination, the mean anomalies associated with smaller cells eliminate only the local surface irregularities of the gravity field without affecting the geoid solution.

One of global geopotential models, GRIM4-S4 (Schwintzer et al., 1997) is adopted to evaluate the reference gravity anomaly and reference geoidal height. Satellite gravity data are given in the form of potential coefficients.

3.2.3 Topographical density data (laterally varying)

The Digital Topographical Density Model (DTDM) becomes necessary if the desired level of accuracy of the geoid model is centimeter or less because, as Martinec (1993) has demonstrated theoretically, the lateral density variation of topographical masses may introduce errors into the geoid starting at the decimeter level. In the present work,

topographical mass density variation effects on the geoid are computed with the use of programs DTE_density and DCTE_density within the PGDP (see Table 3.1). Geoid computation in the Canadian Rocky Mountains, which have the largest relief and density variations in Canada, are the most severely affected by the topographical density effect.

The laterally varying DTDM is stored in a binary file. The topographical density file which used in geoid determination in Canada is called “TopoDensity_CDN_30s.byn” with a 30” by 30” resolution covering the region bounded by north latitudes 30° and 84°, and by east longitudes 215° and 349°. It should be transformed into an ASCII file before being used. The representative density value for each geological unit is taken as the mean value of the density range. In addition, the constant topographical density of 2670kg/m³ is adopted as the actual value over US territory and sea regions in this file.

3.2.4 Other standard input data

Normal gravity field parameters are employed, according to the Reference Ellipsoid GRS-80.

The geopotential model EGM96 (Lemoine et al., 1996) is adopted in computations, which contains fully-normalized, unitless spherical harmonic coefficients completed from degree 2 order 0 to degree and order 360, and their corresponding standard deviations. The EGM96 model represents the latest development in high degree geopotential models which combine satellite data and the available surface and marine gravity data. The long wavelength effect of the far-zone contribution to the geoid surface is generated from this model.

3.3 Problems encountered during data processing

3.3.1 Production of mean DTM files

As mentioned in Section 3.2.1.2, the data set DEM_NA_30s.byn covers the region of North latitude 20° to North latitude 83°, and East longitude 191° to East longitude 350°, stored in binary format.

Firstly by using the program “H_read.c”, see Appendix. (A.1), ASCII grid files can be obtained over the desired region. Such a file is sorted by rows from north to south, with each row sorted from west to east. Mean orthometric heights are stored as integers.

In the Linux operating system, the command format to run “H_read.c” should be,

```
./H_read.e <H_read.job> H.mean
```

where H_read.e is the result of the compilation of program “H_read.c”; “H.mean” is the name of the output file, which can be defined by the user; and file <H_read.job> contains data in the following format:

```
83 0 0  
-150 0 0  
50  
100  
10  
10
```

where the first line number represents the latitude of the most northwest point of the area; the second line represents the longitude of the most northwest point of the area; the third line represents the amplitude of the latitude in degree; the fourth line represents

the amplitude of the longitude in degree; the sixth and the seventh lines represent grid step of latitude and of longitude, respectively. Referring to grid step, 10 or 1 represents the result resolution is 5' or 30", which is designed in program.

The first line of the output file, "H.mean" is a header in the following format:

"Minimum Latitude; maximum latitude; minimum longitude; maximum longitude; step in latitude; step in longitude."

All numbers in the header are in degrees separated by a space and orthometric height data begin from the second line; e.g.,

```
33.00417 82.99583 210.00417 309.99583 0.008333333 0.008333333
231 278 211 367 532 231 782 667 321 289 882 701 829 872 291 211
```

The next step requires running the program "H_grid.c", see Appendix. (A.2). Its option file contains the input, and output file names and the corresponding paths, for example:

```
/data/Computation_Results/DEM/H.mean
/data/Computation_Results/DEM/H_1_1.mean
```

Each latitude, longitude and associated orthometric height are then saved into an output file in a form such as:

```
82.99583 210.00417 231
82.99583 210.01250 278
82.99583 210.02064 211
82.99583 210.02917 ...
```

The mean DTM files are generated better in the order from north to south and from west to east to suit the requirement of programs within PGDP.

3.3.2 Generation of input files for PGDP component programs DAE_NTspace, DAE_Hspace, SIAE_NTspace, SIAE_Hspace and PIAE

As stated in Manual Part II, these programs require four types of input files: “Inner_zone.dat”, “Near_zone.dat”, “Computation_point.dat” and “H-1deg_world.dat”. “Near_zone.dat” and “Computation_point.dat” contain 5’ by 5’ resolution mean orthometric height data. “Inner_zone.dat” contains 30” by 30” resolution mean orthometric height data, and “H-1deg_world.dat” denotes the default set of global orthometric height data with a 1° by 1° resolution.

3.3.2.1 Mean orthometric heights with 5’ by 5’ resolution (DEM_5m)

The generation of mean orthometric heights (with a 5’ by 5’ resolution) can be seen as an extension of the procedure quoted in Section 3.3.1. The solution involves, firstly, a repetition of the method referred to in Section 3.3.1 to obtain DEM_5m coverage for the whole of Canada with an implied range of 33-83° N and 210-310° E. Secondly, the file covering the required area is produced with the use of program “subarea.c”, see Appendix. (A.3). Considering the size of data sets and the convenience of checking the production to avoid mistakes, it is advisable to split the computational area crossing Canada into 10° by 10° sections. One example of the option file “subarea.opt” is:

```

/H.mean 720000
/DEM_5m_1_1
73.0 83.0 210.0 220.0

```

where “H.mean” is DEM_5m as input file covering all of Canada; 72000 is the number of rows in file “H.mean”; “DEM_5m_1_1” is the output file name; the numbers in the third line represent the boundary latitude and longitude of the DEM_5m_1_1’s coverage.

	210°	220°	230°	300°	310°
73°	DEM_5m_1_1	DEM_5m_1_2	...	DEM_5m_1_10	
	DEM_5m_2_1	DEM_5m_2_2	...	DEM_5m_2_10	
53°	DEM_5m_3_1	DEM_5m_3_2	...	DEM_5m_3_10	
	DEM_5m_4_1	DEM_5m_4_2	...	DEM_5m_4_10	
33°	DEM_5m_5_1	DEM_5m_5_2	...	DEM_5m_5_10	

Table 3.2: DEM_5m files covering Canada

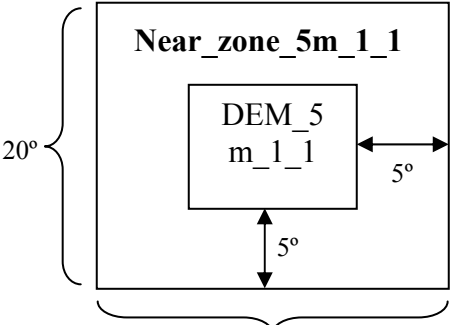


Figure 3.3: Coverage relation between N20° zone.dat and Computation_points.dat

At the final stage, the resulting DEM_5m files should have an appearance similar to Table 3.2, which are the required the “Computation_points.dat”.

The file “Near_zone.dat” is produced by extending 5 additional degrees in each direction of the corresponding “Computation_points.dat” as shown in Figure 3.3. Each final file “Near_zone.dat” file covers a grid area of 20° by 20° after such an operation.

3.3.2.2 Mean orthometric heights with 30'' by

30'' resolution (DEM_30s)

There are two ways to produce DEM_30s. One involves the same method as in DEM_5m’s generation. The other, which involves repeating the use of “H_read.c” and “H_grid.c” to produce DEM_30s files directly, was adopted for practical purposes based on the computational efficiency in terms of running time of this pair of programs.

Compared to the corresponding “Computation_points.dat”, the “Inner_zone.dat” file extends 1 additional degree to each side, as shown in Figure 3.4:

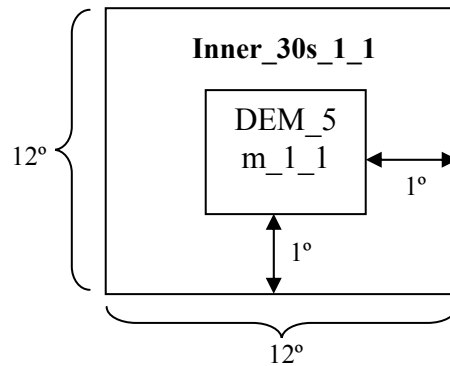


Figure 3.4: Coverage relation between Inner_zone.dat and Computation_points.dat

3.3.3 Preparation of “Inner_zone.dat” for programs

SITE_NTspace, SITE_Hspace, and PITE

The other input files are generated in the same way as described in Section 3.3.2, with the exception of “Inner_zone.dat” which requires that these programs also contain topographical density information. DTM_30s is obtained based on the method outlined in Section 3.3.2.2; it is then combined with the gridded density file covering the same area as shown in Section 3.2.3. Each row of the resulting file includes latitude longitude, orthometric height and topographical density.

3.3.4 Preparation and management of the detailed DTM files

3.3.4.1 Renaming of detailed DTM data files

Because the name of the original detailed DTM files is irregular, renaming the files according to their position provides superior organizational integrity. Usually, the coordinates of the northwestern-most point in the data file are used as the file name. For example, “N66E236_h.byn” denotes a detailed DEM file containing elevations within a $1^{\circ} \times 1^{\circ}$ area bounded by 65-66° N and 236-237° E.

3.3.4.2 Reshaping the regions covered by detailed DTM

GSD provided 12 CDs, each of which contains detailed DTM files corresponding roughly to Canada’s (irregularly shaped) provincial and territorial divisions. To satisfy the computation requirements to deal with the effects of topography, and especially for the convenience of preparing the option files, the detailed DTM files are reorganized into several regularly shaped regions, with adjacent regions having one degree of overlap in latitude / longitude.

3.3.4.3 Generating of detailed DTM files

The program DTE (which combines STC_near_zone, STC_far_zone, SCTC_near_zone, SCTC_far_zone, DTE_density and DCTE_density) requires that the resolution of detailed DTM files with binary format be 3'' by 3''; also, the scheme of the detailed DTM files should be as shown in Figure 3.5 for calculating the 1° by 1° shade region due to the requirement for a 1° Newton spherical integral around the computation point.

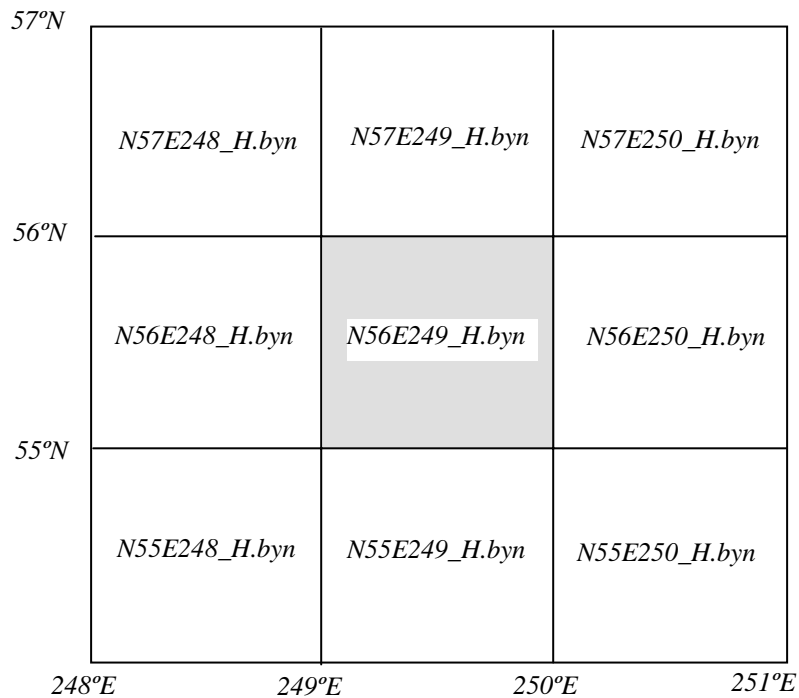


Figure 3.5: Example of the scheme of detailed DTM files

Thus, the detailed DTM data must cover all of the computation area. In actual application, there is lack of such binary DTM files over sea regions (previously

unnecessary due to always zero elevation), absence of files over several regions, and the resolution is relatively lower than 3" by 3" in high latitude areas (see Section 3.2.1.1).

The appropriate programs must be prepared for producing 3" by 3" DTM files for DTE to achieve three goals: (i) to produce the file containing zero elevation over sea regions, with the exact same format as CDED (Canada) (the corresponding program is called "grid1_CDED.c" in Appendix (B.1)) or SRTM (U.S.A.) based on location of the grid cell area; (ii) to interpolate the low-resolution mean DTM with 30" by 30" in ASCII format, into 3" by 3" binary files for regions lacking the corresponding files and to reformat into Binary (the corresponding program is called "grid2_CDED.c" in Appendix (B.2)); and (iii) to solve the problem across high latitude area, firstly the original detailed DTM file is opened to obtain the elevation data with low resolution 3" by 6" or 3" by 12", then the 3" by 3" resolution is achieved by mean of employing linear interpolation, finally the data are arranged back to binary file (the corresponding program is called grid3_CDED.c" in Appendix (B.3)). The difficult point is to generate binary file with special format containing header and orthometric height data.

3.3.5 Programs Reference field and Reference spheroid

The programs Reference_field and Reference_spheroid are interactive. After the commencement of computation, these two programs Reference_field and Reference_spheroid solicit the user's preferences (referred to in the program as

“options”), a task that may be difficult for a novice user. Users are prompted according to the following process questions and general choice areas:

Firstly, mass-conservation condensation should be chosen as the relevant technique of Helmert’s condensation to be applied. The boundary area should begin with 2.5’ and end with 57.5’ in general because the results with 5’ by 5’ resolution. These two programs require that steps in latitude and longitude be the same, at 5’ increments. The maximum degree of approximation should be defined as 20 and the minimum degree should be 0. This set of responses meets the minimum requirements at the program setup stage.

3.3.6 Evaluation of required region for each file

At the beginning of the computation, one should define the limits of the resulted geoid region. Theoretical prerequisites of downward continuation call for one additional degree for eliminating the edge effect; Stokes integration selects the spherical cap with a radius of 6°. Obviously, in respect of the procedure for numerical realization of the geoid model, the region of each file calculated in Real space should be 7° larger than that of the final geoid on each side. The region of each file calculated in NT-space must be 6° larger. All files computed in H-space thus have the same geographic region as the geoid.

This problem becomes complicated if the final geoid model has an irregular shape which results in an increased amount of data processing.

3.3.7 Additional comments

During the procedure of downward continuation, one of the input files, the mean orthometric heights file (DEM_5m) should be exactly 7° by 7° over the computation area. The required input files (named NT_anomaly_top.mean and FA_anomaly.mean) cover at least the computation area. In the fourth line of the options file, all parameters are kept constant; the default fixed computation area is 7° by 7° (84 by 84 rows and columns associated with a 5' by 5' step-size of the data) resulting with a coverage of 5° by 5° being stored to the output files.

The option files of several programs require determination of the dimensions of the data in latitude and longitude which can be calculated from the total size in degree divided by the grid step in degree. For instance: $100 / 0.00833333 = 1200$ and $50 / 0.00833333 = 600$. Usually the order is firstly latitude's dimension, followed by longitude's. However, it should be noted that dimensions of longitude and latitude are used in inverse order in the input file of program Stokes_integral, Residual_gravity.geo. In addition, this input file's data are arranged from south to north and from west to east. This order is different from the order of most other input data files as well.

Before carrying out the computation it is important to learn each original data format and the frequently used auxiliary programs, and to discover how to produce and manipulate input files using both of them to meet our objective.

As for the order of computation, it is unnecessary to run the program multiple times according to Figure 3.1. In practice, the actual processing approach depends on the requirements for preparing input data and other concrete computational power problems.

3.4 Special technical skills required for calculation

3.4.1 Requirement for familiarity with one computer language

At the beginning of computation, it is necessary to understand each program to learn the methodology behind them, and then to use, and perhaps to revise and refine it. During this operation, considerable data manipulation and format transformation are taken place, such as summation or differentiation of two files in point list format, preparation of the sub-area from the regular grid file in point list format, and computation of the minimal, maximal and mean values.

In terms of computer languages, a basic knowledge of C, C++ and Fortran is recommended because all programs in PGDP, which can be readily operated in Linux systems, were written employing these languages.

3.4.2 Capability of writing scripts in Linux

After the beginning of computations, the time-consuming tasks become apparent. A strategically sound approach to processing data involves trying a variety of methods in accommodating and data manipulation. The most efficient tactic is writing scripts to run programs, even to accomplish seemingly straightforward tasks such as generating input and option files automatically. For example, the program DTE requires one option file incorporating the names of five types of input files, eight types of output file names, a

changeable mode referred to the terrain roughness among other parameters, and a required input file called “inpuh.dat” including nine detailed DTM or SRTM files, whose output file is within a 1° by 1° area. Generally one must repeatedly change and save the option and “inpuh.dat” files, then run the program almost 4500 times respectively if the objective of calculation is the Canadian geoid model. However, scripts make them easier. Three scripts are attached in Appendixes. (C.1), (C.2) and (C.3). In addition assembling each set of 1° by 1° numerical results is another challenging job, and mistakes are likely during manual data-handling. Armed with knowledge of writing scripts based on the regularity of the detailed DTM file names and of the expected region’s shape, the task of these files’ organization becomes easier, in light of which the amount of time spent at the workstation diminishes.

3.4.3 Mastering GMT to make graphical plots

Given its complexity, graphical representation of the concepts and outputs of a data processing methodology in PGDP becomes important; a picture is indeed worth a thousand words in relating the meaning and results of this technique. The need to show each step’s numerical results succinctly and unambiguously is obvious. The Generic Mapping Tool (GMT) is the plot-making software of choice for this purpose, which can manipulate geographic and Cartesian data sets to produce illustrations of 3-D perspective views. Most plots presented in Chapter 4, for example, were generated by GMT.

3.5 Descriptive statistics of program operation

Given an onerous and highly complex task such as determination of the Canadian digital geoid model, analysis of PGDP's computational efficiency is critical. The running time span of each program in the PGDP suite is tested in a PC with Pentium 4 CPU and 1.00 GB of RAM in single processing, which are shown in Table 3.3. Each program is listed in the first column; the numbers in third column tell the total number of runs to get the output cover the whole Canada; and the total time in the final column is calculated by run-time multiply number of runs. Based on running time, without considering manipulation of input files and the preparation of option files, determination of the Canadian geoid requires around 2363 computational hours.

Program	Run-time (minute)	Coverage of output	Number of runs	Total time (minute)
DTE	15	1° by 1°	4500	67500
Ellipsoidal_cor	2	10° by 10°	50	100
Geoid_quasigeoid_cor	3	50° by 100°	1	3
SITE_NTspace	114	10° by 10°	50	5700
DAE_NTspace	290	10° by 10°	50	14500
SIAE_NTspace	340	10° by 10°	50	17000
Downward_continuation	52	10° by 10°	50	2600
SITE_Hspace	102	10° by 10°	50	5100
DAE_Hspace	265	10° by 10°	50	13250
SIAE_Hspace	169	10° by 10°	50	8450
Stokes_integral	18	10° by 10°	50	900
PITE	133	10° by 10°	50	6650
				141753 (2363 hours)

Table 3.3: Statistics of computational time span for the production of digital geoid

Chapter 4

Numerical Results and Their

Interpretation

To this point, each procedure in the Stokes-Helmert approach has been thoroughly explained; all associated formulae have been presented in Chapter (2), and the required input data files have been described in Chapter (3). In broader perspective, then, the computation task concerns the whole of the Canadian landmass bounded by north latitudes 42° and 71° , and by east longitudes 224° and 302° , with the exception of a southwest area delimited by $42\text{-}48^\circ\text{ N}$ and $224\text{-}274^\circ\text{ E}$. As described in Section 3.3.6, the coverage of each of the individual numerical results may be different depending on which space it happens. Based on the resolution of the original simple and complete Bouguer gravity anomaly, the Canadian geoid is on a $5'$ by $5'$ grid, which requires that each procedure's results be evaluated with the same grid step. The computational results of each step would be shown in both graphical and tabular form. Generally, the spatial behavior of each component can be shown graphically. The tabulated statistics usually contain minimum, maximum and mean values, as well as standard deviations. The quality and nature of each component can be assessed by the combination of these two kinds of display.

Based on the similarity of required input files and of the used mathematical method behind programs, a couple of operation procedures are organized together and are analyzed in comparison. Both topographical and atmospheric effects are evaluated by a Newton integral computed over the entire globe. The integration is usually split into several sub-domains where data files of differing resolution are needed, with differing division patterns of each integration domain based on the different procedure's operation.

4.1 Direct topographical effect and direct condensed topographical effect

According to the Stokes-Helmert approach, the direct topographical effect (DTE) on gravitational attraction must be computed and subsequently removed to obtain NT-space; following this, the direct condensed topographical effect (DCTE) in gravitational attraction is introduced to reduce the overall change of gravity field.

The DTE, which is evaluated on the Earth's surface, consists of three parts: the spherical terrain correction (STC) effect, the anomalous topographical density distribution effect (DTE-density), and the gravitational attraction of the spherical Bouguer shell. Similarly, the DCTE is computed as a sum of the spherical condensed terrain correction (SCTC) effect and the gravitational attraction of the anomalous condensed topographical density (DCTE-density) plus the effect of the condensed spherical Bouguer shell, all of which are evaluated on the geoid surface.

4.1.1 STC and SCTC

The effect of either STC or of SCTC on gravity is calculated through integration over the entire Earth. The integration is usually split into two parts: (i) integration over an area immediately adjacent to the point of interest, called the near-zone; and (ii) the integration over the rest of the world, referred to as the far-zone. When calculating the effect of the near-zone contribution of STC and SCTC (STC-near-zone and SCTC-near-zone), the DTMs and the 30'' by 30'' mean density data are used. For the far-zone contribution (STC-far-zone and SCTC-far-zone), the 30' by 30' global elevation data are adopted.

4.1.1.1 STC-near-zone and SCTC-near-zone

Near-zone integration is extended up to 5° of spherical cap around the computation point. This cap is then separated into three parts: (i) the innermost zone (a 5' by 5' grid area); (ii) the inner zone (residual 1° by 1° grid area); and (iii) the middle zone (residual 5° by 5°). The Newton integrals are computed using a 3'' by 3'' detailed DTM data within the innermost area centered at the computation point. The DTM_30s data are used for the integration over the inner zone, excepting the innermost zone. The remainder of the spherical cap's integration is completed by using DTM_5m data (see Figure 4.1).

To match the final computational geoid grid step, both STC-near-zone and SCTC-near-zone numerical results are 5' by 5' cell mean values, which are obtained after the averaging of point values within each cell. The number of point values required to compute the mean values depends on the roughness of the terrain. In the option files of

the corresponding programs, the parameter mode reflects this proposition: mode 1 means 1 point value; mode 2 to 6 represent 4, 10, 25, 50 and 100 point values respectively. For better meeting a sufficient level of accuracy, the higher mode is preferred; however, considering the challenge of computationally intensive integrals, the optimal number of point values is determined according to the associated experimental outcome shown by the program “rough.c” collected in Reference Manual III, which should be generally adopted by users. During the author’s computation, the mode 6, i.e., that mode indicating the averaging of values of 100 points is used fixedly due to the availability of the computer array.

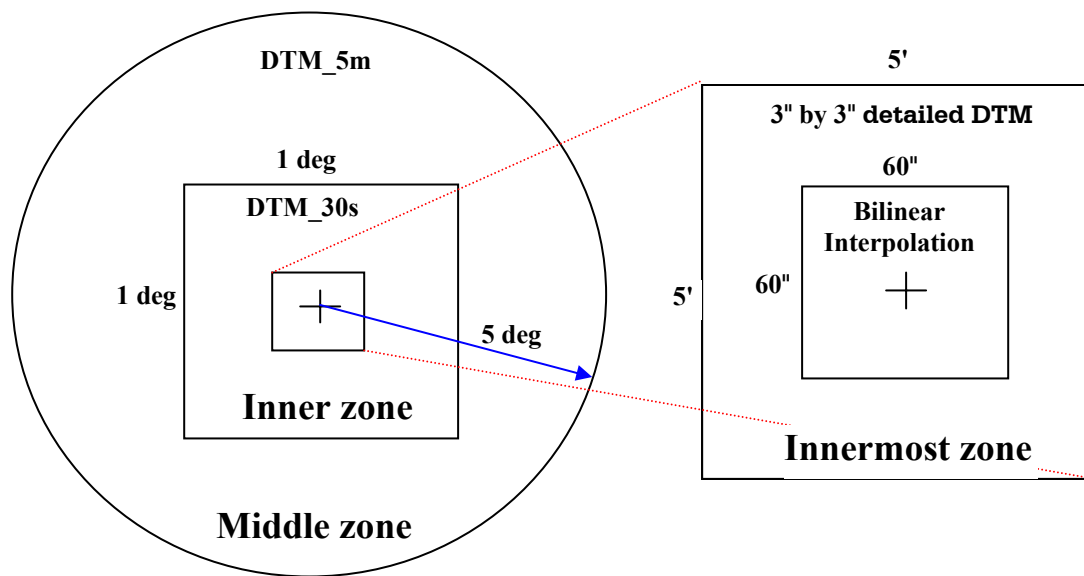


Figure 4.1: Scheme of integration domain

The resulted effects of these two near-zone divisions are shown in Figures 4.2 and 4.3. Basic statistics are shown in Table 4.1. Both the figures and the tabulated values conform to the expected behavior of the STC: the topographical masses within the near-

TERM	Minimum	Maximum	Mean value	Std deviation
STE-near-zone	-4.803	101.818	0.754	±3.449
SCTE-near-zone	-14.120	9.410	0.127	±1.257

Table 4.1: Terrain and condensed terrain effects on gravity – near-zone (mGal)

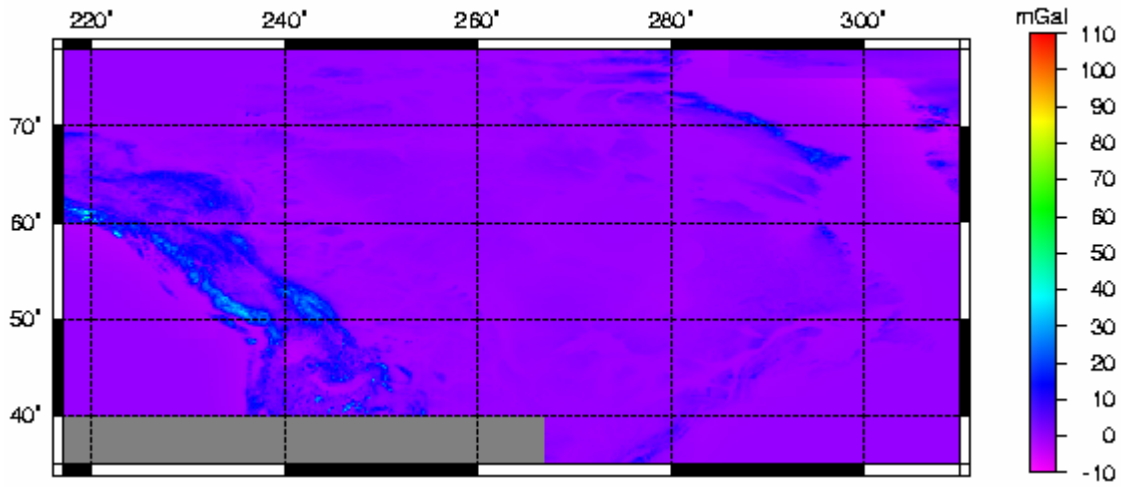


Figure 4.2: Terrain effect on gravity – near zone (mGal)

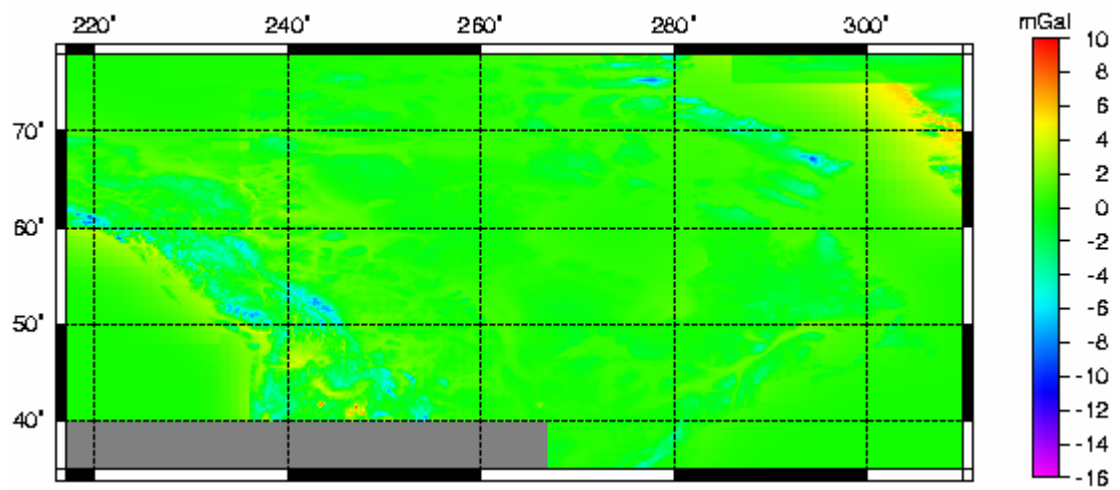


Figure 4.3 Condensed terrain effect on gravity – near zone (mGal)

zone generate a high-frequency gravity field highly correlated with topography. In addition, the addition of the STC-near-zone to free air gravity anomalies increases the smoothness of the latter.

4.1.1.2 STC-far-zone and SCTC-far-zone

These two far-zone contributions to gravity computed over the Canadian landmass are shown in Figures 4.4 and 4.5. A 30' step has been used in the surface numerical integration over the far-zone integration sub-domain. The topographical masses within the near zone generate a high-frequency gravity field and the distant topographical masses are responsible for an attenuated low-frequency gravitational field due to the consequence of Newton's law of gravitation. The statistical results of the STC-far-zone and SCTC-far-zone effects on the gravitational attraction are shown in Table 4.2.

Comparing the statistical parameters in Table 4.2, the far-zone contributions to the terrain effects and to the condensed terrain effects on gravity are with almost exactly reverse characters, although they are taken at the Earth's surface and at the geoid, respectively. In addition, they seem to be independent of the height of the computation point.

4.1.2 DTE-density and DCTE-density

Similar to the effects of STC-near-zone and SCTC-near-zone, DTE-density and DCTE-density are also mean values obtained from the averaging of point values with the same criteria described in Section 4.1.1.1.

TERM	Minimum	Maximum	Mean value	Std deviation
STE-far-zone	-30.063	449.879	7.847	± 50.073
SCTE-far-zone	-448.435	30.589	-7.809	± 50.053

Table 4.2: Terrain and condensed terrain effects on gravity – far-zone (mGal)

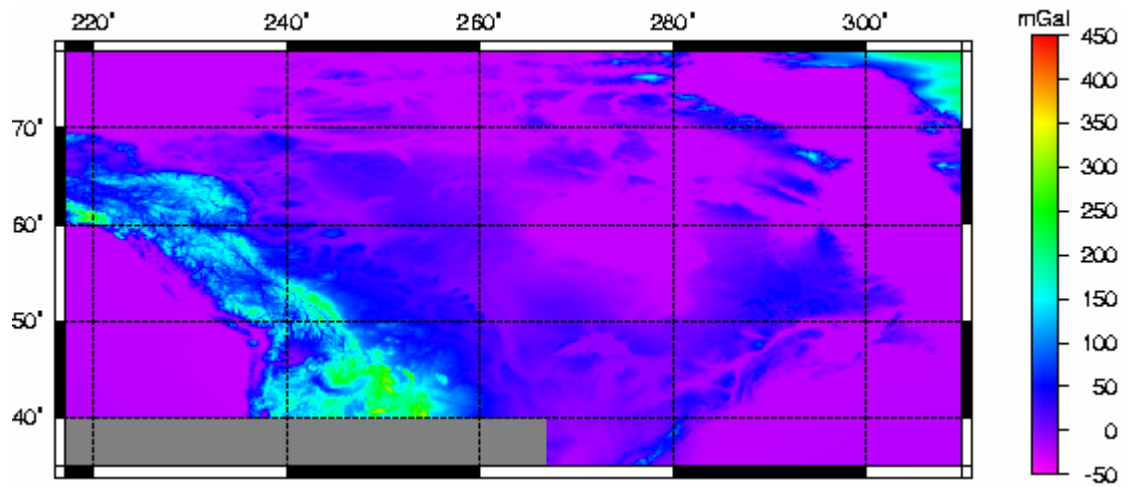


Figure 4.4: Terrain effect on gravity – far zone (mGal)

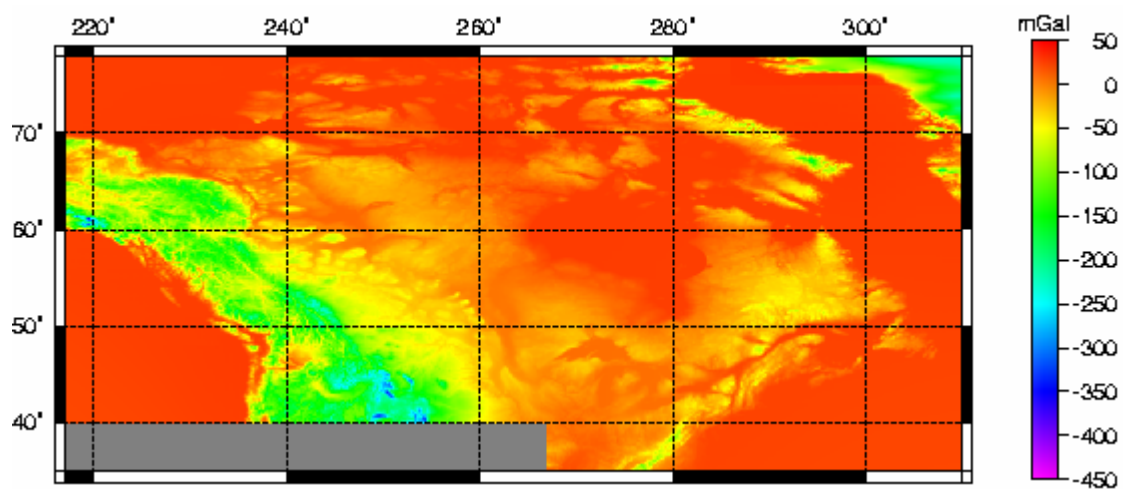


Figure 4.5: Condensed terrain effect on gravity – far zone (mGal)

TERM	Minimum	Maximum	Mean value	Std deviation
DTE-density	-19.048	12.804	0.281	± 1.505
DCTE-density	-0.212	0.075	-0.014	± 0.037

Table 4.3: Anomalous density effects (mGal)

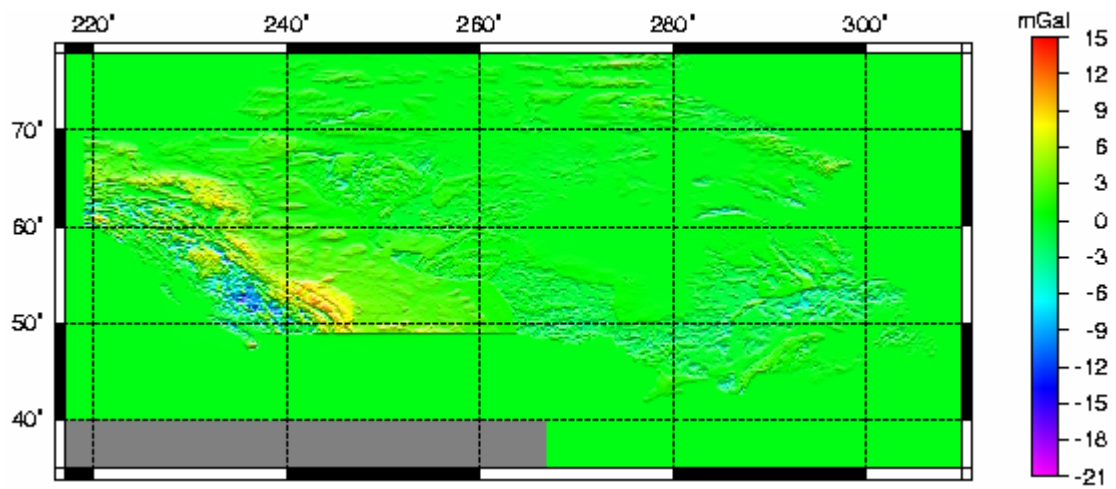


Figure 4.6: Anomalous topographical density effect on gravity (mGal)

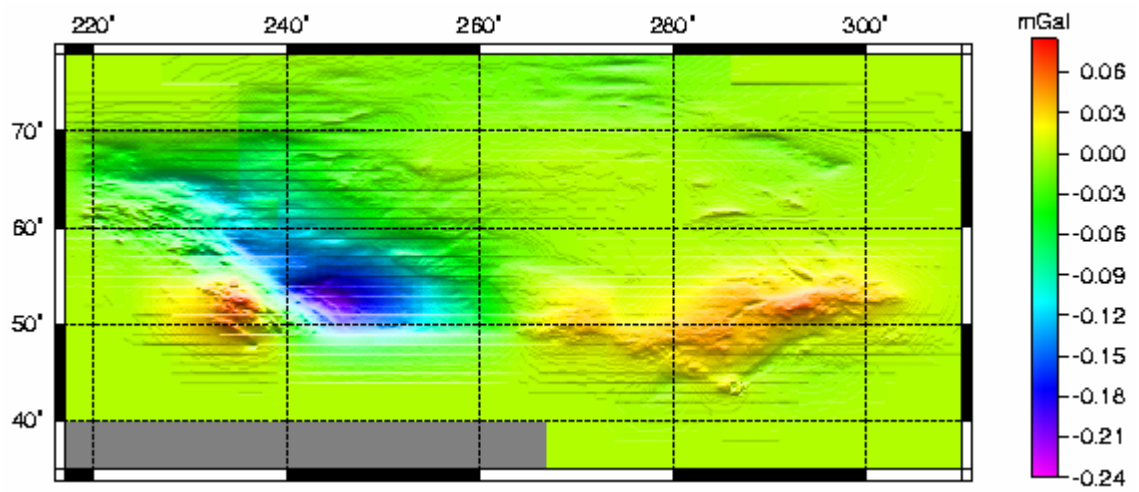


Figure 4.7: Condensed anomalous topographical density effect on gravity (mGal)

Since the almost identical integration kernel is used as for STC-near-zone and SCTC-near-zone, the integration region and the needed data are similar as well excepting the mean laterally varying topographical density data. In most of the topography, the actual lateral density varies from 1.0 g.cm^{-3} (water) to 2.98 g.cm^{-3} (gabbro). Therefore, by disregarding existing water bodies, the variation of topographical density $\delta\rho$ is almost completely within $\pm 0.3 \text{ g.cm}^{-3}$ around the mean value ρ_o . Since the mean global value of $\delta\rho(\Omega)$ is regarded as 0, the far-zone contribution is likely to be very small and can be neglected.

These two anomalous topographical density effects are plotted in Figures 4.6 and 4.7, and the corresponding statistical results are shown in Table 4.3. From these figures and tabulated values, the DTE-density and DCTE-density display a high frequency character, which is correlated with topographical density and topography as well. The large anomalous density effect is concentrated in the Rocky Mountains as expected. The sign of both effects changes between positive and negative due to the nature of the density variation. The DTE-density can reach $\pm 20 \text{ mGal}$. The range of DCTE-density is at the 0.1 mGal level, which is two orders of magnitude smaller than the DTE-density. Thus the implementation of related formula in the program should be rechecked. Since it reaches more than 0.01 mGal (in absolute value), it must be taken into account if a 1 cm accuracy level is the aim (Vaníček and Martinec, 1994). Due to a density data collection problem as mentioned in Section 3.2.3, the effects over the territory of the USA are calculated using a constant density value, which can be seen clearly from Figures 4.6 and 4.7.

The calculation results of the two effects of DTE-density and DCTE-density show that the introduction of the digital topographical density model will significantly improve the accuracy of the geoid evaluation. The results presented here may have underestimated the effects because the mean DTDM of 30'' by 30'' is not sufficient to model the topography density in the Canadian Rocky Mountains. Furthermore, a better density model will be needed to estimate the density effects at 1 cm accuracy covering the larger region and showing more precise density information. The laterally varying density information from the USA should be used in the computation of the southwest part of the Canadian geoid model.

4.1.3 DTE and DCTE

Due to the simplicity of calculation of the Bouguer shell contribution, it is not separately treated in the related program. Figures 4.8 and 4.9 show DTE and DCTE respectively. Table 4.4 shows the statistical results of these effects.

Each component of the gravitational attraction of topography at the surface and the gravitational attraction of condensed topography at the geoid are fully studied and analyzed from above of all. Both of DTE and DCTE are seen to have a local, high-frequency feature. The method of using both local and global DEM to capture the full signal with no loss of accuracy is proposed. In the NT-space, the high frequency signals of topographical effect are eliminated following the removal of topographical masses, which smoothes the gravity field for downward continuation. This is seen as a slight advantage since downward continuation should be done in a field with as much signal (high frequency) removed as possible.

TERM	Minimum	Maximum	Mean value	Std deviation
DTE	-444.244	-14.315	-61.876	± 53.197
DCTE	21.824	523.410	63.084	± 54.978

Table 4.4: DTE and DCTE on gravity (mGal)

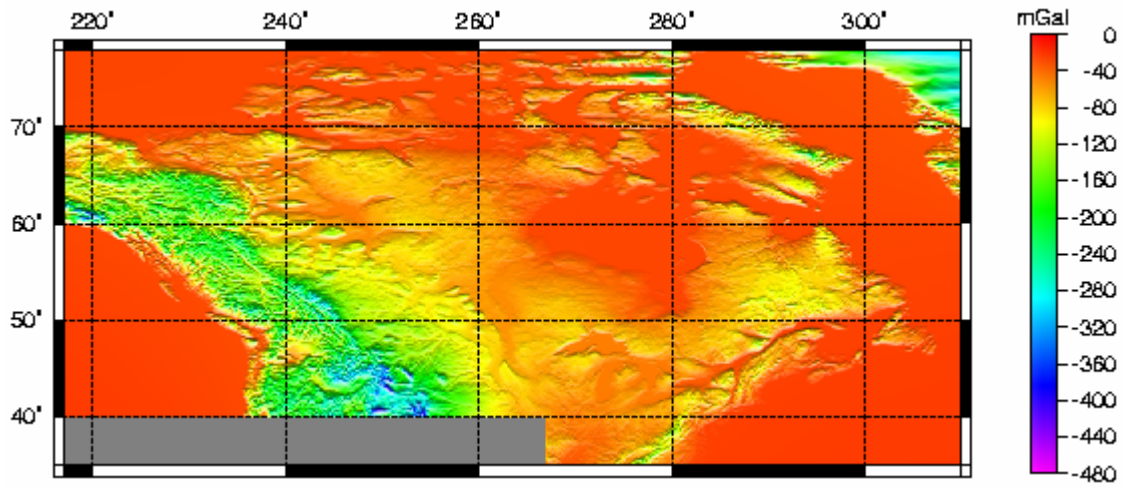


Figure 4.8: Direct topographical effect on gravity (mGal)

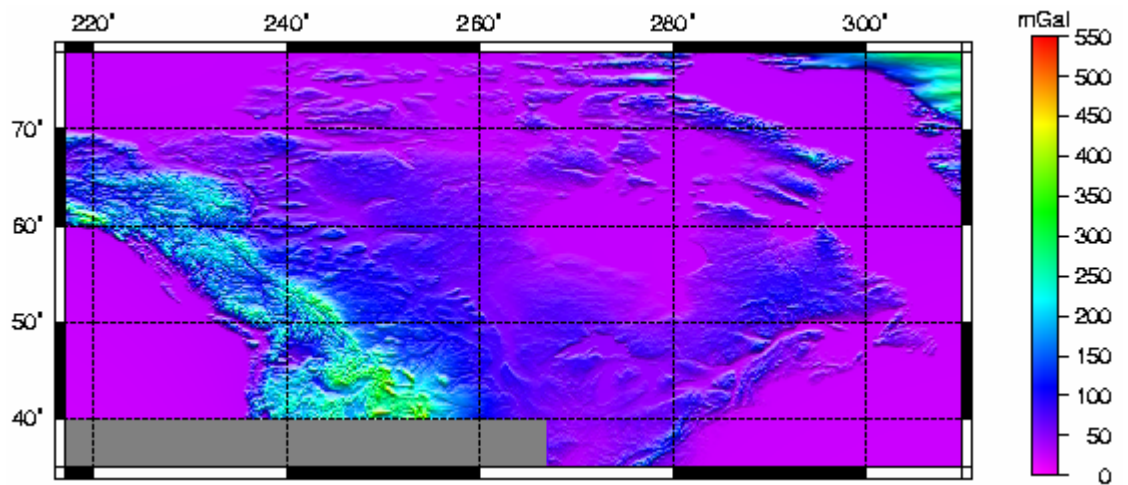


Figure 4.9 Direct condensed topographical effect on gravity (mGal)

4.2 Atmospheric effects

The atmospheric effects on the gravitational attraction contain five parts considered in the Stokes-Helmert approach: the direct atmospheric effect referred to the Earth's surface (DAE-NT); the secondary indirect atmospheric effect referred to the Earth's surface (SIAE-NT); the direct condensed effect referred to the geoid (DCAE-H); the secondary indirect condensed effect referred to the geoid (SICAE-H); and the primary indirect atmospheric effect referred to the geoid (PIAE), which is too small to be taken into account during computation.

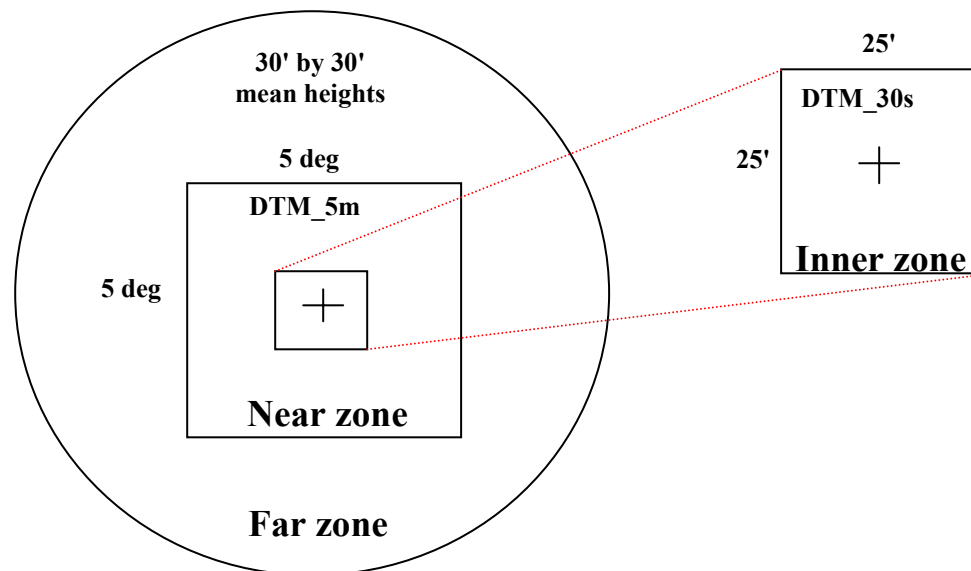


Figure 4.10: Integration scheme for the atmospheric effects

In the evaluation of these atmospheric effects, the Newton integral is used as well as the computing topographical effects. As the integration is to be carried out over the entire Earth's surface, the integration domain is usually split into an inner zone (around

the computation point), near-zone and the far-zone (see Figure 4.10) where DEM_30s, DEM_5m and 30' by 30' mean elevation are used, respectively. The mean DTM files can be obtained by the methods described in Section 3.1. These atmospheric effects can be found in Figures 4.11 to 4.14, and basic statistical results for individual atmospheric effect on gravity can be found in Table 4.5.

Summarizing the result of our numerical investigation over Canada, it follows that the direct atmospheric effect referred to the Earth surface is much smaller than the direct condensed atmospheric effect referred to the geoid. Meanwhile, the secondary indirect effect of atmospheric masses is larger than the secondary indirect effect of condensed atmospheric masses, and the differences (a few milligals) are not negligible.

The direct condensed atmospheric effect and the secondary indirect atmospheric effect have a high-frequency character and are especially strongly correlated with the topography, while the direct atmospheric effect and the secondary indirect condensed atmospheric effect also contain a low-frequency component. The direct atmospheric effect is almost negligible over the ocean, whereas it reaches up to 180 μGal at the Canadian Rocky Mountains.

Based on our numerical investigation of all of the effects caused by atmospheric and condensed atmospheric masses, the 30'' by 30'' DTM data are sufficient for near-zone numerical integration for a region up to 5' of the spherical distance around the computation point, 5' by 5' DTM for the middle-zone up to 3° of the spherical distance, and 1° by 1° mean heights for the far-zone integration sub-domain because of the smooth behavior of the integration kernel.

TERM	Minimum	Maximum	Mean value	Std deviation
DAE-NT	-0.176	-0.001	-0.02	± 0.018
SIAE-NT	1.682	1.801	1.766	± 0.028
DAE-H	-0.842	-0.631	-0.819	± 0.030
SIAE-H	0.758	1.411	0.805	± 0.070

Table 4.5: All effects of atmospheric masses on gravity (mGal)

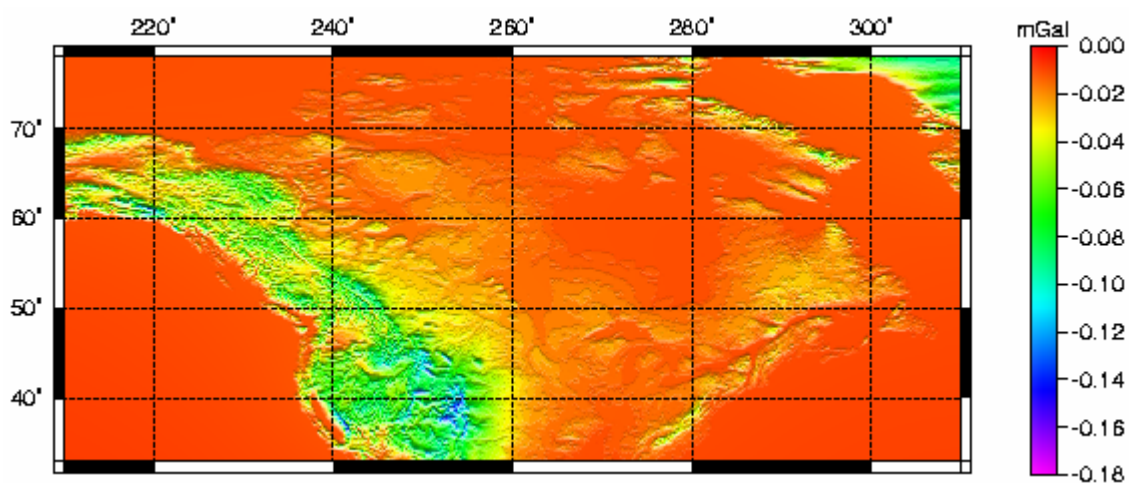


Figure 4.11: Direct atmospheric effect on gravity (mGal)

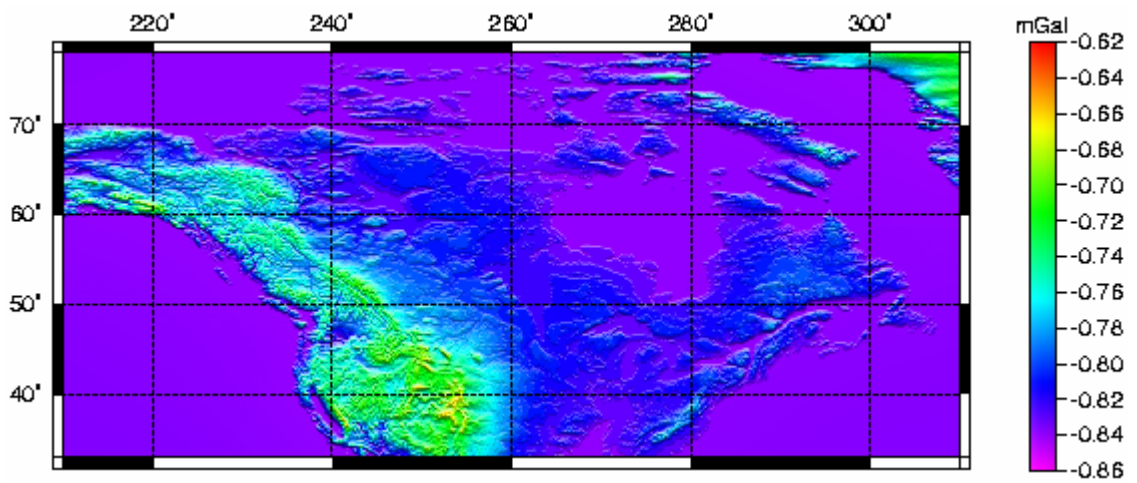


Figure 4.12: Direct condensed atmospheric effect on gravity (mGal)

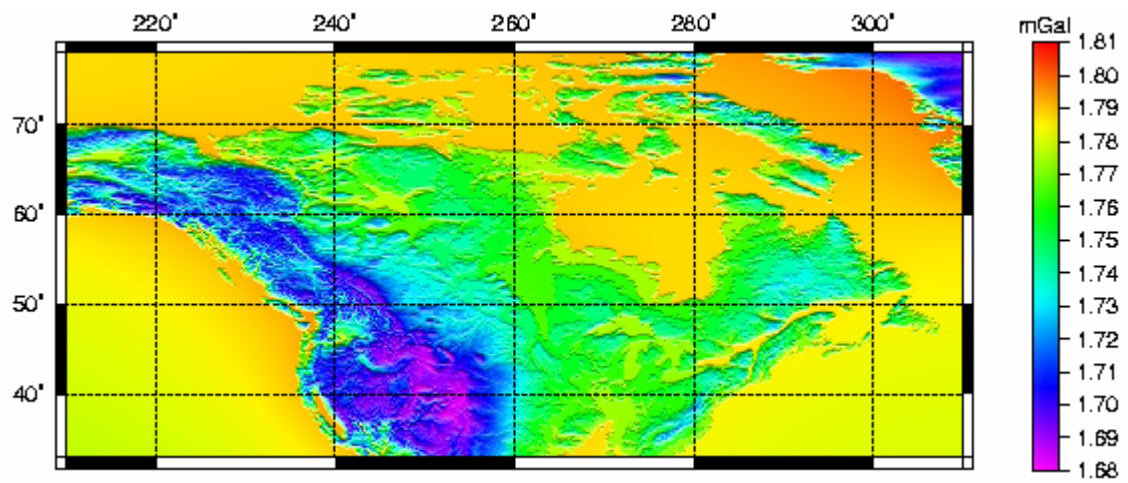


Figure 4.13: Secondary indirect atmospheric effect on gravity (mGal)

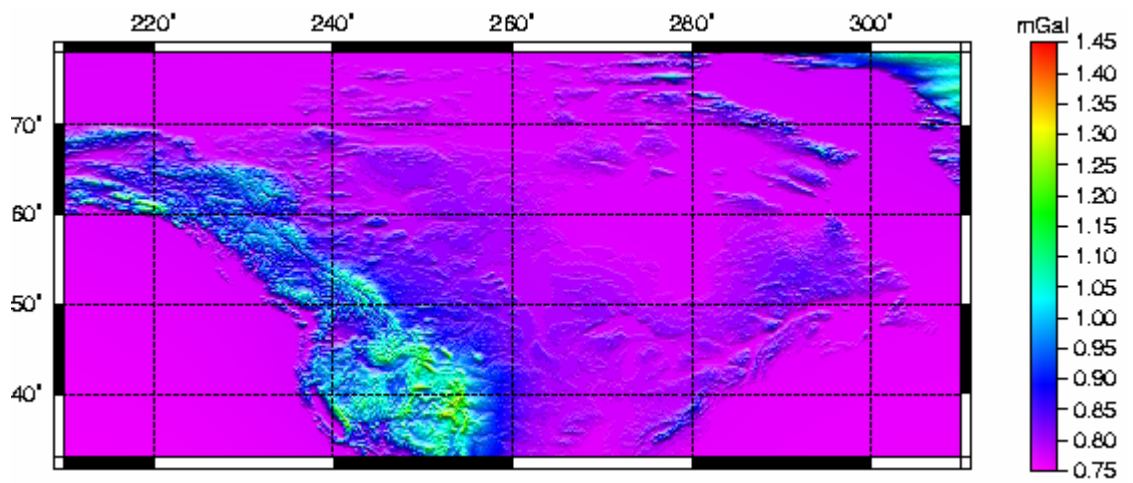


Figure 4.14: Secondary indirect condensed atmospheric effect on gravity (mGal)

The atmospheric effects on the geoid are smaller, may be two orders of magnitude smaller than DTE. However, the effects are then still a few centimeters, required for a centimeter geoid.

4.3 Secondary indirect effect of topography evaluated in NT-space (SITE-NT) and H-space (SICTE-H) respectively, and PITE

While calculating secondary indirect effect of topography in NT-space (SITE-NT), secondary indirect effect of topography in H-space (SICTE-H) and PITE, the splitting of the integration domain is the same as the pattern shown in Figure 4.10. The mean DTMs and 30'' by 30'' DTDM, (see Section 3.2.3) are used as input data for the evaluation of the point value of SITE-NT on the Earth surface, SICTE-H and PITE on the geoid at a spacing of 5' by 5'. The anomalous density effects are evaluated from integration over a spherical cap with a radius of 3°. The far-zone contribution of the lateral density variation effects is not estimated due to lack of global coverage of density data and their small values.

The values of SITE-NT and SICTE-H on gravity are plotted in Figures 4.15 and 4.16. The associated statistical values are shown in Table 4.6. Note that the SITE-NT and the SICTE-H are characterized by long-wavelength pattern and with same value at same gridded points. Consequently, it is not necessary to specify if these effects are referred to the Earth's surface or the geoid, as these are practically the same.

Figure 4.17 shows the PITE on geoidal height. A 30' by 30' grid for the numerical integration is sufficient for a few millimeters precision of the far-zone contribution to PITE. It ranges between -1.040 m and -0.019 m, with the mean value of -0.045m. The PITE affects the geoid up to the meter level in the Canadian Rocky Mountains. More than 96% of PITE values are within the range of -0.2 m to 0.0 m. The PITE is mainly characterized by short wavelength features, which are highly correlated with topography. One important reason for this is that its integral kernel decreases quickly and the near-zone contribution accounts for the largest portion of this effect. The PITE on the geoidal height is always negative and, thus, must be subtracted in absolute value from Helmert's co-geoid systematically.

4.4 Ellipsoidal correction and geoid-quasigeoid correction

The ellipsoidal correction contains two terms. The first is the ellipsoidal correction to the gravity disturbance (Ellipsoidal-cor1). The other is the ellipsoidal correction for the spherical approximation (Ellipsoidal-cor2). These effects can be found in Figures 4.18 to 4.19; Table 4.7 shows the statistical numerical results.

The effect of ellipsoidal correction on gravity disturbance is relatively short wavelength but with correlation to terrain. As for the ellipsoidal correction for the spherical approximation, it is of a very low frequency character. The elevation from the global model EGM96 is applied to the related computation.

TERM	Minimum	Maximum	Mean value	Std deviation
SITE-NT	80.894	149.622	109.923	±12.410
SICTE-H	80.900	149.974	109.947	±12.435

Table 4.6: Secondary indirect topographical effect on gravity (mGal)

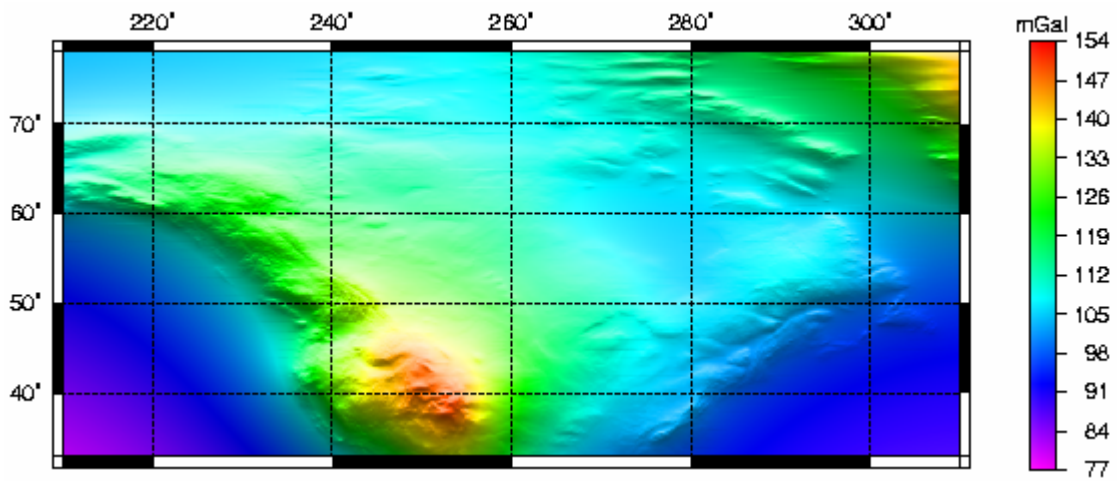


Figure 4.15: Secondary indirect topographical effect on gravity (mGal)

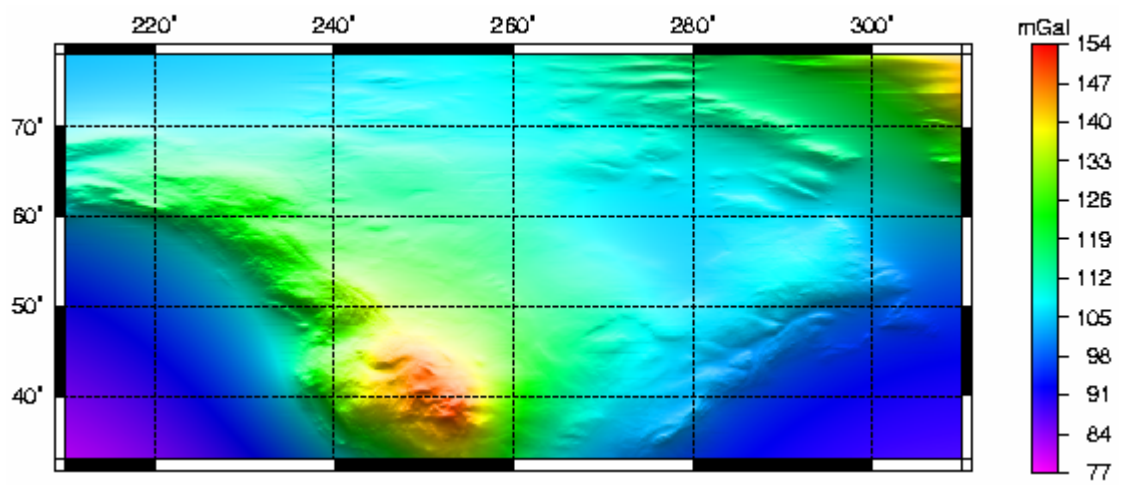


Figure 4.16: Secondary indirect condensed topographical effect on gravity (mGal)

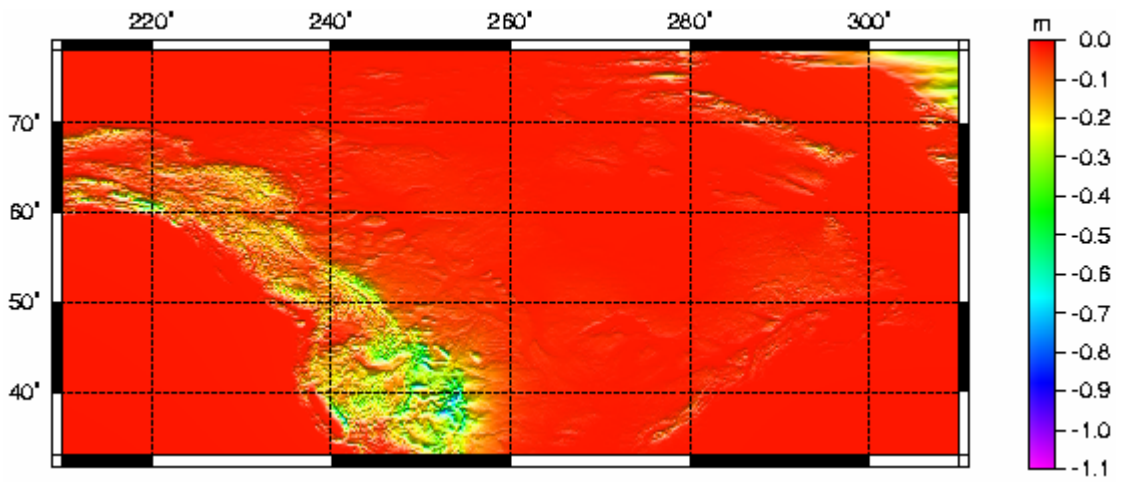


Figure 4.17: Primary indirect topographical effect on geoid (m)

TERM	Minimum	Maximum	Mean value	Std deviation
Ellipsoidal-cor1	-0.158	0.172	0.025	± 0.044
Ellipsoidal-cor2	-0.074	0.022	-0.015	± 0.017
Geoid-quasigeoid-cor	-0.405	0.018	-0.012	± 0.030

Table 4.7: Ellipsoidal correction and Geoid-quasigeoid correction (mGal)

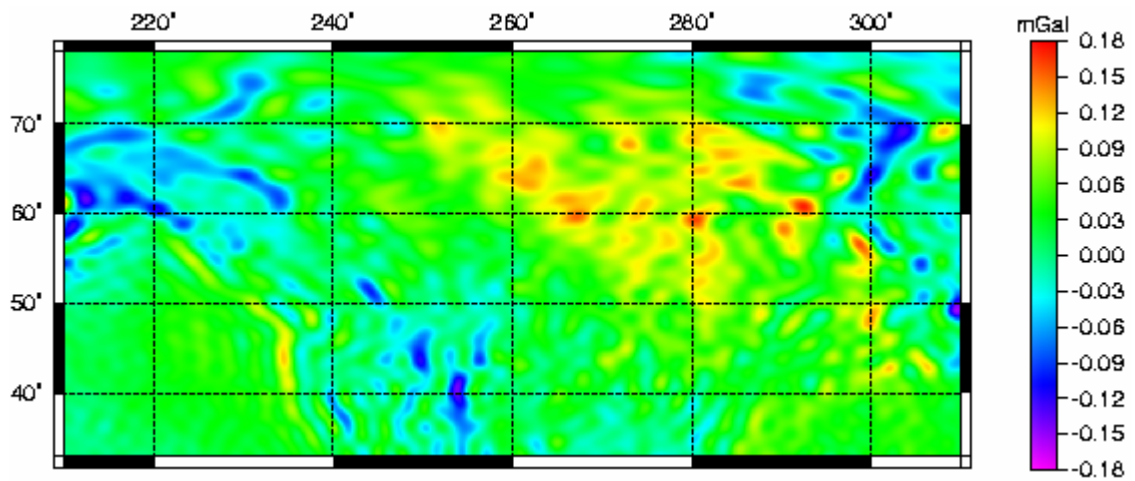


Figure 4.18: Ellipsoidal correction to the gravity disturbance (mGal)

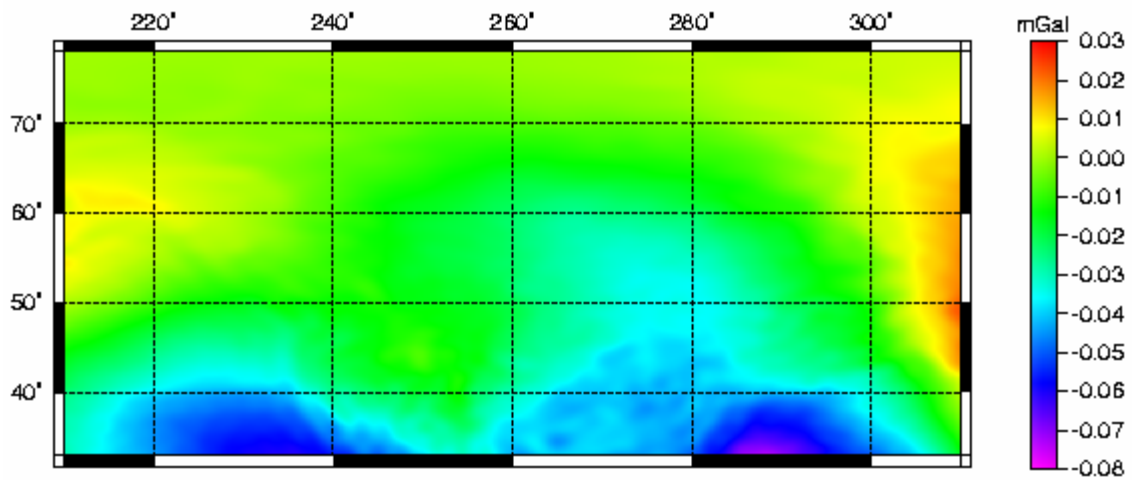


Figure 4.19: Ellipsoidal correction for the spherical approximation (mGal)

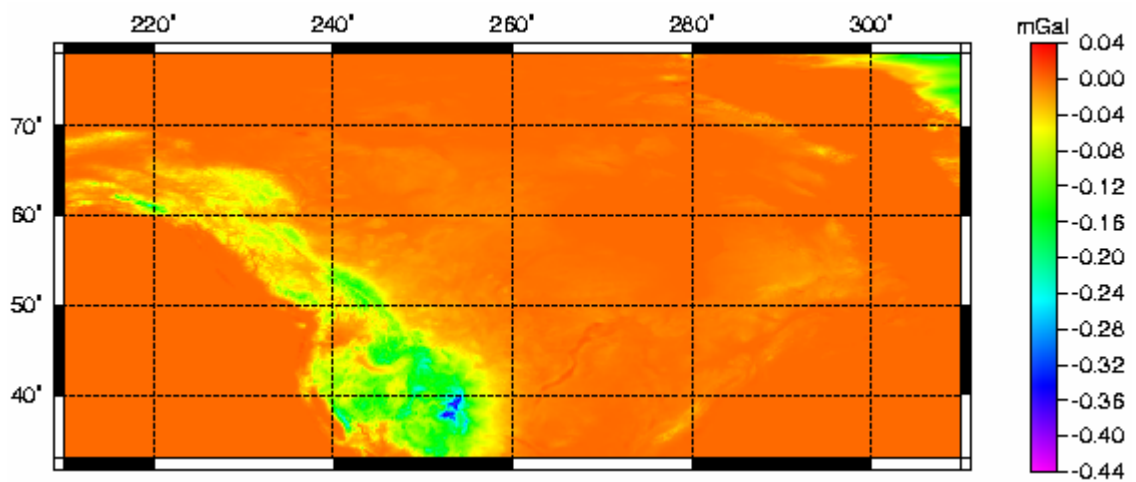


Figure 4.20: Geoid-quasigeoid correction on gravity (mGal)

The geoid-quasigeoid correction is a linear function of the free-air gravity anomaly, orthometric height, and the mean topographical density. Its statistical results are also shown in Table 4.7. The geoid-quasigeoid correction is a long wavelength function while still retaining some correlation to terrain, see Figure 4.20. Each of these three contributions to the resulting geoid amounts to very little of the order of a few millimeters.

4.5 Downward continuation

This program's output is a 5° by 5° file which requires 7° by 7° computation area considering the edge effect and computational area size limitation. The following two of Figures 4.21, and 4.22, depict the NT gravity anomaly on the Earth's surface (GA-E-NT), and the NT gravity anomaly on the geoid (GA-G-NT), respectively. The corresponding statistical values including downward continuation are shown in Table 4.8.

The gravity anomaly in NT-space referred to the Earth's surface seems relatively smooth although having a large range. The gravity anomaly in NT-space referred to the geoid is of short wavelength with a large range as well. The mean downward continuation contribution demonstrates its high frequency character. Although more than 99% of the values are between -10 mGal and 10 mGal, there are some points with rather large and irregular values. Some of them (scattered in USA's Rocky Mountains and along Canada's boundary with Alaska) change sharply from negative to positive or the other way round, which is probably the result of a singularity problem after making sure the correctness of the input files. It causes the graphical plot of NT gravity anomaly

on the geoid to look blurred. Further studies are needed to evaluate the stability of downward continuation.

4.6 Helmert reference gravity anomaly and Helmert reference spheroid

As described in Section 2.3.7.1, based on the frequency decomposition of gravity data, the geoid height can similarly be decomposed into the low frequency reference spheroid and high frequency residual geoid. Both Helmert reference gravity anomaly (Reference-GA) and Helmert reference spheroid are evaluated from the low frequency gravity disturbing potential, which can be accurately determined from the low degree spherical harmonic coefficients of a global geopotential model. Presently GRIM4-S4 is adopted.

The Reference-GA and Helmert's reference spheroid can be found in Figures 4.23 and 4.24. Basic statistical values can be found in Table 4.9. Both of them have a low frequency character. The Helmert co-geoid is the major component of the final geoid.

The global geopotential model is updated frequently with the advancement of satellite techniques. The GRACE Gravity Model 02 (GGM02) can be a better successor which is developed to the degree and order 150 based on only GRACE data.

4.7 Residual Helmert gravity anomaly and residual spheroid

TERM	Minimum	Maximum	Mean value	Std deviation
GA-E-NT	-192.713	346.142	42.543	± 42.033
DC	-72.659	126.776	0.010	± 1.048
GA-G-NT	-264.756	346.142	43.302	± 39.589

Table 4.8: Gravity anomaly in NT-space and downward contribution (mGal)

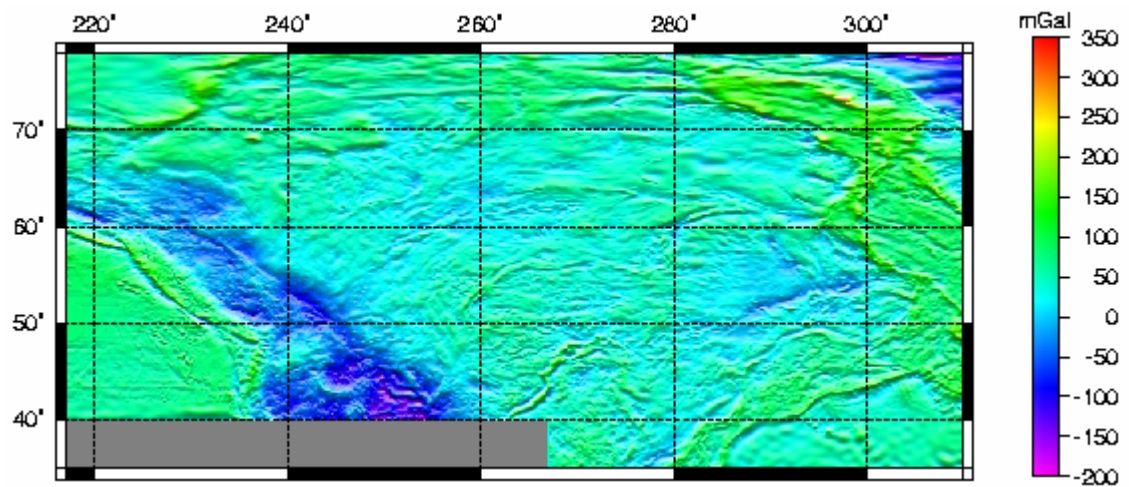


Figure 4.21: NT gravity anomaly on the Earth's surface (mGal)

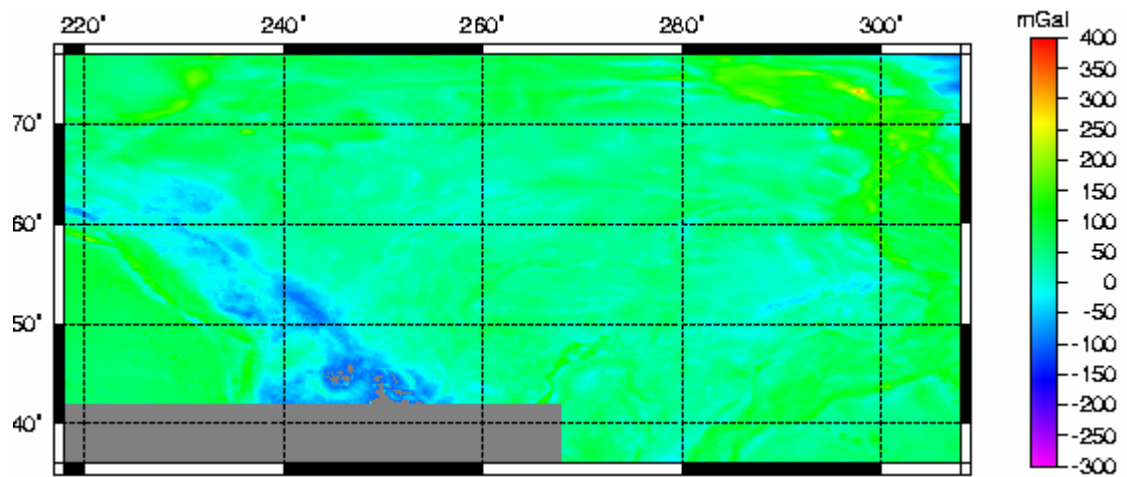


Figure 4.22: NT gravity anomaly on the geoid (mGal)

TERM	Minimum	Maximum	Mean value	Std deviation
Reference-GA	-44.268	29.639	-5.973	± 16.042
Reference spheroid	-48.104	35.362	-17.211	± 18.137

Table 4.9: Reference gravity anomaly (mGal) and reference spheroid (m)

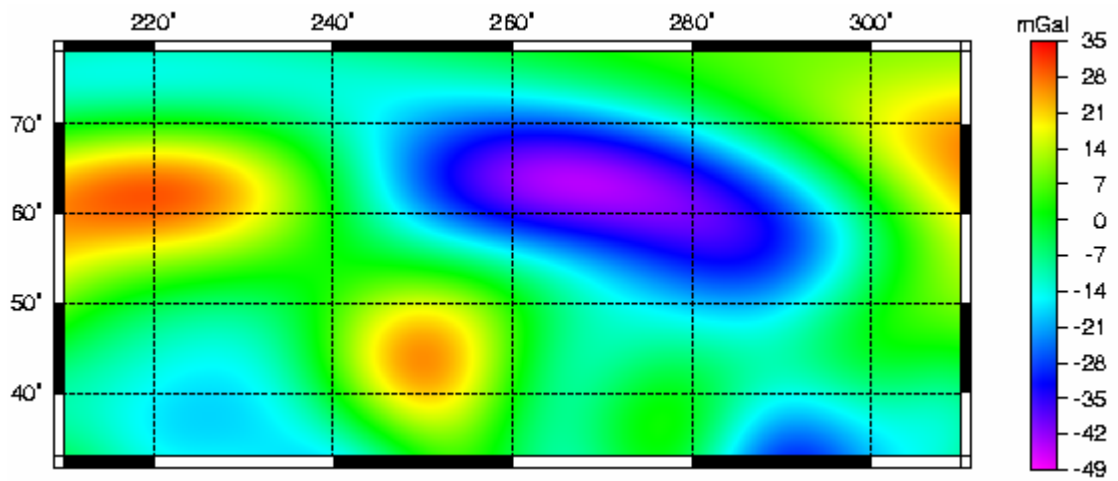


Figure 4.23: Helmert reference gravity anomaly (mGal)

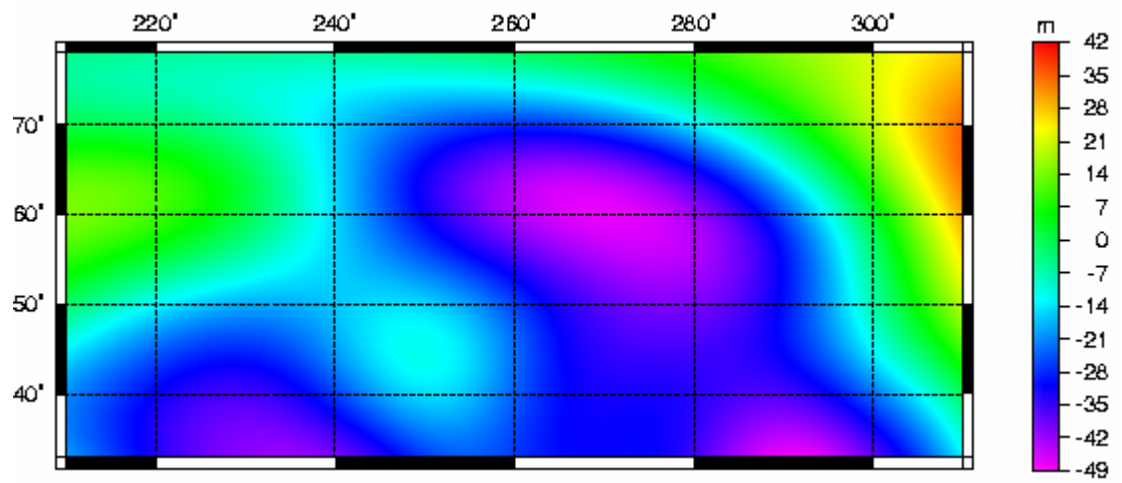


Figure 4.24 Helmert reference spheroid (m)

TERM	Minimum	Maximum	Mean value	Std deviation
Residual gravity anomaly	-187.976	402.1	1.39	± 26.615
Residual co-geoid	-7.105	6.461	0.403	± 2.173

Table 4.10: Residual gravity anomaly (mGal) and residual co-geoid (m)

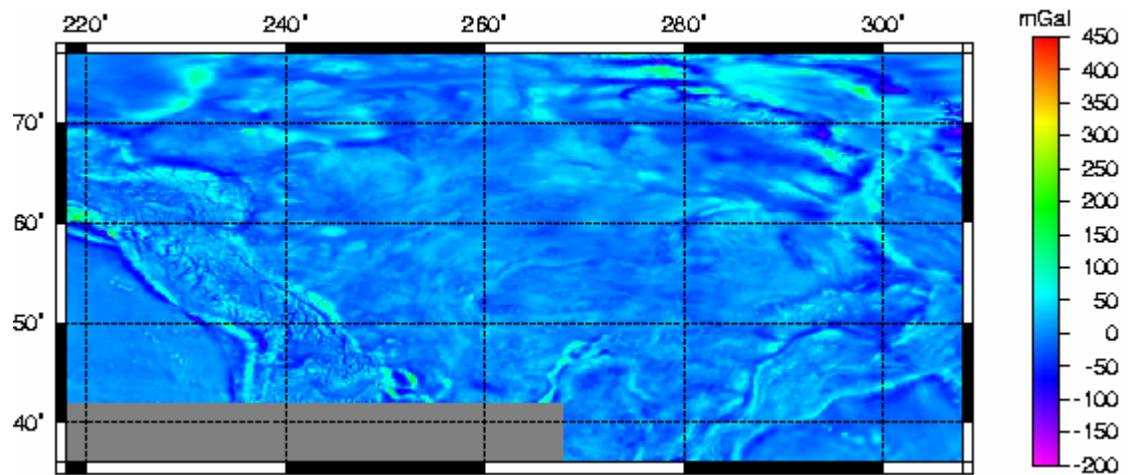


Figure 4.25 Residual gravity anomaly in H-space (mGal)

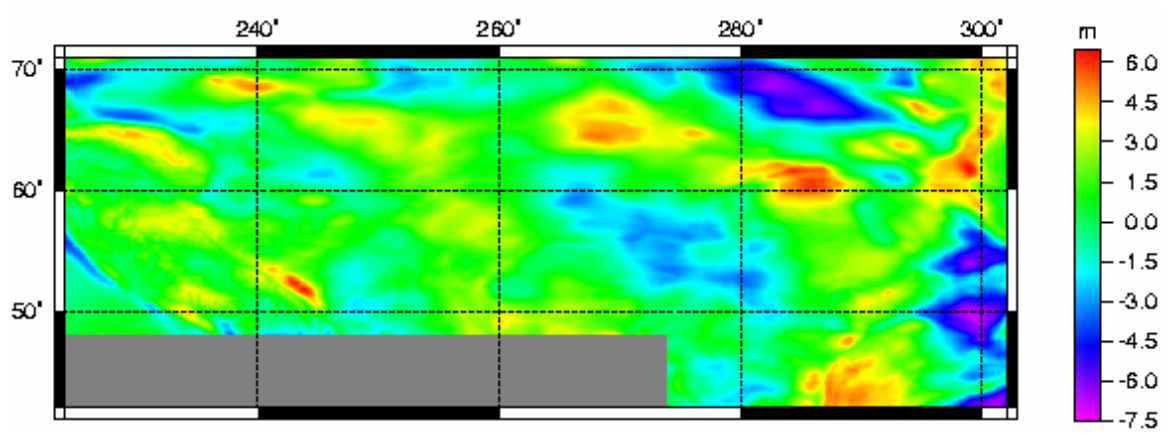


Figure 4.26: Residual co-geoid (m)

The residual Helmert gravity anomaly is calculated by subtracting the Helmert reference gravity anomaly from the Helmert gravity anomaly. The residual co-geoid is obtained by means of the solution of the geodetic boundary value problem. First, employing the Stokes integral the high frequency disturbing gravity potential is calculated. Then the residual co-geoid is calculated according to Bruns formula.

The residual Helmert gravity anomaly (Residual-GA) and residual co-geoid are plotted in Figures 4.25 and 4.26. The corresponding statistics are shown in Table 4.10. Both of the residual Helmert gravity anomaly and residual geoid show the high frequency qualities correlated with terrain as expected.

4.8 Geoid model and the comparison of results with GPS/Leveling data

The final Canadian gravimetric geoid model (see Figure 4.27) is obtained after combining the reference spheroid and residual co-geoid and adding PITE to so obtained co-geoidal height. The associated statistical values are shown in Table 4.11; this seems reasonable because it connects closely with topography.

Currently, the best independent technique for validating geoid model is its comparison to geoid heights derived from GPS ellipsoidal heights and spirit-leveled orthometric heights, simply called GPS/Levelings. The results, as compared with 1736 GPS/Leveling points' data (Figure 4.28 shows the location of GPS/Leveling points.), are shown in Figure 4.29; its statistics can be found in Table 4.11. The differences (which are calculated using bilinear interpolation) between GPS/leveling and the

computed geoid model, and the related standard deviation are little large. To a certain extent, these large differences are resulted from the linear trend of GPS/Leveling data and the bias between the geometric geoid model which can be reflected at these GPS/leveling points and the gravimetric geoid model produced by the data processing methods discussed above. To eliminate these systematic factors, a four-parameter transformation (Sideris, 1993) should be applied.

4.9 Comparison between Canadian geoid models produced in UNB

Before the conceptualization of the three-space Stokes-Helmert's scheme, the two-space (R-space and H-space) Stokes-Helmert's scheme has been employed. Its main principle is firstly to obtain Helmert gravity anomaly on the Earth's surface by a series of gravity corrections based on Helmert's second condensation, and then to implement the downward continuation.

Built on the two-space Stokes-Helmert's approach, a geoid model called Geoid_UNB2000 (see Figure 4.30) was realized, which ranges from -50.193m to 25.991m with a standard deviation $\pm 14.080\text{m}$. The difference between these two UNB geoid models is shown in Figure 4.31, which ranges from -0.951m to 4.550m with a standard deviation $\pm 0.765\text{m}$ in the compared region.

The Geoid_UNB2000 is of a rather low frequency character which is incongruent with the actual complicated gravity anomaly. The difference shows clearly the topographical effects, especially in the regions of Rocky Mountain and Greenland.

TERM	Minimum	Maximum	Mean value	Std deviation
Geoid	26.642	-49.867	-22.894	± 15.162
Differences	-1.5058	1.5996	-0.0873	± 0.626

Table 4.11: Geoid and compared differences with GPS/Leveling (m)

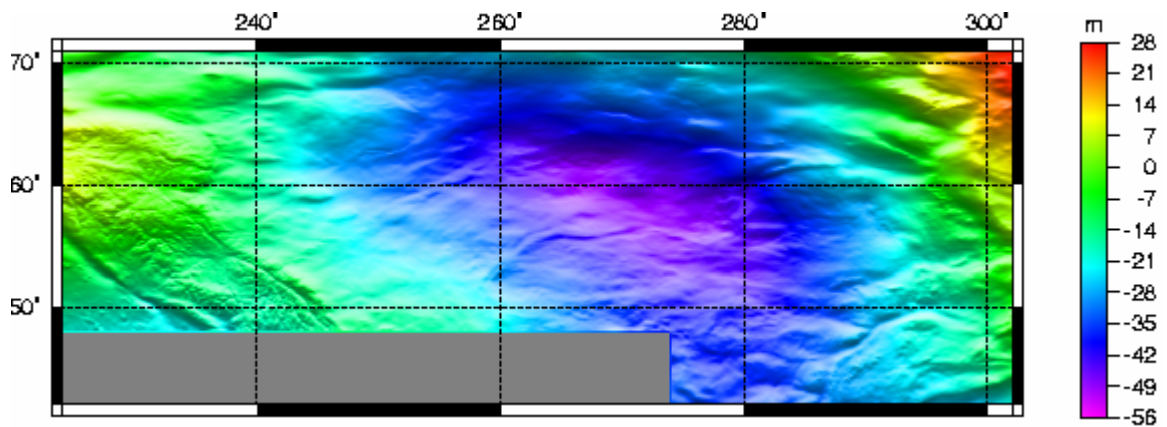


Figure 4.27: Canadian geoid model (m)

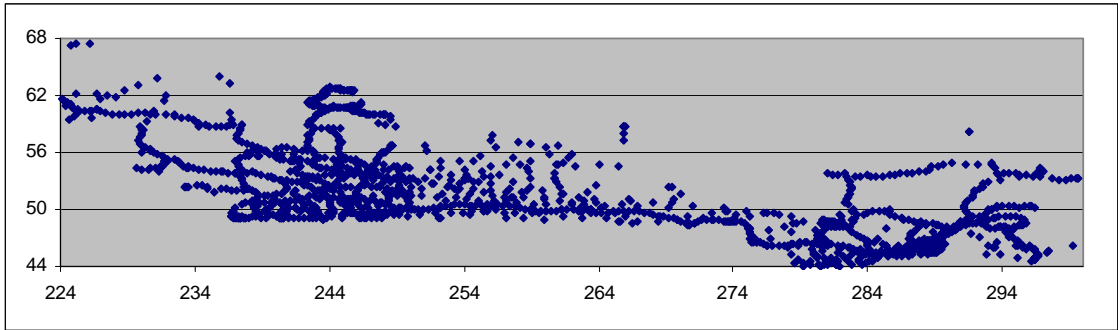


Figure 4.28: Locations of GPS/Leveling points

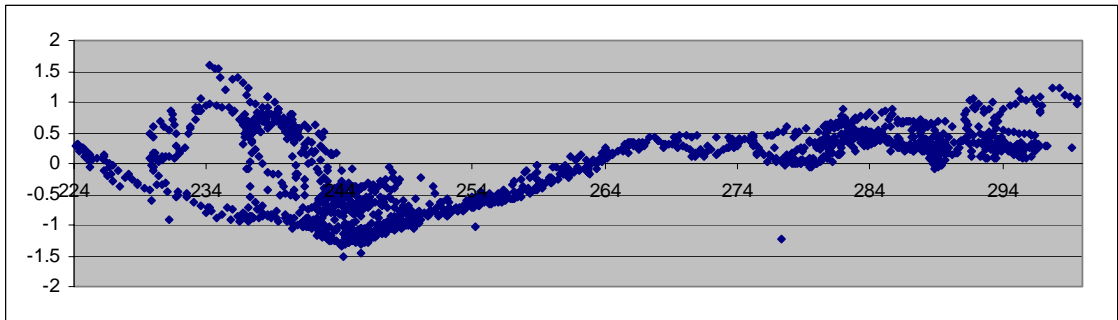


Figure 4.29: Comparing results with GPS/Leveling data (m)

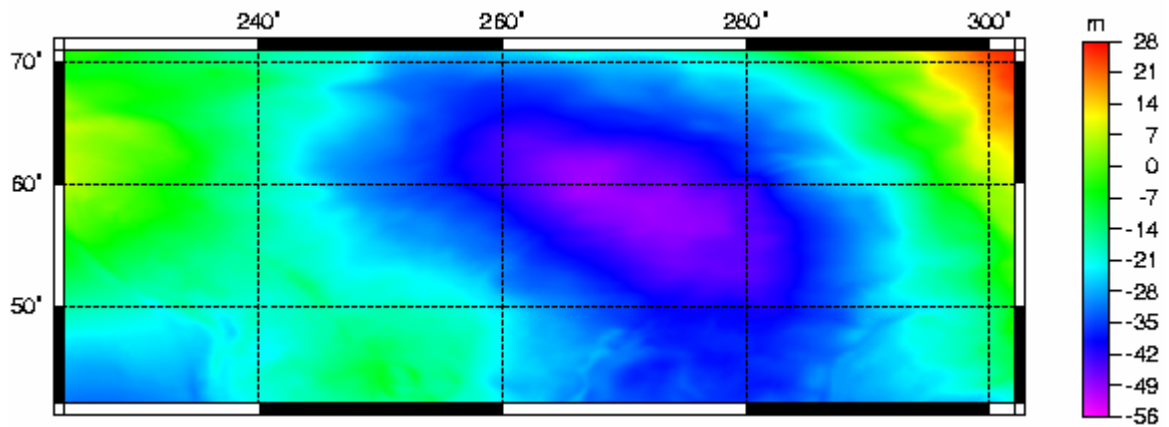


Figure 4.30: Geoid model based on two-space Stokes-Helmert scheme (m)

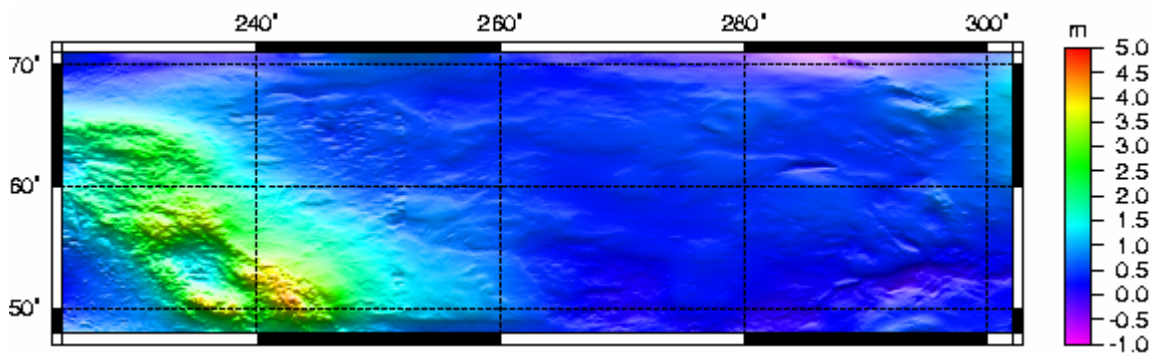


Figure 4.31: Difference between two Canadian geoid models (m)

There are four key factors that make the new model, Geoid_UNB2004 better than its predecessor: (i) the implementation of the free-air gravity anomaly as initial gravity data, which is theoretically more reasonable than Simple Bouguer gravity anomaly adopted in the computation of the Geoid_UNB2000; (ii) the application of the improved theory, in which the NT gravity anomaly on the Earth surface regarded as being smoother than the Helmert gravity anomaly is adopted for the downward continuation; (iii) the consideration of DTE-density and DCTE-density by using the Digital Topographical Density Model; and (iiii) the correction of the PITE program to certify the numerical results consistent with the related theory.

4.10 Comparison Canadian geoid models between UNB's and GSD's

The Canadian Gravimetric Geoid 2000 (CGG2000) was released by the Geodetic Survey Division (GSD) of Canada. It is generally built on the two-space Stokes-Helmert's scheme as well. However, the derivation of the boundary value, i.e., the Helmert gravity anomaly (see Véronneau, 2000) seems rather strange and is obviously different from the corresponding approach used in UNB. Additionally, the procedure of downward continuation is omitted due to its instability.

In order to compare CGG2000 with Geoid_UNB2004, they have to be in the same format. The software GPS-Hv2.1 (GPS·H functions as converter from NAD83 ellipsoidal heights to CGVD28 orthometric heights.) was adopted to interpolate into 5'

by 5' resolution geoid model (Figure 4.32), which is same as Geoid_UNB2004. The boundary was set by north latitudes 48° and 71°, and by east longitudes 224° and 302°.

CGG2000 in the investigated region ranges from -49.115m to 27.171m with a standard deviation ± 15.487 m. The difference between Geoid-UNB2004 and CGG2000 is shown in Figure 4.33, which ranges from -3.171m to 1.563m with a standard deviation ± 0.550 m. The comparison between CGG2000 and GPS/Leveling is depicted in Figure 4.34 and the difference ranges from -1.458m and 0.171m with a standard deviation ± 0.239 m. The systematic biases and tilt should be eliminated by using a four-parameter transformation as well.

Two geoid models have exact same pattern with high frequency character. However, the difference can not be neglected especially in west part and southeast part of sea regions. Additionally, two small areas in Hudson Strait and Foxe Bay still exist the big difference. The difference should be resulted from four main factors: (i) the difference methodology is employed to calculate the Helmert anomaly; (ii) the downward continuation and topographical density variation are not considered in the CGG2000; (iii) the more accuracy detailed DTM for the provinces of British Columbia, Albert and New Brunswick better than 10 meters is used in GSD; and (iiii) the Helmert gravity is adopted as the original gravity data in GSD.

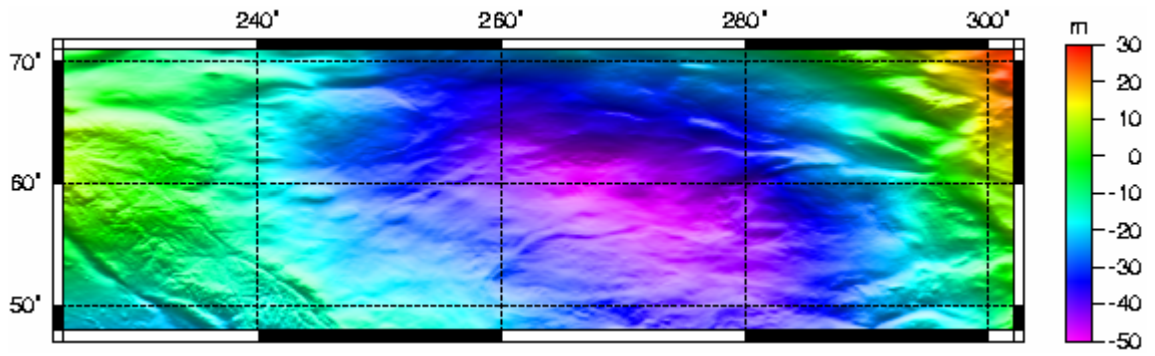


Figure 4.32: CGG2000 of GSD (m)

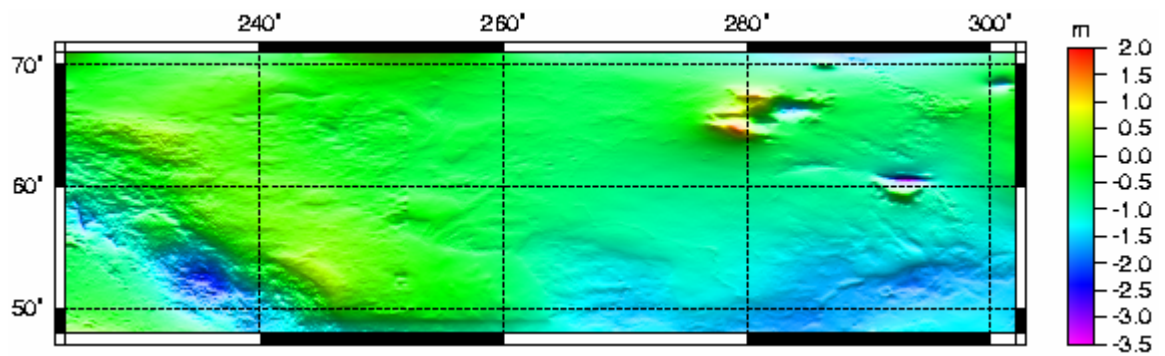


Figure 4.33: Difference between Geoid_UNB2004 and CGG2000 (m)

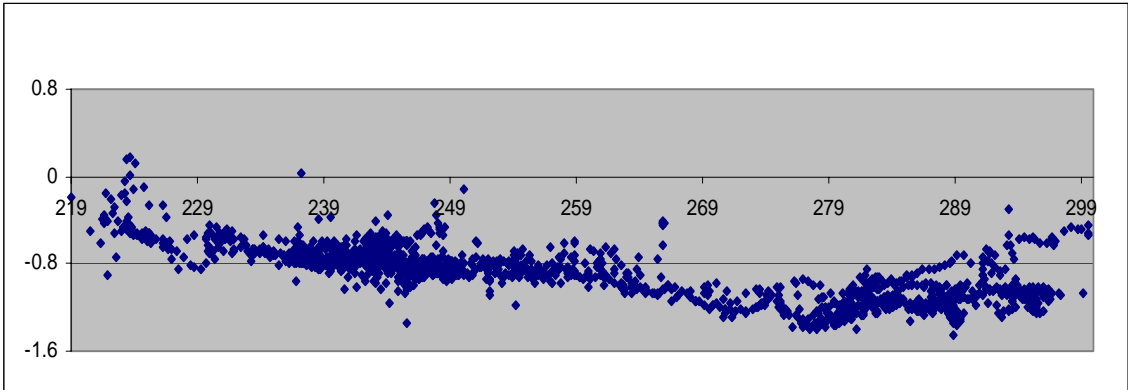


Figure 4.34: Comparison between CGG2000 and GPS/Levelings (m)

Chapter 5

Conclusions and Recommendations

Each program in the package has been numerically tested and results towards the Canadian gravimetric geoid model have been generated. This preliminary solution requires further improvement, as becomes clear from the direct comparison with GPS/Leveling data. The long wavelength part of the differences between the geoid solution and GPS/Leveling is obvious. Other systematic effects, such as the bias and vertical deflection between the geometric geoid model and gravimetric geoid model seem to exist. Treating these effects might reduce the differences.

Both the Digital Terrain Model and the Digital Topographical Density Model are employed in the evaluation of the topographical effect, the secondary indirect topographical effect, the condensed topographical effect, the secondary indirect condensed topographical effect, and the primary indirect topographical effect. According to the integration sub-domain and the corresponding required input data, both of them play an important role in the near zone contribution to the large magnitude of each effect.

Based on the three-space scenario Stokes-Helmert scheme, the application of downward continuation of gravity anomaly from the Earth's surface to the geoid in the NT-space (which amounts to more than one hundred of mGals) is regarded as an essential step. It is obtained by the solution of the inverse Poisson integral equation, which can be evaluated theoretically (Sun and Vaniček, 1998), despite the existence of the Poisson kernel's singularity. However, in practical application, the numerical results seem unstable. Sometimes they change irregularly from a large negative value to a positive one (or vice versa) in the neighboring grids.

The primary indirect topographical effect on geoidal height is calculated by applying Bruns formula (Bruns, 1878) to the residual topographical potential evaluated at the geoid, which is regarded as the difference between the actual geoidal height and the Helmert co-geoidal height and is systematically negative; i.e., the Helmert co-geoid is always above the geoid (Vaniček *et al.*, 1995). The practical numerical results coincide with the theory and are fully suitable for geoid determination over Canada.

During the computation of the Canadian geoid, several problems have been encountered, and the associated recommendations are made as following:

- For precise evaluation of the direct topographical and condensed topographical effects, a more detailed DTM is required, especially over the Rocky Mountains. In the best possible scenario, with the 1" by 1" detailed DTM or even denser, one can meet the 1 cm accuracy, which is the final objective in geoid determination.
- Similar to detailed DTM, the DTDM needs to be more accurate and denser to reflect the reality of its topographical character, especially in mountainous

regions, and to be of larger coverage if the objective is the determination of the geoid across the whole of Canada.

- Because of the instability of the downward continuation, more effort should be made to check the implementation of the associated theoretical methodology.
- The applied programs of SITE_NT, SITE_H, DAE_NT, DAE_H, SIAE_NT, SIAE_H, and PITE were written using old standard C++ language, which can be compiled only by the version GCC 2.56 contained in the Linux operating system. For ease of use in more common applications, it is recommended to employ an updated version of C++.
- Currently, the so-called DTE program, which combines the previous STC_near_zone, STC_far_zone, SCTC_near_zone, SCTC_far_zone, DTE_density, and DCTE_density, can produce DTE-density, DCTE-density, and their two associated output files. One output shows the effects of STC-near-zone, STC-far-zone, and Bouguer shell together; the other displays all the effects of SCTC-near-zone, SCTC-far-zone and condensed Bouguer shell. Neither have any physical meaning.
- Several frequently used programs for transforming data formats or manipulating the data files (such as “grid1_CDED.c”, “grid2_CDED.c” to generate the detailed DTM file, etc.) most of which were coded by the author, should be added to the reference Manual III as auxiliary routines.
- In the process of completely removing the topographical masses and condensing them onto the geoid surface, the estimated orthometric heights are used. Due to

orthometric heights' roughness, the resulting space's harmonicity and its consequent effects on the final digital geoid should be reconsidered.

References

- Bessel, F.W. (1837). “Über den Einfluss der Unregelmässigkeiten der Figur der Erde auf geodätische Arbeiten und ihre Vergleichung mit den Astronomischen Bestimmungen.” *Astronomische Nachrichten*, T.14, No. 269.
- Bruns, H. (1878). *Die Figur der Erde*. Berlin, Publ. Preuss. Geod. Inst.
- Bomford, G. (1971). *Geodesy*. 3rd edition, Clarendon Press.
- Featherstone, W. E., J. Evans, and P. Vaníček (1999). “Optimal selection of the degree of geopotential model and integration radius in regional gravimetric geoid computation.” IUGG General Assembly, Birmingham, July 18 – 30.
- Gauss, C. F. (1828). “Bestimmung des Breitenunterschiedes zwischen den Sternwarten von Göttingen und Altona durch Beobachtungen am Ramsdenschen Zenithsector.” *Vanderschoeck und Ruprecht*, Göttingen.
- Gradshteyn, I. S., and I. M. Ryzhik (1980). *Table of Integrals, Series and Products*. Corrected and enlarged edition, Translated by A. Jeffrey, Academic Press, New York.
- Heck, B. (1993). “A revision of Helmert’s second method of condensation in the geoid and quasigeoid determination.” Presented at 7th I.A.G. Symposium, Geodesy and Physics of the Earth“, No. 112, Potsdam, October 1992.
- Heiskanen, W. H., and H. Moritz (1967). *Physical geodesy*. W. H. Freeman and Co., San Francisco.
- Helmert, F.R. (1884). *Die mathematische und physikalische Theorien der höheren Geodäsie*. B. G. Teubner, Leipzig.

- Hobson, E. W. (1931). "The theory of spherical and ellipsoidal harmonics." *Cambridge University Press*. Cambridge.
- Huang, J., P. Vaníček, and P. Novák (2000). "An alternative algorithm to FFT for the numerical evaluation of Stokes' integral." *Studia Geophysica et Geodaetica*. No. 44, pp. 374-380.
- Huang, J., P. Vaníček, S. D. Pagiatakis, and W. Brink (2001). "Effect of topographical density on the geoid in the Rocky Mountains." *Journal of Geodesy*, Vol. 74. Springer.
- Huang, J., S. Pagiatakis, and P. Vaníček (2001). "On some numerical aspects of downward continuation of gravity anomalies." Paper presented at the IAG General Assembly, Budapest, Sept. 3 to 7.
- Huang, J., P. Vaníček, and S. Pagiatakis (2001). "Computational Methods for the Discrete Downward Continuation of the Earth Gravity." *IAG General Assembly*, Budapest.
- Huang, J. (2002). "Computational Methods for the Discrete Downward Continuation of the Earth Gravity and Effect of Lateral Topographical Mass Density Variation on Gravity and the Geoid." Ph.D. Thesis. University of New Brunswick, Fredericton, N. B., Canada.
- Janák, J., P. Vaníček, and B. Alberts (2001). "Point and mean values of topographical effects". Paper presented at The Digital Earth conference. Fredericton, June 25-28.
- Kellogg, O. D. (1929). *Foundations of potential theory*. Springer. Berlin.
- Lambert, W. D. (1930). "Reduction of the observed values of gravity to the sea level." *Bulletin Géodésique*, No.26.
- Listing, J. B. (1873). "Über unsere jetzige Kenntniss der Gestalt und Grösse der Erde." *Nachrichten von der Köning*. Göttingen VLG der Dietrichschen Buchhandlung.

- MacMillan, W. D. (1930). *The theory of the potential*. Dover, New York.
- Martinec, Z. (1993). "Effect of lateral density variations of topographical masses in view of improving geoid model accuracy over Canada." Final report of the contract DSS No. 23244-2-4356. Geodetic Survey of Canada, Ottawa.
- Martinec, Z., C. Matyska, E. W. Grafarend, and P. Vaniček (1993). "On Helmert's 2nd condensation method." *Manuscripta Geodaetica*, No.18. Springer.
- Martinec, Z., and P. Vaniček (1994a). "Direct topographical effect of Helmert's condensation for a spherical approximation of the geoid." *Manuscripta Geodaetica*, No.19. Springer.
- Martinec, Z., and P. Vaniček (1994b). "Indirect effect of topography in the Stokes-Helmert technique for a spherical approximation of the geoid." *Manuscripta Geodaetica*, No.19, Springer.
- Martinec, Z., P. Vaniček, A. Mainville, and M. Véronneau (1995). "The effect of lake water on geoidal height." *Manuscripta Geodaetica*, No.20. Springer.
- Martinec, Z. (1996). "Stability investigations of a discrete downward continuation problem for geoid determination in the Canadian Rocky Mountains." *Journal of Geodesy*, Vol. 70. Springer.
- Martinec, Z., and P. Vaniček (1996). "Formulation of the boundary-value problem for geoid determination with a higher-degree reference field." *Geophysical Journal International*, No. 126, pp. 219-228.
- Martinec, Z., P. Vaniček, A. Mainville, and M. Véronneau (1996). "Evaluation of topographical effects in precise geoid computation from densely sampled heights." *Journal of Geodesy*, Vol. 70, Springer.
- Martinec, Z. (1998). "Boundary value problems for gravimetric determination of a precise geoid." *Lecture notes in earth sciences*, Vol. 73, Springer.

- Molodensky, M. S., V. F. Yeremeev, and M. I. Yurkina (1960). *Methods for Study of the External Gravitational Field and Figure of the Earth*. TRUDY Ts NIIGAiK, 131, Geodezizdat, Moscow. English transl.: Israel Program for Scientific Translation, pp 248, Jerusalem 1962.
- Moritz, H. (1980). *Advanced Physical Geodesy*, H. Wichmann, Karlsruhe.
- Najafi, M. A. (1996). "Contributions towards the computation of a precise regional geoid." Ph.D. Thesis, University of New Brunswick, Fredericton, NB, Canada.
- Novák, P., and P. Vaníček (1998). "Atmospheric Corrections for the Evaluation of Mean Helmert's Gravity Anomalies." Paper presented at CGU Annual Meeting, Quebec City, May 18-20.
- Novák, P. (2000). "Evaluation of gravity data for the Stokes-Helmert solution to the geodetic boundary-value problem." Ph.D. Thesis, University of New Brunswick, Fredericton, NB, Canada.
- Novák, P., P. Vaníček, Z. Martinec, and M. Véronneau (2001). "Effect of the spherical terrain on gravity and the geoid." *Journal of Geodesy*, Vol.75, Springer.
- Novák, P., P. Vaníček, M. Véronneau, S. Holmes, and W. E. Featherstone (2001). "On the accuracy of modified Stokes's integration in high-frequency gravimetric geoid determination." *Journal of Geodesy*, Vol.74, Springer.
- Pick, M., J. Pícha, V. Vyskočil (1973). *Theory of the Earth's Gravity Field*. Elsevier, Amsterdam.
- Pizzeti, P. (1911). Sopra il calcolo teorico delle deviazioni del geoide dall' ellissoide. Atti Reale Accademia delle Scienze, V. 46, Torino.
- Ralston, A. (1965). *A First Course in Numerical Analysis*. McGraw-Hill, New York.

- Sideris, M., P. Vaniček, J. Huang, and I. N. Tsiavos (1999). "Comparison of downward continuation techniques of terrestrial gravity anomalies." Paper presented at IUGG General Assembly, Birmingham, July 18 – 30.
- Sjöberg, L. E. (1998). "The atmospheric geoid and gravity corrections." *Bolletino di Geodesia e Scienze Affini*, 57.
- Sjöberg, L. E. (1999). "The IAG approach to the atmospheric geoid correction in Stokes' formula and a new strategy." *Journal of Geodesy*, V.73, Springer.
- Smith, D. A. (2000). "Gravity and the geoid at NGS." Retrieved 29 October 2004 from the World Wide Web. <http://www.ngs.noaa.gov/GEOID/PRESENTATIONS/>
- Stokes, G. G. (1849). "On the variation of gravity on the surface of the Earth." *Transactions of the Cambridge Philosophical Society*, No. 8.
- Somigliana, C. (1929). "Teoria Generale del Campo Gravitazionale dell'Ellissoide di Rotazione." *Memoire della Societa Astronomica Italiana*, IV. Milano.
- Sun, W., and P. Vaniček (1995). "Downward continuation of Helmert's gravity disturbance." *IUGG General Assembly*, Boulder, Colo., July 1995.
- Sun, W., and P. Vaniček (1998). "On some problems of the downward continuation of the 5'x 5' mean Helmert gravity disturbance." *Journal of Geodesy*, Vol. 72. Springer.
- Tenzer, R., P. Vaniček, and S. Sluijs (2002). "The far-zone contribution to upward continuation of gravity anomalies." *Acta Geodaetica*, V. 3., Geographic service of the Army of the Czech Republic, Military Topographic Institute, Prague.
- Tenzer, R., P. Vaniček, and S. Sluijs (2002). "On Some Numerical Aspects of Primary Indirect Topographical Effect Computation in the Stokes-Helmert Theory of the Geoid Determination." *Acta Geodaetica*, Vol. 4., Geographic service of the Army of the Czech Republic, Military Topographic Institute, Prague.

- Tenzer, R., P. Vaníček, and P. Novák (2003). “Far-zone contributions to topographical effects in the Stokes-Helmert method of the geoid determination.” *Studia Geophysica et geodaetica*, Academy of Science of the Czech Republic, Geophysical Institute in Prague, Prague, Czech Republic.
- Tenzer, R., and P. Vaníček (2003). “New Result for UNB Geoid.” Paper presented at the Annual scientific meeting, Canadian Geophysical Union, May 10 - 14, Banff, Canada.
- Tenzer, R., P. Novák, J. Janák, J. Huang, M. Najafi, P. Vajda, and M. Santos (2003). “A Review of the UNB Approach for Precise Geoid Determination Based on the Stokes-Helmert Method.” Honoring the academic life of Petr Vaníček, M. Santos (Ed.), Department of Geodesy and Geomatics Engineering, Technical Report No. 218, Fredericton, NB, Canada.
- Tenzer, R., and P. Vaníček (2003). “Formulation of the Stokes-Helmert method of geoid determination for the No Topography space.” *Journal of Geodesy*, Springer.
- Vaníček, P., and E. Krakiwsky (1986). *Geodesy: The concepts*. 2nd rev. ed., Elsevier Science B.V., Amsterdam.
- Vaníček, P., and A. Kleusberg (1987). “The Canadian geoid – Stokesian approach. Compilation of a precise regional geoid.” *Manuscripta Geodaetica*, No.12, Springer.
- Vaníček, P., and L. E. Sjöberg (1989). “Kernel modification in generalized Stokes's technique for geoid determination.” Paper presented at the General Meeting of IAG Edinburgh, Scotland, Aug. 3-12, Sea Surface Topography and the Geoid (Eds. H. Sünkel and T. Baker), Springer, 1990.
- Vaníček, P., and L. E. Sjöberg (1991). “Reformulation of Stokes's Theory for Higher Than Second-Degree Reference Field and Modification of Integration Kernels.” *Journal of Geophysical research*, V. 96, No.B4.

- Vaniček, P., and N. Christou (1993). "Geoid and its geophysical interpretations." *CRC Press*, Boca Raton, Fla., USA. 343 pp.
- Vaniček, P., and Z. Martinec (1994). "The Stokes-Helmert scheme for the evaluation of a precise geoid." *Manuscripta Geodaetica*, No.19., Springer.
- Vaniček, P., M. Najafi, Z. Martinec, L. Harrie, and L. E. Sjöberg (1995). "Higher-degree reference field in the generalised Stokes-Helmert scheme for geoid computation." *Journal of Geodesy*, Vol. 70, Springer.
- Vaniček P., Sun W., Ong P., Martinec Z., Najafi M., Vajda P., Horst B., 1996: Downward continuation of Helmert's gravity. *Journal of Geodesy*, Vol. 71, Springer.
- Vaniček, P., M. Véronneau, and Z. Martinec (1997). "Determination of mean Helmert's anomalies on the geoid." *IAG General Assembly*, Rio de Janeiro, Sept. 3 to 9.
- Vaniček, P., and W. E. Featherstone (1998). "Performance of three types of Stokes's kernel in the combined solution for the geoid." *Journal of Geodesy*, Vol.72, Springer.
- Vaniček, P., J. Huang, P. Novák, S. D. Pagiatakis, M. Véronneau, Z. Martinec, W. E. Featherstone (1999). "Determination of the boundary values for the Stokes-Helmert problem." *Journal of Geodesy*, Vol.73, Springer.
- Vaniček, P., and P. Novák (1999). "Comparison between planar and spherical models of topography." Paper presented at CGU Annual Meeting, Banff, May 9 -12, 1999.
- Vaniček, P., J. Janák, and J. Huang (2000). "Mean Vertical Gradient of Gravity". Poster presentation at GGG2000 conference, Banff, July 28 – August 3.

- Vaniček, P., and J. Janák (2000). "Truncation of 2D spherical convolution integration with an isotropic kernel." Paper presented at the Algorithms 2000 conference, Tatranska Lomnica, Slovakia, September 15-18.
- Vaniček, P., and J. Janák (2001). "The UNB technique for precise geoid determination." Paper presented at CGU annual meeting, Banff, May 26, 2000.
- Vaniček, P., P. Novák, and Z. Martinec (2001). "Geoid, topography, and the Bouguer plate or shell." *Journal of Geodesy*, V.75, Springer.
- Vaniček, P., R. Tenze, and J. Huang (2003). "The role of No Topography space in the Stokes-Helmert technique for geoid determination." Paper presented at the Annual scientific meeting, Canadian Geophysical Union, May 10 - 14, 2003, Banff, Canada.
- Vaniček, P., J. Janák, and W. E. Featherstone (2003). "Truncation of spherical convolution integrals with an isotropic kernel." *Studia Geophysica et geodaetica*, Academy of Science of the Czech Republic, Geophysical Institute in Prague, Prague, Czech Republic.
- Véronneau, M. (2000). "The Canadian gravimetric geoid model of 2000 (CGG2000)." GSD.
- Wichiencharoen, C. (1982). "The indirect effects on the computation of geoid undulations." Report No.336, Ohio State University, Columbus.
- Yang, H., R. Tenzer, P. Vaniček, and M. Santis (2004). "Atmospheric effect in the three-space scenario for the Stokes-Helmert method of geoid determination." Paper presented at the AGU and CGU Joint Conference, May 17-21, Montreal, Canada.

Appendix A

A.1 H_read.c

```
#include <stdio.h>

/* Program for working with binary DEM file.
Input file:
1st row: Latitude of NW corner in (deg min sec), must be < 84 00 00,
2nd row: Longitude of NW corner in (deg min sec), must be > -170 00 00,
3rd row: Area in latitude in (deg min sec),
4th row: Area in longitude in (deg min sec),
5th row: Step in latitude 1: 30x30 sec, 2: 60x60 sec, etc.,
6th row: Step in longitude 1: 30x30 sec, 2: 60x60 sec, etc.
Output file :
ascii, from north to south, from west to east
header: latmin, latmax, lonmin, lonmax, dlat, dlon (in degrees). */

main()
{
FILE *fr;
short int i,j,p,q,value,dlat,dlon;
int nwr,nwc,r,c,n,m,n1,n2,n3,w1,w2,w3,nn1,nn2,nn3,nw1,nw2,nw3;
long int k,south,north,west,east,nns,nws,val;
double meanval,latmin,latmax,lonmin,lonmax,dla,dlo;

/* reading of the input file data */

scanf("%d %d %d",&nn1,&nn2,&nn3);
scanf("%d %d %d",&nw1,&nw2,&nw3);
scanf("%d %d %d",&n1,&n2,&n3);
scanf("%d %d %d",&w1,&w2,&w3);
scanf("%d",&m);
scanf("%d",&n);

/* reading of the binary file header */

fr = fopen("DEM_NA_30s.byn","rb");
fread(&south, sizeof(long), 1, fr);
```

```

SwapByte( &south, 0, sizeof( long ));
fread(&north, sizeof(long), 1, fr);
SwapByte( &north, 0, sizeof( long ));
fread(&west, sizeof(long), 1, fr);
SwapByte( &west, 0, sizeof( long ));
fread(&east, sizeof(long), 1, fr);
SwapByte( &east, 0, sizeof( long ));
fread(&dlat, sizeof(short), 1, fr);
SwapByte( &dlat, 0, sizeof( short ));
fread(&dlon, sizeof(short), 1, fr);
SwapByte( &dlon, 0, sizeof( short ));

/* writing of the output file header */

dla=30*m/3600.0;
dlo=30*n/3600.0;
latmax=((nn3/60.0+nn2)/60.0+nn1)-dla/2;
latmin=latmax-((n3/60.0+n2)/60.0+n1)+dla;
lonmin=(-(nw3/60.0+nw2)/60.0+nw1)+dlo/2;
lonmax=lonmin+((w3/60.0+w2)/60.0+w1)-dlo;

printf("%10.5lf%10.5lf%11.5lf%11.5lf%13.10lf%13.10lf\n\n",latmin,latmax,360.0+lon
min,360.0+lonmax,dla,dlo);

/* computing of the start reading position */

nns=nn1*3600+nn2*60+nn3;
nws=nw1*3600-nw2*60-nw3;
r=(n1*3600+n2*60+n3)/30;
c=(w1*3600+w2*60+w3)/30;
nwr=(north+15-nns)/30;
nwc=(15-west+nws)/30;
i=nwr; j=nwc;
k=80+(38400*(nwr))+(2*(nwc));
fseek(fr, k, SEEK_SET);

/* reading and processing the data */

if (m==1 && n==1) {
for(i=nwr;i<nwr+r;i++) {
for(j=nwc;j<nwc+c;j++) {
fread(&value, sizeof( short ), 1, fr);
SwapByte(&value, 0, sizeof( short ));
printf("%5d",value);
}
printf("\n\n");
}
}

```

```

    k=k+38400;
    fseek(fr, k, SEEK_SET);
}
}
else {
    val=0;
    for(i=1;i<=(r/m);i++) {
        for(j=1;j<=(c/n);j++) {
            for(p=1;p<=m;p++) {
                for(q=1;q<=n;q++) {
                    fread(&value, sizeof ( short ), 1, fr);
                    SwapByte(&value, 0, sizeof( short ));
                    val=val+value;
                }
            }
            k=k+38400;
            fseek(fr, k, SEEK_SET);
        }
        meanval=val/(m*n);
        val=0;
        printf("%5.0f",meanval);
        k=k-(m*38400)+(2*n);
        fseek(fr, k, SEEK_SET);
    }
    printf("\n\n");
    k=k+(m*38400)-2*n*(c/n);
    fseek(fr, k, SEEK_SET);
}
}
fclose(fr);
}

int SwapByte( char *buf, int start_byte , int num_bytes )
{
    char    temp;
    if (num_bytes == 2) {
        temp = buf[start_byte];
        buf[start_byte] = buf[start_byte + 1];
        buf[start_byte + 1] = temp;
        return( 1 );
    }
    else if (num_bytes == 4) {
        temp = buf[start_byte];
        buf[start_byte] = buf[start_byte + 3];
        buf[start_byte + 3] = temp;
        temp = buf[start_byte + 1];
        buf[start_byte + 1] = buf[start_byte + 2];

```

```

    buf[start_byte + 2] = temp;
    return( 1 );
}
else if (num_bytes == 8) {
    temp = buf[start_byte];
    buf[start_byte] = buf[start_byte + 7];
    buf[start_byte + 7] = temp;
    temp = buf[start_byte + 1];
    buf[start_byte + 1] = buf[start_byte + 6];
    buf[start_byte + 6] = temp;
    temp = buf[start_byte + 2];
    buf[start_byte + 2] = buf[start_byte + 5];
    buf[start_byte + 5] = temp;
    temp = buf[start_byte + 3];
    buf[start_byte + 3] = buf[start_byte + 4];
    buf[start_byte + 4] = temp;
    return( 1 );
}
else {
    printf("swap_bytes: num_bytes not one of 2 or 4.\n");
    exit(1);
}
}

```

A.2 H_grid.c

```

#include <stdio.h>
#include <math.h>
main()
{
    FILE *fr, *fw;
    int i,j,r,c;
    float h;
    float *val;
    double bmin,bmax,lmin,lmax,db,dl,lon,lat;
    char ifile[80], ofile[80];
    h = 0.0;
    fr = fopen("H_grid.opt","r");
    fscanf(fr,"%s",ifile);
    fscanf(fr,"%s",ofile);
    fclose(fr);
    fr = fopen(ifile,"r");
    fscanf(fr,"%lf %lf %lf %lf %lf %lf",&bmin,&bmax,&lmin,&lmax,&db,&dl);
    r = floor((bmax - bmin)/db + 1.1);
    c = floor((lmax - lmin)/dl + 1.1);

```



```

val = (float *) malloc((r*c + 1) * sizeof (float));
for (i=0; i < r; i++) {
    for (j=0; j < c; j++) {
        fscanf(fr, "%f", &val[i*c + j]);
    }
}
fclose(fr);
fw = fopen(ofile, "w");
for (i=0; i < r; i++) {
    lat = bmax - i*db;
    for (j=0; j < c; j++) {
        lon = lmin + j*dl;
        fprintf(fw, "%10.5lf%10.5lf%7.1fn", lat, lon, val[i*c + j]);
    }
}
fclose(fw);
}

```

A.3 subarea.c

```

#include <stdio.h>
#include <math.h>

main()
{
    FILE *fr, *fw;
    int i,j,n,r,c;
    double val,a1,a2;
    double *lat1, *lon1, *val1;
    double bmin,bmax,lmin,lmax,step,lon,lat;
    char ifile[80], ofile[80];
    step = 0.0833333333;
    fr = fopen("subarea.opt", "r");
    fscanf(fr, "%s %d", ifile, &n);
    fscanf(fr, "%s", ofile);
    fscanf(fr, "%lf %lf %lf %lf", &bmin, &bmax, &lmin, &lmax);
    fclose(fr);
    r = floor((bmax - bmin)/step + 0.1);
    c = floor((lmax - lmin)/step + 0.1);
    printf("\n %d %d\n", r, c);
    val1 = (double *) malloc((r*c+1)*sizeof(double));
    lat1 = (double *) malloc((r*c+1)*sizeof(double));
    lon1 = (double *) malloc((r*c+1)*sizeof(double));
    fr = fopen(ifile, "r");

```

```

fw = fopen(ofile,"w");
j = 0;
for (i=0; i < n; i++) {
    fscanf(fr, "%lf %lf %lf",&lat,&lon,&val);
    if(lat > bmin && lat < bmax && lon > lmin && lon < lmax) {
        lat1[j] = lat;
        lon1[j] = lon;
        val1[j] = (double) val;
        j++;
    }
}
printf("\n%d\n",j);
fclose(fr);
for (i=0; i < r; i++) {
    for (j=0; j < c; j++) {
        fprintf(fw, "%9.4lf%9.4lf%9.3lf\n",lat1[i*c+j],lon1[i*c+j],val1[i*c+j]);
        /* fprintf(fw, "%9.4lf%9.4lf%9.3lf\n",lat1[i*c+j],lon1[i*c+j],val1[i*c+j]); */
    }
}
fclose(fw);
}

```

Appendix B

B.1 grid1_CDED.c

```
#include <stdio.h>
```

```
/* It was written by Huaining Yang in Sep. 22, 2004.
```

```
It was used to produce detailed DTM with resolution 3" by 3" in Binary format with  
hight of zeor.
```

```
Using gcc -lm -o./grid002.e grid002.c to compile the program;
```

```
Using ./grid002.e N66W233_H.byn 36 230 to run the program. */
```

```
typedef struct binfile_data
```

```
{  
    FILE    *File;  
    char    Name[80];  
    double  South;  
    double  North;  
    double  West;  
    double  East;  
    double  DLat;  
    double  DLon;  
    double  Factor;  
    double  FactorSD;  
    short int NLat;  
    short int NLon;  
    short   StdDev;  
    short   Global;  
    short   Type;  
    short   SizeOf;  
    short   Datum;  
    short   Ellipsoid;  
    short   ByteOrder;  
    short   Scale;  
} BINFILE;
```

```
int SwapByte( char *buf, int start_byte , int num_bytes )
```

```

{
    char    temp;
    if (num_bytes == 2) {
        temp = buf[start_byte];
        buf[start_byte] = buf[start_byte + 1];
        buf[start_byte + 1] = temp;
        return( 1 );
    }
    else if (num_bytes == 4) {
        temp = buf[start_byte];
        buf[start_byte] = buf[start_byte + 3];
        buf[start_byte + 3] = temp;
        temp = buf[start_byte + 1];
        buf[start_byte + 1] = buf[start_byte + 2];
        buf[start_byte + 2] = temp;
        return( 1 );
    }
    else if (num_bytes == 8) {
        temp = buf[start_byte];
        buf[start_byte] = buf[start_byte + 7];
        buf[start_byte + 7] = temp;
        temp = buf[start_byte + 1];
        buf[start_byte + 1] = buf[start_byte + 6];
        buf[start_byte + 6] = temp;
        temp = buf[start_byte + 2];
        buf[start_byte + 2] = buf[start_byte + 5];
        buf[start_byte + 5] = temp;
        temp = buf[start_byte + 3];
        buf[start_byte + 3] = buf[start_byte + 4];
        buf[start_byte + 4] = temp;
        return( 1 );
    }
    else {
        printf("swap_bytes: num_bytes not one of 2 or 4.\n");
        exit(1);
    }
}

```

```

short ReadBinaryFileHeaderSwap( BINFILE *BinFile )
{
    double Scale, Tmp8;
    long int Tmp4;
    short int Tmp2 , i;

    if( !(BinFile->File = fopen( BinFile->Name, "rb")))

```

```

return( 0 );

fread( &Tmp4 , sizeof( long ) , 1 , BinFile->File );
SwapByte( (char *)&Tmp4 , 0 , 4 );
BinFile->South = Tmp4/3600.0;
fread( &Tmp4 , sizeof( long ) , 1 , BinFile->File );
SwapByte( (char *)&Tmp4 , 0 , 4 );
BinFile->North = Tmp4/3600.0;
fread( &Tmp4 , sizeof( long ) , 1 , BinFile->File );
SwapByte( (char *)&Tmp4 , 0 , 4 );
BinFile->West = Tmp4/3600.0;
fread( &Tmp4 , sizeof( long ) , 1 , BinFile->File );
SwapByte( (char *)&Tmp4 , 0 , 4 );
BinFile->East = Tmp4/3600.0;
fread( &Tmp2 , sizeof( short ) , 1 , BinFile->File );
SwapByte( (char *)&Tmp2 , 0 , 2 );
BinFile->DLat = Tmp2/3600.0;
fread( &Tmp2 , sizeof( short ) , 1 , BinFile->File );
SwapByte( (char *)&Tmp2 , 0 , 2 );
BinFile->DLon = Tmp2/3600.0;

fread( &Tmp2 , sizeof( short ) , 1 , BinFile->File );
SwapByte( (char *)&Tmp2 , 0 , 2 );
BinFile->Global = Tmp2;
fread( &Tmp2 , sizeof( short ) , 1 , BinFile->File );
SwapByte( (char *)&Tmp2 , 0 , 2 );
BinFile->Type = Tmp2;
fread( &Tmp8 , sizeof( double ) , 1 , BinFile->File );
SwapByte( (char *)&Tmp8 , 0 , 8 );
BinFile->Factor = Tmp8;
fread( &Tmp2 , sizeof( short ) , 1 , BinFile->File );
SwapByte( (char *)&Tmp2 , 0 , 2 );
BinFile->SizeOf = Tmp2;
fread( &Tmp2 , sizeof( short ) , 1 , BinFile->File );
SwapByte( (char *)&Tmp2 , 0 , 2 );
BinFile->StdDev = Tmp2;
fread( &Tmp8 , sizeof( double ) , 1 , BinFile->File );
SwapByte( (char *)&Tmp8 , 0 , 8 );
BinFile->FactorSD = Tmp8;
fread( &Tmp2 , sizeof( short ) , 1 , BinFile->File );
SwapByte( (char *)&Tmp2 , 0 , 2 );
BinFile->Datum = Tmp2;
fread( &Tmp2 , sizeof( short ) , 1 , BinFile->File );
SwapByte( (char *)&Tmp2 , 0 , 2 );
BinFile->Ellipsoid = Tmp2;
fread( &Tmp2 , sizeof( short ) , 1 , BinFile->File );

```

```

SwapByte( (char *)&Tmp2 , 0 , 2 );
BinFile->ByteOrder = Tmp2;
fread( &Tmp2 , sizeof( short ) , 1 , BinFile->File );
SwapByte( (char *)&Tmp2 , 0 , 2 );
BinFile->Scale = Tmp2;

/* Read the dummy bytes */

for( i = 0 ; i < 7 ; i++ )
    fread( &Tmp4 , sizeof( long ) , 1 , BinFile->File );

Scale = ( BinFile->Scale ) ? 1000.0 : 1.0;
BinFile->South /= Scale;
BinFile->North /= Scale;
BinFile->West /= Scale;
BinFile->East /= Scale;
BinFile->DLat /= Scale;
BinFile->DLon /= Scale;

BinFile->NLat = ( BinFile->North - BinFile->South ) / BinFile->DLat + 1.5;
BinFile->NLon = ( BinFile->East - BinFile->West ) / BinFile->DLon + 1.5;

return( 1 );
}

double ReadBinaryFileDataSwap( BINFILE *BinFile )
{
    double Value;
    short int Tmp2;
    long int Tmp4;

    if( BinFile->SizeOf == 4 )
    {
        if( fread( &Tmp4 , sizeof( long ) , 1 , BinFile->File ) == 1 )
        {
            SwapByte( (char *)&Tmp4 , 0 , 4 );
            Value = Tmp4/BinFile->Factor;
        }
        else
            Value = 9999.0;
    }
    else
    {
        if( fread( &Tmp2 , sizeof( short ) , 1 , BinFile->File ) == 1 )
        {
            SwapByte( (char *)&Tmp2 , 0 , 2 );

```

```

if( Tmp2 != 32767 )
    { Value = Tmp2/BinFile->Factor; }
else
    { Value = 9999.0; }
}
else
    { Value = 9999.0; }
}

return( Value );
}

```

```

void WriteHeadFileSwap(long int North,long int West,long int South,long int East,
short int DLat,short int DLon,double factor,double FactorSD,
short int StdDev,short int Global,short int type,short int Sizeof,
short int Datum,short int Ellipsoid,short int ByteOrder,short int Scale,FILE *XYZ)

```

```

{
long int longint;
int s,t;

```

```

SwapByte( (char *)&South , 0 , 4 );
fwrite(&South,sizeof(long),1,XYZ);

```

```

SwapByte( (char *)&North , 0 , 4 );
fwrite(&North,sizeof(long),1,XYZ);

```

```

SwapByte( (char *)&West , 0 , 4 );
fwrite(&West,sizeof(long),1,XYZ);

```

```

SwapByte( (char *)&East , 0 , 4 );
fwrite(&East,sizeof(long),1,XYZ);

```

```

SwapByte( (char *)&DLat , 0 , 2 );
fwrite(&DLat,sizeof(short),1,XYZ);

```

```

SwapByte( (char *)&DLon , 0 , 2 );
fwrite(&DLon,sizeof(short),1,XYZ);

```

```

SwapByte( (char *)&Global , 0 , 2 );
fwrite(&Global,sizeof(short),1,XYZ);

```

```

SwapByte( (char *)&type , 0 , 2 );
fwrite(&type,sizeof(short),1,XYZ);

```

```

SwapByte( (char *)&factor , 0 , 8 );
fwrite(&factor,sizeof(double),1,XYZ);

```

```
SwapByte( (char *)&Sizeof , 0 , 2 );  
fwrite(&Sizeof,sizeof(short),1,XYZ);
```

```
SwapByte( (char *)&StdDev , 0 , 2 );  
fwrite(&StdDev,sizeof(short),1,XYZ);
```

```
SwapByte( (char *)&FactorSD , 0 , 8 );  
fwrite(&FactorSD,sizeof(double),1,XYZ);
```

```
SwapByte( (char *)&Datum , 0 , 2 );  
fwrite(&Datum,sizeof(short),1,XYZ);
```

```
SwapByte( (char *)&Ellipsoid , 0 , 2 );  
fwrite(&Ellipsoid,sizeof(short),1,XYZ);
```

```
SwapByte( (char *)&ByteOrder , 0 , 2 );  
fwrite(&ByteOrder,sizeof(short),1,XYZ);
```

```
SwapByte( (char *)&Scale , 0 , 2 );  
fwrite(&Scale,sizeof(short),1,XYZ);
```

```
longint=0;  
for( s = 0 ; s < 7 ; s++ )  
{  
SwapByte( (char *)&longint , 0 , 4 );  
fwrite(&longint , sizeof( long ) , 1 , XYZ );  
}  
}
```

```
int main(int argc, char *argv[])  
{  
BINFILE BinFile;  
FILE *XYZ;  
  
char buffer[80], xyzname[80], gridfile[80], tempstr[10];  
double value, latitude, longitude;  
long int i, j, east, west, size1, size2;  
short int newheight;  
short flag;  
long int gridinterval,max_lat,max_lon,min_lat,min_lon;  
  
if(argc<2){  
printf("usage: %s inputfiles outputfile\n",argv[0]);
```



```

        return 1;
    }

strcpy(buffer,argv[1]);
max_lat=atoi(argv[2]);
min_lon=atoi(argv[3]);
min_lat=max_lat-1;
max_lon=min_lon+1;
size1 = size2 = 1201;
gridinterval=3;

strcpy( BinFile.Name , buffer );
ReadBinaryFileHeaderSwap( &BinFile );

strcpy(gridfile,"");
strcat(gridfile,"N");
sprintf(tempstr,"%d",max_lat);
strcat(gridfile,tempstr);
strcat(gridfile,"W");
sprintf(tempstr,"%d",min_lon);
strcat(gridfile,tempstr);
strcat(gridfile,"_H.byn");
printf("%s\n",gridfile);

strcpy( xyzname, gridfile );
XYZ = fopen(xyzname, "wb");
if ((max_lon>180) && (min_lon>180))
    {
        east=max_lon-360;
        west=min_lon-360;
    }

WriteHeadFileSwap(max_lat*3600,west*3600,min_lat*3600,east*3600,gridinterval,
gridinterval, BinFile.Factor, BinFile.FactorSD, BinFile.StdDev, BinFile.Global,
BinFile.Type, BinFile.SizeOf,BinFile.Datum, BinFile.Ellipsoid, BinFile.ByteOrder,
BinFile.Scale,XYZ);

for(i=0; i<1201; i++)
    {
        for(j=0; j<1201; j++)
            {
                newheight=0;
                SwapByte( (char *)&newheight , 0 , 2 );
                fwrite(&newheight,sizeof(short),1,XYZ);
            }
    }

```

```

fclose(BinFile.File);
fclose( XYZ );
return 0;

}

```

B.2 grid2_CDED.c

```

#include <stdio.h>
#include <math.h>

```

```

/* It was written by Huaining Yang in Sep. 29, 2004.
   It was used to produce detailed DTM with resolution
   3" by 3" in Binary format using 30" mean DTM data file.
   Using gcc -lm -o./grid004.e grid004.c to compile the program;
   Using ./grid004.e N66W233_H.byn DTM_30s.dat 36 230 to run the program. */

```

```

typedef struct binfile_data
{
    FILE    *File;
    char    Name[80];
    double  South;
    double  North;
    double  West;
    double  East;
    double  DLat;
    double  DLon;
    double  Factor;
    double  FactorSD;
    short int NLat;
    short int NLon;
    short   StdDev;
    short   Global;
    short   Type;
    short   SizeOf;
    short   Datum;
    short   Ellipsoid;
    short   ByteOrder;
    short   Scale;
} BINFILE;

```

```

int SwapByte( char *buf, int start_byte , int num_bytes )
{
    char    temp;
    if (num_bytes == 2) {
        temp = buf[start_byte];
        buf[start_byte] = buf[start_byte + 1];
        buf[start_byte + 1] = temp;
        return( 1 );
    }
    else if (num_bytes == 4) {
        temp = buf[start_byte];
        buf[start_byte] = buf[start_byte + 3];
        buf[start_byte + 3] = temp;
        temp = buf[start_byte + 1];
        buf[start_byte + 1] = buf[start_byte + 2];
        buf[start_byte + 2] = temp;
        return( 1 );
    }
    else if (num_bytes == 8) {
        temp = buf[start_byte];
        buf[start_byte] = buf[start_byte + 7];
        buf[start_byte + 7] = temp;
        temp = buf[start_byte + 1];
        buf[start_byte + 1] = buf[start_byte + 6];
        buf[start_byte + 6] = temp;
        temp = buf[start_byte + 2];
        buf[start_byte + 2] = buf[start_byte + 5];
        buf[start_byte + 5] = temp;
        temp = buf[start_byte + 3];
        buf[start_byte + 3] = buf[start_byte + 4];
        buf[start_byte + 4] = temp;
        return( 1 );
    }
    else {
        printf("swap_bytes: num_bytes not one of 2 or 4.\n");
        exit(1);
    }
}

```

```

short ReadBinaryFileHeaderSwap( BINFILE *BinFile )
{
    double Scale, Tmp8;
    long int Tmp4;
    short int Tmp2 , i;

```

```

if( !(BinFile->File = fopen( BinFile->Name, "rb")))
    return( 0 );

fread( &Tmp4 , sizeof( long ) , 1 , BinFile->File );
SwapByte( (char *)&Tmp4 , 0 , 4 );
BinFile->South = Tmp4/3600.0;
fread( &Tmp4 , sizeof( long ) , 1 , BinFile->File );
SwapByte( (char *)&Tmp4 , 0 , 4 );
BinFile->North = Tmp4/3600.0;
fread( &Tmp4 , sizeof( long ) , 1 , BinFile->File );
SwapByte( (char *)&Tmp4 , 0 , 4 );
BinFile->West = Tmp4/3600.0;
fread( &Tmp4 , sizeof( long ) , 1 , BinFile->File );
SwapByte( (char *)&Tmp4 , 0 , 4 );
BinFile->East = Tmp4/3600.0;
fread( &Tmp2 , sizeof( short ) , 1 , BinFile->File );
SwapByte( (char *)&Tmp2 , 0 , 2 );
BinFile->DLat = Tmp2/3600.0;
fread( &Tmp2 , sizeof( short ) , 1 , BinFile->File );
SwapByte( (char *)&Tmp2 , 0 , 2 );
BinFile->DLon = Tmp2/3600.0;

fread( &Tmp2 , sizeof( short ) , 1 , BinFile->File );
SwapByte( (char *)&Tmp2 , 0 , 2 );
BinFile->Global = Tmp2;
fread( &Tmp2 , sizeof( short ) , 1 , BinFile->File );
SwapByte( (char *)&Tmp2 , 0 , 2 );
BinFile->Type = Tmp2;
fread( &Tmp8 , sizeof( double ) , 1 , BinFile->File );
SwapByte( (char *)&Tmp8 , 0 , 8 );
BinFile->Factor = Tmp8;
fread( &Tmp2 , sizeof( short ) , 1 , BinFile->File );
SwapByte( (char *)&Tmp2 , 0 , 2 );
BinFile->SizeOf = Tmp2;
fread( &Tmp2 , sizeof( short ) , 1 , BinFile->File );
SwapByte( (char *)&Tmp2 , 0 , 2 );
BinFile->StdDev = Tmp2;
fread( &Tmp8 , sizeof( double ) , 1 , BinFile->File );
SwapByte( (char *)&Tmp8 , 0 , 8 );
BinFile->FactorSD = Tmp8;
fread( &Tmp2 , sizeof( short ) , 1 , BinFile->File );
SwapByte( (char *)&Tmp2 , 0 , 2 );
BinFile->Datum = Tmp2;
fread( &Tmp2 , sizeof( short ) , 1 , BinFile->File );
SwapByte( (char *)&Tmp2 , 0 , 2 );
BinFile->Ellipsoid = Tmp2;

```

```

fread( &Tmp2 , sizeof( short ) , 1 , BinFile->File );
SwapByte( (char *)&Tmp2 , 0 , 2 );
BinFile->ByteOrder = Tmp2;
fread( &Tmp2 , sizeof( short ) , 1 , BinFile->File );
SwapByte( (char *)&Tmp2 , 0 , 2 );
BinFile->Scale = Tmp2;

/* Read the dummy bytes */

for( i = 0 ; i < 7 ; i++ )
    fread( &Tmp4 , sizeof( long ) , 1 , BinFile->File );

Scale = ( BinFile->Scale ) ? 1000.0 : 1.0;
BinFile->South /= Scale;
BinFile->North /= Scale;
BinFile->West /= Scale;
BinFile->East /= Scale;
BinFile->DLat /= Scale;
BinFile->DLon /= Scale;

BinFile->NLat = ( BinFile->North - BinFile->South ) / BinFile->DLat + 1.5;
BinFile->NLon = ( BinFile->East - BinFile->West ) / BinFile->DLon + 1.5;

return( 1 );
}

double ReadBinaryFileDataSwap( BINFILE *BinFile )
{
    double Value;
    short int Tmp2;
    long int Tmp4;

    if( BinFile->SizeOf == 4 )
    {
        if( fread( &Tmp4 , sizeof( long ) , 1 , BinFile->File ) == 1 )
        {
            SwapByte( (char *)&Tmp4 , 0 , 4 );
            Value = Tmp4/BinFile->Factor;
        }
        else
            Value = 9999.0;
    }
    else
    {
        if( fread( &Tmp2 , sizeof( short ) , 1 , BinFile->File ) == 1 )
        {

```

```

SwapByte( (char *)&Tmp2 , 0 , 2 );
if( Tmp2 != 32767 )
    { Value = Tmp2/BinFile->Factor; }
else
    { Value = 9999.0; }
}
else
    { Value = 9999.0; }
}

return( Value );
}

```

```

void WriteHeadFileSwap(long int North,long int West,long int South,long int East,
short int DLat,short int DLon,double factor,double FactorSD,
short int StdDev,short int Global,short int type,short int Sizeof,
short int Datum,short int Ellipsoid,short int ByteOrder,short int Scale,FILE *XYZ)

```

```

{
    long int longint;
    int s,t;

```

```

    SwapByte( (char *)&South , 0 , 4 );
    fwrite(&South,sizeof(long),1,XYZ);

```

```

    SwapByte( (char *)&North , 0 , 4 );
    fwrite(&North,sizeof(long),1,XYZ);

```

```

    SwapByte( (char *)&West , 0 , 4 );
    fwrite(&West,sizeof(long),1,XYZ);

```

```

    SwapByte( (char *)&East , 0 , 4 );
    fwrite(&East,sizeof(long),1,XYZ);

```

```

    SwapByte( (char *)&DLat , 0 , 2 );
    fwrite(&DLat,sizeof(short),1,XYZ);

```

```

    SwapByte( (char *)&DLon , 0 , 2 );
    fwrite(&DLon,sizeof(short),1,XYZ);

```

```

    SwapByte( (char *)&Global , 0 , 2 );
    fwrite(&Global,sizeof(short),1,XYZ);

```

```

    SwapByte( (char *)&type , 0 , 2 );
    fwrite(&type,sizeof(short),1,XYZ);

```

```

    SwapByte( (char *)&factor , 0 , 8 );

```

```

fwrite(&factor,sizeof(double),1,XYZ);

SwapByte( (char *)&Sizeof , 0 , 2 );
fwrite(&Sizeof,sizeof(short),1,XYZ);

SwapByte( (char *)&StdDev , 0 , 2 );
fwrite(&StdDev,sizeof(short),1,XYZ);

SwapByte( (char *)&FactorSD , 0 , 8 );
fwrite(&FactorSD,sizeof(double),1,XYZ);

SwapByte( (char *)&Datum , 0 , 2 );
fwrite(&Datum,sizeof(short),1,XYZ);

SwapByte( (char *)&Ellipsoid , 0 , 2 );
fwrite(&Ellipsoid,sizeof(short),1,XYZ);

SwapByte( (char *)&ByteOrder , 0 , 2 );
fwrite(&ByteOrder,sizeof(short),1,XYZ);

SwapByte( (char *)&Scale , 0 , 2 );
fwrite(&Scale,sizeof(short),1,XYZ);

longint=0;
for( s = 0 ; s < 7 ; s++ )
{
fwrite(&longint , sizeof( long ) , 1 , XYZ );
}
}

```

```

int main(int argc, char *argv[])
{
BINFILE BinFile;
FILE *XYZ,*fr,*fp,*fpp;

char buffer1[80], buffer2[80],xyzname[80], xyzfile[80],abcfile[80];
char gridfile[80], tempstr[10], tempfile[80];
int m, n, i, j,s,t,temph,value;
int *h3, *h30, *hh30, rh30, ch30; /* dimensions of height 30" file */
double dbh30, dlh30; /* step of 30" data */
double bh30min,bh30max,lh30min,lh30max; /* min and max of 30" data */
double latitude, longitude;
long int east, west, size1, size2;
short int newheight;

```

```

short flag;
long int gridinterval,max_lat,max_lon,min_lat,min_lon;

int *h1,*h2;

if(argc<2)
{
    printf("usage: %s inputfiles outputfile\n",argv[0]);
    return 1;
}

strcpy(buffer1,argv[1]);
strcpy(buffer2,argv[2]);
max_lat=atoi(argv[3]);
min_lon=atoi(argv[4]);
min_lat=max_lat-1;
max_lon=min_lon+1;
size1 = size2 = 1201;
gridinterval=3;

fr = fopen(buffer2,"r");
fscanf(fr,"%lf %lf %lf %lf",&bh30min,&bh30max,&lh30min,&lh30max);
fscanf(fr,"%lf %lf",&dbh30,&dlh30);
printf("%lf %lf %lf %lf %lf
%lf\n",bh30min,bh30max,lh30min,lh30max,dbh30,dlh30);

rh30 = floor((bh30max - bh30min)/dbh30 + 1.1); /* Num. of rows */
ch30 = floor((lh30max - lh30min)/dlh30 + 1.1); /* Num. of columns */
h30 = (int *) malloc((rh30*ch30+1) * sizeof(int));

for(i = 0; i < rh30; i++)
{
    for(j = 0; j < ch30; j++)
    {
        fscanf(fr,"%d",&h30[i*ch30 + j]);
    }
}
fclose(fr);

m=floor((bh30max-max_lat)/dbh30);
n=floor((min_lon-lh30min)/dbh30);
strcpy(tempfile,"tempfile1");
fp=fopen(tempfile,"w");
for (i=0; i<121; i++)

```



```

        {
            for (j=0;j<121;j++)
            {
value=(h30[((m+i)*ch30+n+j)]+h30[((m+i)*ch30+n+j+1)]+h30[((m+i+1)*ch30+n+j)]+
h30[((m+i+1)*ch30+n+j+1)]/4;
                fprintf(fp," %d",value);
            }
        }
        fclose(fp);
        free(h30);

fp=fopen(tempfile,"r");
        hh30 = (int *) malloc((121*121+1)*sizeof(int));
        for (i=0; i<121; i++)
        {
            for (j=0;j<121;j++)
            {
                fscanf(fp, "%d", &hh30[i*121+j]);
            }
        }
        fclose(fp);

        strcpy(xyzfile,"tempfile2");
        fpp=fopen(xyzfile,"w");
        for (i=1; i<=121; i++)
        {
            for (j=1;j<=121;j++)
            {
                if (fmod(j,121)==0)
                {
                    fprintf(fpp," %d",hh30[(i-1)*121+j-1]);
                }
                else
                {
                    fprintf(fpp," %d",hh30[(i-1)*121+j-1]);
                    for (t=1;t<=9;t++)
                    {
                        value=hh30[(i-1)*121+j-1]+t*(hh30[(i-1)*121+j]-hh30[(i-1)*121+j-
1])/10;
                        fprintf(fpp," %d",value);
                    }
                }
            }
        }
    }
}

```

```

fclose(fpp);
free(hh30);

fp=fopen(xyzfile,"r");
strcpy(abcfile,"tempfile3");
fpp=fopen(abcfile,"w");
h1=(int *)malloc(1202*sizeof(int));
h2=(int *)malloc(1202*sizeof(int));

for(j=0;j<1201;j++)
{
fscanf(fp,"%d",&h1[j]);
}
for (i=1;i<121;i++) {
for(j=0;j<1201;j++) {
fscanf(fp,"%d",&h2[j]);
fprintf(fpp," %d",h1[j]);
}
}

for(t=1;t<=9;t++) {
for(j=0;j<1201;j++) {
temph=h1[j]+t*(h2[j]-h1[j])/10;
fprintf(fpp," %d",temph);
}
}
h1=(int*)realloc(h1,1201*sizeof(int));
for(j=0;j<1201;j++) {
h1[j]=h2[j];
}
h2=(int*)realloc(h2,1201*sizeof(int));
}

for(j=0;j<1201;j++) {
fprintf(fpp," %d",h1[j]);
}
fclose(fp);
fclose(fpp);

free(h1);
free(h2);

fp=fopen(abcfile,"r");
h3 = (int *) malloc((1201*1201+1) * sizeof(int));

```

```

for (i=0; i<1201; i++)
{
    for (j=0;j<1201;j++)
    {
        fscanf(fp, "%d", &h3[i*1201+j]);
    }
}
fclose(fp);

```

```

strcpy( BinFile.Name , buffer1 );
ReadBinaryFileHeaderSwap( &BinFile );

```

```

strcpy(gridfile,"");
strcat(gridfile,"N");
sprintf(tempstr,"%d",max_lat);
strcat(gridfile,tempstr);
strcat(gridfile,"W");
sprintf(tempstr,"%d",min_lon);
strcat(gridfile,tempstr);
strcat(gridfile,"_H.byn");
printf("%s\n",gridfile);

```

```

strcpy( xyzname, gridfile );
XYZ = fopen(xyzname, "wb");
if ((max_lon>180) && (min_lon>180))
{
    east=max_lon-360;
    west=min_lon-360;
}

```

```

WriteHeadFileSwap(max_lat*3600,west*3600,min_lat*3600,east*3600,gridinterval,
gridinterval, BinFile.Factor, BinFile.FactorSD, BinFile.StdDev, BinFile.Global,
BinFile.Type, BinFile.SizeOf,BinFile.Datum, BinFile.Ellipsoid, BinFile.ByteOrder,
BinFile.Scale,XYZ);

```

```

m=0;
for(i=0; i<1201; i++)
{
    for(j=0; j<1201; j++)
    {
        newheight=h3[m];
        SwapByte( (char *)&newheight , 0 , 2 );
        fwrite(&newheight,sizeof(short),1,XYZ);
        m++;
    }
}

```

```

    }

    fclose(BinFile.File);
    fclose( XYZ );
    free(h3);

}

```

B.3 grid3_CDED.c

```

#include <stdio.h>
#include <math.h>
#include <stdlib.h>
#include <string.h>
#include <stdarg.h>

```

```

/* This program was written by Huaining Yang in Sep. 12, 2004.
   This program is to divide 1 by 2 degree with 3" by 6" resolution or 1 by 4
   degree with 3" by 12" resolution Binary DTM into 1 by 1 degree with 3" by 3",
   which is compiled using gcc -lm -o./grid001.e grid001.c,
   and using ./grid001.e -inF BinaryFilename to run.  */

```

```

typedef struct binfile_data
{
    FILE      *File;
    char      Name[80];
    double    South;
    double    North;
    double    West;
    double    East;
    double    DLat;
    double    DLon;
    double    Factor;
    double    FactorSD;
    short int NLat;
    short int NLon;
    short     StdDev;
    short     Global;
    short     Type;
    short     SizeOf;
    short     Datum;
    short     Ellipsoid;
    short     ByteOrder;
}

```

```

    short    Scale;
} BINFILE;

void WriteHeaderSwap(long int North,long int West,long int South,long int East,
short int DLat,short int DLon,double factor,double FactorSD, short int StdDev,
short int Global,short int type,short int Sizeof, short int Datum,
short int Ellipsoid,short int ByteOrder,short int Scale,FILE *fp);
int SwapByte( char *buf, int start_byte , int num_bytes );
short ReadBinaryFileHeaderSwap( BINFILE *BinFile );
double ReadBinaryFileDataSwap( BINFILE *BinFile );

main(int argc, char **argv)

{
char inputfile[100],tempfile[100],gridfile[100],tempstr[10];
float max_lat,max_lon,min_lat,min_lon;
long int *latitude,*longitude;
int *height;
float templat,templon,tempheight;
int size1,size2, NN, NNN;
long int i,j,k,ii,jj;
long int grid_maxlat,grid_minlat,grid_minlon,grid_maxlon;
int m,n,gridinterval;
int num_lat, num_lon;
int minlat,maxlat,minlon,maxlon;
long int tempv,south,north,west,east;
short int sum, newheight;
long int newlon,newlat;

FILE *fp,*fp2;

BINFILE BinFile;
FILE *XYZ;
char xyzname[80],buffer[80];
double value1, latitude1, longitude1;
short flag;

while (*(++argv))
{
if (!strcmp (*argv, "-inF"))
{
if (!(++argv))
printf(" Need input file !!! ");
strcpy(buffer,*argv);
}
else

```

```

    printf("Hi, wrong input formate");
}

//read binary file .....then save these data into new ascii file--tempfile1
strcpy( BinFile.Name , buffer );
ReadBinaryFileHeaderSwap( &BinFile );

strcpy(xyzname,"tempfile1");
XYZ = fopen(xyzname, "w");

fprintf(XYZ,
"%12.4f%12.4f%12.4f%12.4f%6i%6i\n",BinFile.North,BinFile.West+360,
BinFile.South,BinFile.East+360,BinFile.NLat,BinFile.NLon);

m = BinFile.DLat*3600;
n = BinFile.DLon*3600;
printf("gridspan is %lf %lf %d %d\n",BinFile.DLat,BinFile.DLon, m, n);

for(i=0; i<BinFile.NLat; i++)
{
    latitude1 = BinFile.North - i*BinFile.DLat;
    for(j=0; j<BinFile.NLon; j++)
    {
        longitude1 = BinFile.West + j*BinFile.DLon;
        value1 = ReadBinaryFileDataSwap(&BinFile);
        if (value1 != 9999 )
            fprintf(XYZ, "%12.6f%12.6f%12.3f\n", latitude1, longitude1,
value1);
    }
}
fclose(BinFile.File);
fclose( XYZ );

// get data from .tempfile1, .....
// then divide whole region into 1 degree by 1 degree grid
// then at each of 1 by 1, find and interpolate 3 second by 3 second,
// and save 1x1 data into a atomic file(NW_H.byn) in the form of binary

latitude=malloc(10*sizeof(int));
longitude=malloc(10*sizeof(int));
height=malloc(10*sizeof(int));

gridinterval=3;
strcpy(inputfile,xyzname);
strcpy(tempfile,"tempfile2");
fp=fopen(inputfile,"r");

```

```

fscanf(fp,"%f%f%f%f%f%d
%d",&max_lat,&min_lon,&min_lat,&max_lon,&size1,&size2);
fclose(fp);

for(ii=max_lat;ii>min_lat;ii--) {
  for(jj=min_lon;jj<max_lon;jj++)
    {   grid_maxlat=ii;
        grid_minlat=ii-1;
        grid_minlon=jj;
        grid_maxlon=jj+1;

        strcpy(gridfile,"");
        strcat(gridfile,"N");

        sprintf(tempstr,"%d",grid_maxlat);
        strcat(gridfile,tempstr);
        strcat(gridfile,"W");
        sprintf(tempstr,"%d",grid_minlon);
        strcat(gridfile,tempstr);
        strcat(gridfile,"_H.byn");

        fp=fopen(inputfile,"r");
        fscanf(fp,"%f%f%f%f%f%d
%d",&max_lat,&min_lon,&min_lat,&max_lon,&size1,&size2);
        fp2=fopen(tempfile,"w");
        printf("output file...%s\n",gridfile);

        NN=0;
        while (!feof(fp))
          {
            fscanf(fp,"%f%f%f\n",&templat,&templon,&tempheight);
            if (templon <0) templon+=360.00;
            if (((templat>=grid_minlat) && (templat<=grid_maxlat))
                {
                  if (((templon>=grid_minlon) && (templon<=grid_maxlon))
                      {
                        fprintf(fp2,"%f%f%f\n",templat,templon,tempheight);
                        NN++;
                      }
                }
            }
          }
        fclose(fp);
        fclose(fp2);

```

```

//relog data from gridfile and save these data into array
latitude/longitude/height
latitude=realloc(latitude,NN*sizeof(int));
longitude=realloc(longitude,NN*sizeof(int));
height=realloc(height,NN*sizeof(int));

fp=fopen(tempfile,"r");

NNN=0;
minlat=90*3600;
maxlat=-90*3600;
minlon=3600*360;
maxlon=-3600*180;

while (!feof(fp))
{
    fscanf(fp,"%f%f%f\n",&templat,&templon,&tempheight);
    templon=(int)(templon*3600);
    templat=(int)(templat*3600);
    if (templon<minlon) minlon=templon;
    if (templon>maxlon) maxlon=templon;
    if (templat<minlat) minlat=templat;
    if (templat>maxlat) maxlat=templat;

    latitude[NNN]=templat;
    longitude[NNN]=templon;
    height[NNN]=tempheight;
    NNN++;
}
fclose(fp);

fp=fopen(gridfile,"wb");
num_lat=3600/gridinterval;
num_lon=num_lat;
if ((grid_maxlon>180) && (grid_minlon>180))
{
    east=grid_maxlon-360;
    west=grid_minlon-360;
}

WriteHeaderSwap(grid_maxlat*3600,west*3600,grid_minlat*3600,east*3600,gridinter
val, gridinterval, BinFile.Factor, BinFile.FactorSD,
BinFile.StdDev, BinFile.Global, BinFile.Type,
BinFile.SizeOf, BinFile.Datum, BinFile.Ellipsoid, BinFile.ByteOrder,
BinFile.Scale,fp);

```



```

for(i=1;i<=NN;i++)
{
if (n == 6)
{
if (fmod(i,601)==0)
{
newheight=height[i-1];
SwapByte( (char *)&newheight , 0 , 2 );
fwrite(&newheight,sizeof(short),1,fp);
}
else {
newheight=height[i-1];
SwapByte( (char *)&newheight , 0 , 2 );
fwrite(&newheight,sizeof(short),1,fp);

newheight=(height[i-1]+height[i])/2.0;
SwapByte( (char *)&newheight , 0 , 2 );
fwrite(&newheight,sizeof(short),1,fp);
}
}
}

else
{
if (fmod(i,301)==0)
{
newheight=height[i-1];
SwapByte( (char *)&newheight , 0 , 2 );
fwrite(&newheight,sizeof(short),1,fp);
}
else{
newheight=height[i-1];
SwapByte( (char *)&newheight , 0 , 2 );
fwrite(&newheight,sizeof(short),1,fp);

newheight=(height[i-1]+height[i])/2.0;
SwapByte( (char *)&newheight , 0 , 2 );
fwrite(&newheight,sizeof(short),1,fp);

newheight=(height[i-1]+height[i])/2.0;
SwapByte( (char *)&newheight , 0 , 2 );
fwrite(&newheight,sizeof(short),1,fp);
}
}
}

```

```

        }
    }
    fclose(fp);
}
}
free(latitude);
free(longitude);
free(height);
}

```

```

void WriteHeaderSwap(long int North,long int West,long int South,long int East,
short int DLat,short int DLon,double factor,double FactorSD,
short int StdDev,short int Global,short int type,short int Sizeof,
short int Datum,short int Ellipsoid,short int ByteOrder,short int Scale,FILE *fp)

```

```

{
long int longint;
int s,t;

```

```

SwapByte( (char *)&South , 0 , 4 );
fwrite(&South,sizeof(long),1,fp);

```

```

SwapByte( (char *)&North , 0 , 4 );
fwrite(&North,sizeof(long),1,fp);

```

```

SwapByte( (char *)&West , 0 , 4 );
fwrite(&West,sizeof(long),1,fp);

```

```

SwapByte( (char *)&East , 0 , 4 );
fwrite(&East,sizeof(long),1,fp);

```

```

SwapByte( (char *)&DLat , 0 , 2 );
fwrite(&DLat,sizeof(short),1,fp);

```

```

SwapByte( (char *)&DLon , 0 , 2 );
fwrite(&DLon,sizeof(short),1,fp);

```

```

SwapByte( (char *)&Global , 0 , 2 );
fwrite(&Global,sizeof(short),1,fp);

```

```

SwapByte( (char *)&type , 0 , 2 );
fwrite(&type,sizeof(short),1,fp);

```

```

SwapByte( (char *)&factor , 0 , 8 );
fwrite(&factor,sizeof(double),1,fp);

```

```
SwapByte( (char *)&Sizeof , 0 , 2 );  
fwrite(&Sizeof,sizeof(short),1,fp);
```

```
SwapByte( (char *)&StdDev , 0 , 2 );  
fwrite(&StdDev,sizeof(short),1,fp);
```

```
SwapByte( (char *)&FactorSD , 0 , 8 );  
fwrite(&FactorSD,sizeof(double),1,fp);
```

```
SwapByte( (char *)&Datum , 0 , 2 );  
fwrite(&Datum,sizeof(short),1,fp);
```

```
SwapByte( (char *)&Ellipsoid , 0 , 2 );  
fwrite(&Ellipsoid,sizeof(short),1,fp);
```

```
SwapByte( (char *)&ByteOrder , 0 , 2 );  
fwrite(&ByteOrder,sizeof(short),1,fp);
```

```
SwapByte( (char *)&Scale , 0 , 2 );  
fwrite(&Scale,sizeof(short),1,fp);
```

```
longint=0;  
for( s = 0 ; s < 7 ; s++ )  
{  
    SwapByte( (char *)&longint , 0 , 4 );  
    fwrite(&longint , sizeof( long ) , 1 , fp );  
}  
}
```

```
int SwapByte( char *buf, int start_byte , int num_bytes )  
{  
    char    temp;  
    if (num_bytes == 2) {  
        temp = buf[start_byte];  
        buf[start_byte] = buf[start_byte + 1];  
        buf[start_byte + 1] = temp;  
        return( 1 );  
    }  
    else if (num_bytes == 4) {  
        temp = buf[start_byte];  
        buf[start_byte] = buf[start_byte + 3];  
        buf[start_byte + 3] = temp;  
        temp = buf[start_byte + 1];  
        buf[start_byte + 1] = buf[start_byte + 2];  
        buf[start_byte + 2] = temp;  
    }  
}
```

```

    return( 1 );
}
else if (num_bytes == 8) {
    temp = buf[start_byte];
    buf[start_byte] = buf[start_byte + 7];
    buf[start_byte + 7] = temp;
    temp = buf[start_byte + 1];
    buf[start_byte + 1] = buf[start_byte + 6];
    buf[start_byte + 6] = temp;
    temp = buf[start_byte + 2];
    buf[start_byte + 2] = buf[start_byte + 5];
    buf[start_byte + 5] = temp;
    temp = buf[start_byte + 3];
    buf[start_byte + 3] = buf[start_byte + 4];
    buf[start_byte + 4] = temp;
    return( 1 );
}
else {
    printf("swap_bytes: num_bytes not one of 2 or 4.\n");
    exit(1);
}
}

```

```

short ReadBinaryFileHeaderSwap( BINFILE *BinFile )
{
    double Scale, Tmp8;
    long int Tmp4;
    short int Tmp2 , i;

    if( !(BinFile->File = fopen( BinFile->Name, "rb")) )
        return( 0 );

    fread( &Tmp4 , sizeof( long ) , 1 , BinFile->File ); //read south
    SwapByte( (char *)&Tmp4 , 0 , 4 );
    BinFile->South = Tmp4/3600.0;

    fread( &Tmp4 , sizeof( long ) , 1 , BinFile->File ); //read north
    SwapByte( (char *)&Tmp4 , 0 , 4 );
    BinFile->North = Tmp4/3600.0;

    fread( &Tmp4 , sizeof( long ) , 1 , BinFile->File ); //read west
    SwapByte( (char *)&Tmp4 , 0 , 4 );
    BinFile->West = Tmp4/3600.0;

    fread( &Tmp4 , sizeof( long ) , 1 , BinFile->File ); //read east
    SwapByte( (char *)&Tmp4 , 0 , 4 );
}

```

```

BinFile->East = Tmp4/3600.0;

fread( &Tmp2 , sizeof( short ) , 1 , BinFile->File ); //dlat
SwapByte( (char *)&Tmp2 , 0 , 2 );
BinFile->DLat = Tmp2/3600.0;

fread( &Tmp2 , sizeof( short ) , 1 , BinFile->File ); //dlon
SwapByte( (char *)&Tmp2 , 0 , 2 );
BinFile->DLon = Tmp2/3600.0;

fread( &Tmp2 , sizeof( short ) , 1 , BinFile->File ); //global
SwapByte( (char *)&Tmp2 , 0 , 2 );
BinFile->Global = Tmp2;

fread( &Tmp2 , sizeof( short ) , 1 , BinFile->File ); // factor
SwapByte( (char *)&Tmp2 , 0 , 2 );
BinFile->Type = Tmp2;

fread( &Tmp8 , sizeof( double ) , 1 , BinFile->File );
SwapByte( (char *)&Tmp8 , 0 , 8 );
BinFile->Factor = Tmp8;

fread( &Tmp2 , sizeof( short ) , 1 , BinFile->File );
SwapByte( (char *)&Tmp2 , 0 , 2 );
BinFile->SizeOf = Tmp2;

fread( &Tmp2 , sizeof( short ) , 1 , BinFile->File );
SwapByte( (char *)&Tmp2 , 0 , 2 );
BinFile->StdDev = Tmp2;

fread( &Tmp8 , sizeof( double ) , 1 , BinFile->File );
SwapByte( (char *)&Tmp8 , 0 , 8 );
BinFile->FactorSD = Tmp8;

fread( &Tmp2 , sizeof( short ) , 1 , BinFile->File );
SwapByte( (char *)&Tmp2 , 0 , 2 );
BinFile->Datum = Tmp2;

fread( &Tmp2 , sizeof( short ) , 1 , BinFile->File );
SwapByte( (char *)&Tmp2 , 0 , 2 );
BinFile->Ellipsoid = Tmp2;

fread( &Tmp2 , sizeof( short ) , 1 , BinFile->File );
SwapByte( (char *)&Tmp2 , 0 , 2 );
BinFile->ByteOrder = Tmp2;

```

```

fread( &Tmp2 , sizeof( short ) , 1 , BinFile->File );
SwapByte( (char *)&Tmp2 , 0 , 2 );
BinFile->Scale = Tmp2;

/* Read the dummy bytes */

for( i = 0 ; i < 7 ; i++ )
{
    fread( &Tmp4 , sizeof( long ) , 1 , BinFile->File );
}

Scale = ( BinFile->Scale ) ? 1000.0 : 1.0;
BinFile->South /= Scale;
BinFile->North /= Scale;
BinFile->West /= Scale;
BinFile->East /= Scale;
BinFile->DLat /= Scale;
BinFile->DLon /= Scale;

BinFile->NLat = ( BinFile->North - BinFile->South ) / BinFile->DLat + 1.5;
BinFile->NLon = ( BinFile->East - BinFile->West ) / BinFile->DLon + 1.5;

printf( ".\n" );
printf( "%lf %lf\n" , BinFile->North , BinFile->South );
printf( "%lf %lf\n" , BinFile->East , BinFile->West );
printf( "NLat %d NLon %d\n" , BinFile->NLat , BinFile->NLon );

return( 1 );
}

double ReadBinaryFileDataSwap( BINFILE *BinFile )
{
    double Value;
    short int Tmp2;
    long int Tmp4;

    if( BinFile->SizeOf == 4 )
    {
        if( fread( &Tmp4 , sizeof( long ) , 1 , BinFile->File ) == 1 )
        {
            SwapByte( (char *)&Tmp4 , 0 , 4 );
            Value = Tmp4/BinFile->Factor;
        }
        else
            Value = 9999.0;
    }
}

```

```
else
{
if( fread( &Tmp2 , sizeof( short ) , 1 , BinFile->File ) == 1 )
{
SwapByte( (char *)&Tmp2 , 0 , 2 );
if( Tmp2 != 32767 )
{
Value = Tmp2/BinFile->Factor;

}
else
{ Value = 9999.0; }
}
else
{ Value = 9999.0; }
}

return( Value );
}
```

Appendix C

C.1

```
#!/bin/sh
#
# Preparation of the option files for DTE program
# Witen by Huaining Yang
#
if test -z "$1"
then
    echo "Lantitude should be inputed"
else
    if test -z "$2"
    then
        echo "Longtitude should be inputed"
    else
        LANTITUDE=$1
        LONGITUDE=$2
        FILENAME=`echo $LANTITUDE $LONGITUDE | awk
        '{printf("DTE_NTglobal_N%sW%s.opt\n", $1, $2);}'`
        echo $FILENAME
        cat DTE_TEMPLATE | sed "s/NUM_LANTITUDE/$LANTITUDE/g" \
            | sed "s/NUM_LONGTITUDE/$LONGITUDE/g" \
            > $FILENAME
    fi
fi
```

C.2

```
#!/bin/sh
#
# Preparation of the Input files for DTE program
# Written by Huaining Yang
#
for (( i=59; i<=61; i++))
do
```



```

for (( j=269; j<=272; j++))
do
    Lat=$i
    Lon=$j

    #echo "i=$i; j=$j"

    FILENAME=`echo $Lat $Lon | awk '{printf("input_N%sW%s\n",
$1,$2);}'`
    echo "LANTITUDE and LONGITUDE should be $Lat $Lon"

    a=`echo 360-$j | bc`
    Weight=`echo $i-1 | bc`
    Value=`echo $i+1 | bc`
    Zhou=`echo $a-1 | bc`
    Ting=`echo $a+1 | bc`

    echo $FILENAME
    cat INPUT_TEMPLATE | sed "s/LAT/$Lat/g" \
        | sed "s/LON/$a/g" \
            | sed "s/VALUE/$Value/g"\
            | sed "s/WEIGHT/$Weight/g"\
            | sed "s/ZHOU/$Zhou/g"\
            | sed "s/TING/$Ting/g"\
            > $FILENAME

done
done

```

C.3

```

#!/bin/sh
#
# Running DTE program batchly and automatically
# Written by Huaining Yang
#
for (( i=48; i<=60; i++))
do
    for (( j=232; j<=248; j++))
    do
        if [ -f DTE_N${i}W${j}.c ]
        then
            echo "DTE_N${i}W${j}.c file exist"
            gcc -lm -o./aa.e DTE_N${i}W${j}.c
            echo ""# DTE_N${i}W${j}.c was opened #""
        fi
    done
done

```

```
./aa.e
echo ""### the calculation of DTE_N${i}W${j}.c successfully ###""
else
echo "Sorry, $1 file does not exist"
fi
done
done
```

Vita

- Candidate's full name:** Huaining Yang
- Date / place of birth:** November 27, 1975 / Henan, P. R. China
- Permanent address:** Huaining Yang
No 18 Jing Wu Road
Room 24, Building 2,
Zhengzhou, Henan Province
P. R. China, 450002
- Schools attended:** Primary and secondary school in Henan, 1983 – 1991
High school in Henan, 1991 - 1994
- Universities attended:** Jiaozuo Institute of Technology, Jiaozuo, 1994 – 1998
Universit